15334

NATIONAL LIBRARY
OTTAWA

CANADA

BIBLIOTHÈQUE NATIONALE
OTTAWA

NAME OF AUTHOR.....TERANCE E.M. SAMBROOK.....

TITLE OF THESIS.....RADIOLYSIS OF LIQUID.....
.....NITROUS OXIDE.....
.....

UNIVERSITY.....ALBERTA (EDMONTON).....

DEGREE FOR WHICH THESIS WAS PRESENTED.....PhD.....

YEAR THIS DEGREE GRANTED.....1973.....

Permission is hereby granted to THE NATIONAL LIBRARY OF CANADA to microfilm this thesis and to lend or sell copies of the film.

The author reserves other publication rights, and neither the thesis nor extensive extracts from it may be printed or otherwise reproduced without the author's written permission.

(Signed).....T. Sambrook.....

PERMANENT ADDRESS:
.....Bryn Gwyn.....
.....Glyn Ceiriog., DENBYS,
.....WALES U.K.....

DATED.....5.3.....1973.

NL-91 (10-68)

THE UNIVERSITY OF ALBERTA

RADIOLYSIS OF LIQUID NITROUS OXIDE

by

© TERANCE ERNEST MARIUS SAMBROOK

A THESIS

SUBMITTED TO THE FACULTY OF GRADUATE STUDIES AND RESEARCH

IN PARTIAL FULFILMENT OF THE REQUIREMENTS FOR THE DEGREE

OF

DOCTOR OF PHILOSOPHY

DEPARTMENT OF CHEMISTRY

EDMONTON, ALBERTA

Spring 1973

THE UNIVERSITY OF ALBERTA

FACULTY OF GRADUATE STUDIES AND RESEARCH

The undersigned certify that they have read, and recommend to the Faculty of Graduate Studies and Research for acceptance, a thesis entitled

"RADIOLYSIS OF LIQUID NITROUS OXIDE"

submitted by TERANCE ERNEST MARIUS SAMBROOK in partial fulfilment of the requirements for the degree of Doctor of Philosophy.

.....
Supervisor

.....

.....

.....

.....

.....
External Examiner

Date Feb 22/73

A B S T R A C T

The γ-radiolysis of liquid nitrous oxide has been investigated. The products formed are nitrogen, oxygen and nitrogen dioxide, yielding $G(N_2) = 13.1 \pm 0.2$, $G(O_2) = 2.6 \pm 0.1$ and $G(NO_2) = 5.6 \pm 0.2$ respectively. A mechanism is presented, which is consistent with the results obtained, and includes a novel combination of N_2O^+ and N_2O^- ions in the neutralisation reaction.

To support the mechanism, over thirty compounds were added to nitrous oxide solutions, and the changes in product yields measured. Generally the nitrogen yield decreased, whereas the yields of oxygen and nitrogen dioxide were eliminated as the additive concentration increased.

Efficient electron scavengers, such as nitrogen dioxide and chloroform, have lower ionisation potentials than nitrous oxide and when added to the nitrous oxide system, scavenged both electrons and positive ions. The results obtained complement the mechanism.

With the addition of nitrous oxide to alkane solutions, nitrous oxide scavenged some of the electrons generated in the alkane, and thus inhibited hydrogen formation. Nitrous oxide was hence interfering with normal neutralisation reactions of the alkanes, resulting in a decrease in the hydrogen yield and an increase in the nitrogen yield.

A specific study was carried out to determine $G(H_2O)$ in the hydrocarbon/nitrous oxide system, and the results obtained accounted for the oxygen atoms released during radiolysis.

ACKNOWLEDGEMENTS

I would like to express my appreciation to Dr. G. R. Freeman, my research director, for his guidance during this project.

The understanding and patience of my wife Ida, and constant if distant encouragement of my parents are deeply appreciated.

Special thanks are due to Mrs. M. Waters who typed the final draft of this thesis, and also to those members of the radiation chemistry group who offered assistance.

TABLE OF CONTENTS

		Page
ABSTRACT.		iii
ACKNOWLEDGEMENTS		v
LIST OF TABLES		x
LIST OF FIGURES		xv
INTRODUCTION.		1-20
A	GENERAL	1
B	ABSORPTION OF IONISING RADIATION	2
C	REACTIVE INTERMEDIATES	3
	(a) Positive Ions	4
	(b) Negative Ions	5
	(c) Excited Molecules	6
	(d) Neutral Free Radicals	7
D	ANOMALIES CONCERNING RADIOLYSIS IN THE LIQUID PHASE	8
E	RADIOLYSIS OF NITROUS OXIDE	11
	(a) Gas Phase	11
	(b) Liquid Phase	15
F	ADDITIVE STUDIES WITH NITROUS OXIDE	15
G	OBJECT OF THE PRESENT WORK.	19
EXPERIMENTAL.		21-47
A	MATERIALS	21
	(a) Nitrous Oxide	21

Page

(b) Compounds Used as Gaseous Additives 21

(c) Compounds Used as Liquid Additives 22

(d) Materials Used in the Gas Chromatographic Units 23

(e) Miscellaneous 24

B APPARATUS 24

(a) High Vacuum System 24

(b) The Gas Chromatographic Unit 30

(c) Spectrophotometric Analysis 34

C TECHNIQUES 34

(a) Preparation of Pure Nitrous Oxide 34

(b) Gaseous Additives 37

(c) Liquid Additives 38

(d) Gas Analysis 41

(e) Nitrogen Dioxide Determination as Nitrite . 43

(f) Water Analysis 44

D IRRADIATION 46

(a) The γ-ray Source 46

(b) Dosimetry 46

RESULTS 48-144

A DEFINITION OF TERMS USED. 48

(a) G Value 48

(b) g Value 48

Page

(c) Electron Fraction 48

(d) Nitrogen Yields 48

B THE RADIOLYSIS OF LIQUID NITROUS OXIDE 49

C ADDITIVE STUDIES. 49

D PRODUCT YIELDS 52

(a) High Electron Affinity Compounds 52

(b) Alkanes 62

(c) Alkenes 74

(d) Halo-compounds 79

(e) Oxygen-containing Compounds 103

(f) Alkynes 118

(g) Cyclo-compounds 118

(h) Miscellaneous 132

(i) Water Analysis 137

DISCUSSION 145-196

A LIQUID NITROUS OXIDE 145

(a) Structures of Nitrous Oxide and Its Ions using Mechanism I 152

B ANALYSIS OF THE ADDITIVE STUDIES 155

(a) Alkanes 155

(b) Alkenes 161

(c) Water Analysis 167

(d) Halo-compounds 171

Page

(e) Oxygen-containing Compounds. 181

(f) Alkynes. 183

(g) Cyclo-compounds 183

(h) Miscellaneous 187

(i) High Electron Affinity Compounds 190

REFERENCES 197

LIST OF TABLES

Table		Page
II-1	Densities of additives at selected temperatures	39
II-2	Various irradiation temperatures used	40
III-1	G values for the radiolysis of liquid nitrous oxide at -90°C	50
III-2	G values using sulphur hexafluoride as the additive at -90°C and -45°C	53
III-3	$G(NO_2)$ and $g(NO_2)$ values using sulphur hexafluoride as the additive at -90°C	56
III-4	G values using carbon dioxide as the additive at -47°C	58
III-5	G values using nitrogen dioxide as the additive at -45°C	60
III-6	G values using n-hexane as the additive at -90°C	63
III-7	G values of nitrogen dioxide using alkanes as the additives at -90°C	65
III-8	G values using n-butane as the additive at -90°C	67
III-9	G values using propane as the additive at -90°C	70
III-10	G values using ethane as the additive at -90°C	72
III-11	G values using 1-hexene as the additive at -90°C	75
III-12	G values of nitrogen dioxide using alkenes as the additives at -90°C	77
III-13	G values using 1-butene as the additive at -90°C	80
III-14	G values using propene as the additive at -90°C	82

Table		Page
III-31	G values of nitrogen dioxide using neohexane, toluene and methyl acetylene as additives at -90°C	123
III-32	G values using cyclopentane as the additive at -90°C	125
III-33	G values using cyclopentene as the additive at -90°C	128
III-34	G values using cyclopropane as the additive at -90°C	130
III-35	G values using toluene as the additive at -90°C	133
III-36	G values using 1,3-butadiene as the additive at -90°C	135
III-37	G values using neohexane as the additive at -90°C	138
III-38	Determination of $G(H_2O)$ in nitrous oxide using n-butane as the additive at -90°C	140
III-39	Determination of $G(H_2O)$ in nitrous oxide using 1-butene as the additive at -90°C	143
IV-1	Material balance for Mechanism I using G(ionisation) values of 3,4 and 5 respectively	147
IV-2	Material balance for Mechanism II (invoking O^- ions) using G(ionisation) values of 3, 4 and 5 respectively.	148
IV-3a	Decrease in product yields with addition of the alkanes	157
IV-3b	G values obtained for the pure alkanes	157
IV-4	Ionisation potentials of the alkanes	158
IV-5a	Decrease in product yields with addition of the alkenes	162

Table		Page
III-15	G values using ethene as the additive at -90°C	84
III-16	G values using methyl fluoride as the additive at -90°C	86
III-17	G values using methyl chloride as the additive at -90°C	89
III-18	G values of nitrogen dioxide using methyl chloride and methyl bromide as the additives at -90°C	92
III-19	G values using methyl bromide as the additive at -90°C	94
III-20	G values using methyl iodide as the additive at -63°C	96
III-21	G values using n-propyl bromide as the additive at -90°C	99
III-22	G values using chloroform as the additive at -63°C	101
III-23	G values using carbon tetrachloride as the additive at -23°C	104
III-24	G values using acetone as the additive at -90°C	106
III-25	G values of nitrogen dioxide using methanol and acetone as additives at -90°C	109
III-26	G values using acetaldehyde as the additive at -90°C	111
III-27	G values using methanol as the additive at -90°C	113
III-28	G values using ethanol as the additive at -90°C	116
III-29	G values using acetylene as the additive at -90°C	119
III-30	G values using methyl acetylene as the additive at -90°C	121

Table		Page
IV-5b	$G(H_2)$ values obtained for the pure alkenes	162
IV-6	Ionisation potentials and electron affinities of the alkenes	164
IV-7a	Decrease in product yields with addition of the halo-compounds	172
IV-7b	G values obtained for the pure halo-compounds	172-173
IV-8a	Ionisation potentials and electron affinities of the halo-compounds	175
IV-8b	$G(N_2)$ values at 0.01 mole fraction nitrous oxide	175
IV-9a	Decrease in product yields with addition of the oxygen-containing compounds	179
IV-9b	G values obtained for the pure oxygen-containing compounds	179
IV-10	Ionisation potentials of the oxygen-containing compounds	180
IV-11a	Decrease in product yields with addition of the alkynes	182
IV-11b	Ionisation potentials of the alkynes	182
IV-12a	Decrease in product yields with addition of the cyclo-compounds	184
IV-12b	$G(H_2)$ values obtained for the pure cyclo-compounds	184
IV-13	Ionisation potentials of the cyclo-compounds	186
IV-14a	Decrease in product yields with addition of the miscellaneous compounds	188
IV-14b	Ionisation potentials of the miscellaneous compounds	188
IV-15a	Decrease in product yields with addition of the high electron affinity compounds	191

Table		Page
IV-15b	Ionisation potentials and electron affinities of the high electron affinity compounds	191

LIST OF FIGURES

Figure		Page
II-1	Main vacuum manifold	25
II-2	Sample preparation manifold	27
II-3	Sample bulbs	28
II-4	Gas analysis system	31
II-5	Water analysis system	33
II-6	Nitrous oxide preparation system	36
III-1	Product yields using sulphur hexafluoride as the additive. Irradiation temperatures are -90°C and -45°C	54
III-2	Effect of sulphur hexafluoride on the $G(NO_2)$ yield. Irradiation temperature is -90°C	57
III-3	Product yields with carbon dioxide as the additive. Irradiation temperature is -47°C	59
III-4	Product yields with nitrogen dioxide as the additive. Irradiation temperature is -45°C	61
III-5	Product yields using n-hexane as the additive. Irradiation temperature is -90°C	64
III-6	Effect of the alkanes on the $G(NO_2)$ yield. Irradiation temperature is -90°C	66
III-7	Product yields with n-butane as the additive. Irradiation temperature is -90°C	68
III-8	Product yields with propane as the additive. Irradiation temperature is -90°C	71
III-9	Product yields with ethane as the additive. Irradiation temperature is -90°C	73
III-10	Product yields using 1-hexene as the additive. Irradiation temperature is -90°C	76
III-11	Effect of the alkenes on the $G(NO_2)$ yield. Irradiation temperature is -90°C	78

Figure		Page
III-12	Product yields with 1-butene as the additive. Irradiation temperature is -90°C	81
III-13	Product yields with propene as the additive. Irradiation temperature is -90°C	83
III-14	Product yields with ethene as the additive. Irradiation temperature is -90°C	85
III-15	Product yields using methyl fluoride as the additive. Irradiation temperature is -90°C	87
III-16	Product yields with methyl chloride as the additive. Irradiation temperature is -90°C	90
III-17	Effect of the halo-compounds on the $G(NO_2)$ yield. Irradiation temperature is -90°C	93
III-18	Product yields with methyl bromide as the additive. Irradiation temperature is -90°C	95
III-19	Product yields with methyl iodide as the additive. Irradiation temperature is -63°C	97
III-20	Product yields with n-propyl bromide as the additive. Irradiation temperature is -90°C	100
III-21	Product yields with chloroform as the additive. Irradiation temperature is -63°C	102
III-22	Product yields with carbon tetrachloride as the additive. Irradiation temperature is -23°C	105
III-23	Product yields using acetone as the additive. Irradiation temperature is -90°C	108
III-24	Effect of the oxygen-containing compounds on the $G(NO_2)$ yield. Irradiation temperature is -90°C	110
III-25	Product yields with acetaldehyde as the additive. Irradiation temperature is -90°C	112
III-26	Product yields with methanol as the additive. Irradiation temperature is -90°C	114
III-27	Product yields with ethanol as the additive. Irradiation temperature is -90°C	117

Figure		Page
III-28	Product yields using acetylene as the additive. Irradiation temperature is -90°C	120
III-28	Product yields with methyl acetylene as the additive. Irradiation temperature is -90°C	122
III-30	Effect of methyl acetylene, toluene and neohexane respectively on the $G(NO_2)$ yield. Irradiation temperature is -90°C	124
III-31	Product yields using cyclopentane as the additive. Irradiation temperature is -90°C	126
III-32	Product yields with cyclopentene as the additive. Irradiation temperature is -90°C	129
III-33	Product yields with cyclopropane as the additive. Irradiation temperature is -90°C	131
III-34	Product yields using toluene as the additive. Irradiation temperature is -90°C	134
III-35	Product yields with 1,3-butadiene as the additive. Irradiation temperature is -90°C	136
III-36	Product yields with neohexane as the additive. Irradiation temperature is -90°C	139
III-37	Yield of $G(H_2O)$ upon addition of n-butane. Irradiation temperature is -90°C	141
III-38	Yield of $G(H_2O)$ upon addition of 1-butene. Irradiation temperature is -90°C	144

INTRODUCTION

A. GENERAL

Radiation chemistry is the study of the chemical effects resulting from the absorption of high energy ionising radiation by material (1). The passage of such radiation through liquids yields excited, ionic and free radical species. These intermediates then react further to give stable products.

Certain compounds added to a system can react with intermediates during radiolysis. For example, nitrous oxide reacts with electrons and results in the formation of nitrogen, a stable product which is easily measured. Nitrous oxide is therefore used as an additive for elucidating mechanisms in various systems. Information can thus be obtained about electron reactions, leading to a better understanding of radiolytic processes.

Ion-electron neutralisation in the radiolysis of an alkane normally produces hydrogen.

$$RH \longrightarrow\!\!\!\!\!\!\sim\!\!\!\!\!\!\sim\!\!\!\!\!\!\longrightarrow RH^+ + e^- \qquad (1)$$

$$RH^+ + e^- \longrightarrow H_2 + \text{products} \qquad (2)$$

In the presence of nitrous oxide, some of the electrons generated in the alkane are scavenged, thus altering the neutralisation reaction and preventing the formation of

hydrogen via reaction (2). The negative ion N_2O^- formed in (3) results in nitrogen through (4).

$$e^- + N_2O \longrightarrow N_2O^- \qquad (3)$$

$$N_2O^- + RH^+ \longrightarrow N_2, \text{ but no } H_2 \qquad (4)$$

By measuring these changes in product yields, data are gathered about the normal neutralisation reactions.

Although nitrous oxide has been used as an electron scavenger in many systems, it has not been thoroughly investigated itself. This thesis is therefore concerned with the study of the radiolysis of liquid nitrous oxide.

B. ABSORPTION OF IONISING RADIATION

Radiolysis reactions are initiated by the absorption of high energy ionising radiation in a system. The actual processes by which energy is transferred from the radiation to the molecules in the system merit consideration. γ rays interact in several ways with the medium they traverse. The two main processes by which energy is transferred from 1 MeV γ rays, such as those used in the present work, are briefly outlined below.

The photoelectric effect must be considered when using materials of high atomic number, such as methyl bromide and iodide. A γ photon interacts with the atom as a whole, and the orbital electron ejected essentially

acquires all the energy of the absorbed photon.

Compton scattering is the predominant process for 1 MeV photons in materials of low atomic number, such as hydrocarbons and nitrous oxide. An incident γ ray collides with an atomic electron which absorbs on average about half of the photon's energy. The electron released thus acquires about 0.5 MeV, and produces further ionisations, and excitations by interacting with molecules as it darts through the system. This initial electron is called a "primary" electron, and in turn it sets in motion many "secondary" electrons. The secondary electrons can create further ionisations and excitations. Hence "activated" zones are created along the path of the ionising particles.

In the liquid phase many of the ions and electrons recombine within about 10^{-10} sec, but others may have a lifetime of 10^{-6} sec or longer.

C. REACTIVE INTERMEDIATES

Reactive intermediates such as positive ions, electrons, excited molecules, free radicals and negative ions can take part in several types of reactions in forming the final products. A brief explanation of the more important reactions is warranted and therefore is summarised below.

(a) Positive Ions

A charge transfer, or electron abstraction reaction, can occur if the ionisation potential of a neutral molecule B is less than that of the neutral counterpart of the ion A^+.

$$A^+ + B \longrightarrow A + B^+ \qquad (5)$$

If A is a polyatomic molecule then its ionisation potential could be greater than the "recombination energy" of the electron. Thus for reaction (5) to proceed efficiently, the ionisation potential of B should be equal to or less than the "recombination energy" of the ion A^+. These reactions are helpful in studying various positive ions such as the excited propane ion formed in the following reaction (2).

$$Xe^+(^2P_{3/2}, {}^2P_{1/2}) + C_3H_8 \rightarrow Xe + C_3H_8^{+*} \qquad (6)$$

In the radiolysis of hydrocarbons using nitrous oxide as the additive, a charge transfer reaction can occur between the N_2O^+ ion and the neutral hydrocarbon molecule.

$$N_2O^+ + RH \longrightarrow N_2O + RH^+ \qquad (7)$$

Johnson and Warman (3) noted that by using nitrous oxide in the radiolysis of propane, the hydrogen yield decreased. They deduced that no hydrogen atoms are formed when the electrons are scavenged by nitrous oxide.

Other reactions of positive ions include proton transfer hydrogen atom and hydrogen transfer, and condensation reactions.

(b) Negative Ions

Thermal electrons can be captured by neutral molecules possessing positive electron affinities, and hence can form negative ions (4).

$$AB + e^- \longrightarrow AB^{-*} \qquad (8)$$

The fate of the vibrationally excited ions, with respect to dissociation, depends upon such factors as the initial energy of the electron, the electron affinity of the neutral molecule AB, and the dissociation energy of the A-B bond. Thus dissociation or autodetachment can occur unless the anion is quickly stabilized.

$$AB^{-*} \longrightarrow A + B^- \text{ (dissociation)} \qquad (9)$$

$$AB^{-*} \longrightarrow AB + e^- \text{ (autodetachment)} \qquad (10)$$

Hence the formation of a relatively stable AB^- ion is dependent upon a rapid de-excitation of the anion. The excess energy of the excited ion is removed by collision stabilisation with a neutral molecule.

$$AB^{-*} + M \rightarrow AB^- + M^* \qquad (11)$$

Information from the study of the pressure dependence from the electron capture cross-sections of nitrous oxide indicate that the ion N_2O^- is stabilised by collisions (5,6). The nitrous oxide negative ion N_2O^- has

a decomposition lifetime of $\sim 10^{-4}$ sec in the gas phase (7), and the estimated lifetime in another study was 2×10^{-5} sec (8). By comparison the lifetime of a more complex ion, SF_6^-, is 10^{-4} sec (9). These negative ions can undergo ion-molecule reactions, and can be neturalised by positive ions. For example, when two high electron affinity compounds are present in a radiolytic system, an electron transfer reaction is proposed to occur (7).

$$N_2O^- + SF_6 \longrightarrow N_2O + SF_6^- \qquad (12)$$

$$N_2O^- + DI \longrightarrow N_2O + DI^- \qquad (13)$$

(c) Excited Molecules

Excited molecules are generated directly in the radiolytic system and formed from ion neutralisation reactions. Much of the knowledge concerning the reactions of excited molecules is acquired from photolysis studies using photon energies below the ionisation potential of the compound under investigation. The decomposition of nitrous oxide after the absorption of 1470 Å light can occur according to the following equations (10,11).

$$N_2O \xrightarrow{h\nu} N_2O^* \longrightarrow N_2 + O \qquad (14)$$

$$\longrightarrow NO + N \qquad (15)$$

Reactions of excited molecules also include autoionisation and energy transfer. Excited cyclohexane molecules, for example, are reported to transfer energy to cyclohexane and benzene (12,13). Holroyd proposed that energy transfer reactions occur between cyclohexane and nitrous oxide in the photolysis of cyclohexane - nitrous oxide mixtures and 1470 Å light (14).

$$C_6H_{12}^{*} + N_2O \longrightarrow C_6H_{12} + N_2O^{*} \qquad (16)$$

(d) Neutral Free Radicals

Free radicals may be formed from ion-molecule reactions, and from the decomposition of excited molecules and ions.

$$C_2H_5OH^{+} + C_2H_5OH \longrightarrow C_2H_5OH_2^{+} + CH_3CHOH \qquad (17)$$

$$C_6H_{14}^{*} \longrightarrow CH_3 + C_5H_{11} \qquad (18)$$

$$N_2O^{*} \longrightarrow N_2 + O \qquad (19)$$

Free radicals are detected in a radiolytic system with the addition of radical scavengers such as iodine, and thereby information is obtained regarding the role of these radicals. Electron spin resonance spectroscopy is frequently used to detect radicals, as in the esr studies of irradiated nitrous oxide (15,16). Reactions

of neutral free radicals of particular importance in the present work are abstraction (e.g. reaction 20) and combination (e.g. reaction 21).

$$OH + RH \longrightarrow H_2O + R\cdot \qquad (20) \quad \text{(ref. 17)}$$

(where RH is a hydrocarbon)

$$O + O + M \longrightarrow O_2 + M \qquad (21) \quad \text{(ref. 18)}$$

Other reactions include addition to double bonds, disproportionation, and abstraction.

D. ANOMALIES CONCERNING RADIOLYSIS IN THE LIQUID PHASE

Mechanistic postulates concerning the radiolysis of solutions are frequently augmented by direct comparison with similar studies in the gas phase. This section briefly discusses differences between processes in the two phases.

The passage of γ rays through a liquid causes the ionised and excited species to be intially concentrated in spheres of about 10 Å diameter and roughly 10^3 Å apart along the paths of high energy electrons (4). Secondary electrons drift about 100 Å from their parent positive ions while becoming thermalised. Therefore it is quickly rationalised that in the liquid phase, most of these low energy electrons recombine with their parent ions. The majority of the free radicals formed also recombine. These clusters or spheres of intermediates are referred

to as spurs and due to the close proximity of these intermediates, the latter have a high probability of reacting together. Those species which by random diffusion evade initial recombination percolate into the bulk of the solution. From conductivity experiments, the free ion yield G_{fi} (where G_{fi} is the number of pairs of free ions formed per 100 eV of energy absorbed) is estimated to be about 0.1 in many liquid hydrocarbons (19-22).

By comparison, the spurs in the gas phase are about 1 μ in diameter and separated by about 10^2 μ (4). The secondary electrons have a high probability (close to unity) of escaping from their positive ions and pairs of free radicals formed have little probability of recombination. The free ion yield in gas phase hydrocarbons is therefore considerably higher being around 4 (23).

The low yield in the liquid phase indicates that only a small fraction of the ejected electrons escape the coloumbic fields of their parent positive ions. Therefore considering that the product yields from electron scavenging studies are far in excess of 0.1, then the electrons which are scavenged are those which would otherwise have recombined in the spurs.

Electron affinity values obtained from measurement in the gas phase are often quoted indiscriminately from one phase to another. In fact values in the liquid phase

vary with such factors as the polarity and structure of the solution.

$$e^-_{solv} + AB_{solv} \longrightarrow AB^-_{solv} \qquad (22)$$

In the above reaction, the sum of the solvation energies of the neutral molecule AB and the electron probably does not equal the solvation energy of the negative ion AB^-. Solvation processes can also enhance the dissociation of negative ions, and alter the probability of ion-molecule reactions, especially in polar solvents (4).

Excited molecules and ions which would have decomposed in the gas phase have a good probability of being stabilised by collision in liquids. Collisional stabilisation apparently accounts for the behaviour of such compounds as carbon dioxide and methyl chloride which are good electron scavengers in the liquid phase, and are quite ineffective as scavengers in the gas phase.

The geminate recombination processes could also differ between the two phases, as the recombining electron suffers many more collisions in the liquid phase due to the close proximity of neighbouring molecules. However, the recombination energy will still be greater than the bond energy of the molecule so a probable result is decomposition of the excited molecule.

Ionisation potentials are lower in the liquid

phase than in the gas phase by about 1 - 1.5 eV (24). In the radiolysis of liquid hydrocarbons, using nitrous oxide as the additive, the reduction in the hydrogen yield has often been interpreted as an indication of the number of electrons scavenged. There is however a danger in this interpretation, as in the gas phase the yield of hydrogen from neutralisation processes is less than the ion yield (25-27). A charge transfer reaction is probably more efficient in the liquid phase, as collisions with other molecules are likely to occur before vibration relaxation of the ion.

In conclusion, extrapolation of gas phase data into liquid phase mechanisms should be undertaken with caution, giving due regard to the above examples.

E. RADIOLYSIS OF NITROUS OXIDE

(a) Gas Phase

Nitrous oxide has been used extensively as a dosimeter (28-41), but its role as such is somewhat limited due to the uncertainty in the resultant nitrogen yields. However, various groups have contributed significantly towards a greater insight to the overall mechanism in the radiolysis of gaseous nitrous oxide.

Harteck and Dondes (30) proposed that nitrous oxide was a reproducible dosimeter, and included the equations given below in their mechanism.

$$N_2O \longrightarrow N_2O^* \longrightarrow N_2 + O \quad \sim 80\% \quad (23)$$

$$N_2O \longrightarrow N_2O^+ + e^- \longrightarrow N + NO \quad \sim 20\% \quad (24)$$

Jones and Sworski studied the effects of temperature pressure and electric field on nitrous oxide dosimetry (38). They used the above equations in their mechanism, drawing their conclusions from an early study of nitrous oxide (28,29) and from information gained with the photolysis of nitrous oxide (10,18).

Further reactions of nitrogen and oxygen atoms with nitrous oxide are endothermic if the former are in their ground states (42). However, the nitrogen atom can react with the product nitric oxide, and the oxygen atoms recombine (43).

$$N + NO \longrightarrow N_2 + O \quad (25)$$

$$O + O + M \longrightarrow O_2 + M \quad (26)$$

Applied electric field experiments with nitrous oxide gave various results from group to group (44,45), and also values from temperature effect studies varied. For example, Jones and Sworski (38) and Gorden and Ausloos (37) agreed that the nitrogen yield obtained is greatly dependent on temperature but Boyd et al (41) determined that $G(N_2)$ showed no dependence on temperature below 200°C. Values of $G(N_2)$ even at a standard temperature show great

deviations. Jones and Sworski obtained a $G(N_2)$ value of 10.0 ± 0.2 agreeing with the results of Moseley and Truswell, Harteck and Dondes, and Flory. However, higher results such as $G(N_2) = 13.1 \pm 0.2$ (36) and $G(N_2) = 11.0 \pm 0.4$ (33) display the overiding deficiency of nitrous oxide as a gas phase dosimeter due to the inconsistent nitrogen yields obtained.

The radiolysis of gaseous nitrous oxide containing additives has been investigated (46-50). Conventionally the product yields for the pure system are determined, then additives such as the electron scavengers sulphur hexafluoride and carbon tetrachloride are added, and the changes in the yields are recorded. A mechanism is then proposed compatible with the experimental results.

Thermal electrons are proposed to react with nitrous oxide in the gas phase to form nitrogen by dissociative attachment (51-53).

$$N_2O + e^- \longrightarrow N_2 + O^- \qquad (27)$$

Burtt and Kircher suggested that the O^- ion reacted further (31).

$$O^- + N_2O \longrightarrow N_2 + O_2^- \qquad (28)$$

$$O^- + N_2O \longrightarrow NO + NO^- \qquad (29)$$

The formation of O_2^- from the bombardment of O^- ions on

gaseous nitrous oxide, studied in a mass spectrometer (31), led to a general acceptance of reactions (28) and (29). Therefore, according to this proposal, the capture of one electron by nitrous oxide leads to more than one mole of nitrogen formed. Using other electron scavengers as additives in the nitrous oxide system, Hummel (46,49) obtained results consistent with the above mechanism, and also suggested further reactions which could generate additional O^- ions.

$$NO^- + N_2O \longrightarrow NO + N_2 + O^- \qquad (30)$$

However, in a similar study with electron scavengers, Takao et al (47,50) determined that in the radiolysis of nitrous oxide, one electron decomposed one molecule of nitrous oxide subsequently leading to the formation of one molecule of nitrogen. Hence the ionic reactions, involving O^- yielding more than one molecule of nitrogen per scavenged electron, could not explain their results.

They suggested that the electron attachment to nitrous oxide was not initially dissociative, and the negative ion N_2O^- was sufficiently long-lived to undergo neutralisation reactions.

$$e^- + N_2O \longrightarrow N_2O^- \qquad (3)$$

Sears (48), studying the effect of electron scavengers on nitrous oxide, also cast doubt on reactions (28) and (29), since Paulson (54) found that charge transfer from O^- to impurity O_2 could account for the O_2^- observed by Burtt and Henis (52).

(b) Liquid Phase

Little work has been done on the radiolysis of pure liquid nitrous oxide (48,55). Robinson and Freeman (55) included in their mechanism the reaction of O^- with N_2O (reactions (28) and (29)), followed by a neutralisation reaction.

$$N_2O^+ + O_2^-(NO^-) \rightarrow N_2O^* + O_2(NO) \qquad (32)$$

Although the reaction of a ground state oxygen atom with nitrous oxide is endothermic, they suggested that equivalent reactions involving excited oxygen atoms could occur. The value obtained for $G(N_2)$ was 12.9 ± 0.2. Sears, using different techniques, obtained a value of 11.2 ± 0.5 for the radiolysis of liquid nitrous oxide at -88°C (48).

F. ADDITIVE STUDIES WITH NITROUS OXIDE

Nitrous oxide, being an electron scavenger, is used frequently in systems to ascertain the extent of the ionic reactions involved (3,7,14,17,56-82). Referring to saturated hydrocarbon systems, a gradual decrease in

hydrogen yield and increase in nitrogen yield is generally observed with increasing nitrous oxide concentration. The nitrogen yields obtained are usually greater than the expected yields of nitrogen resulting from the scavenging of electrons. Several suggestions have been made to account for this apparent "additional yield" of nitrogen and are briefly discussed below.

Various workers have determined that hydrogen atom reactions have little effect on the nitrogen yield. For example, Sato et al (65) determined that the addition of cyclohexene (a hydrogen atom scavenger) to the cyclohexane/nitrous oxide system does not decrease the nitrogen yield. Robinson and Freeman (75) in a radiolysis study of alkanes observed that nitrogen yields obtained from the addition of nitrous oxide were independent of the alkane type, thus confirming that nitrous oxide reacts with electrons and not hydrogen atoms. Sagert (78), Charlesby (64) and others (79,80) determined that hydrocarbon free radicals could not be percursors of nitrogen. A probable source of this "excess yield" of nitrogen therefore lies in the secondary reactions of nitrous oxide. Holroyd proposed that above a certain nitrous oxide concentration (~20mM), an energy transfer reaction between an excited molecule and nitrous oxide could occur. He concluded this from his studies of the 1470 Å photolysis of cyclohexane and nitrous oxide

solutions (14).

$$C_6H_{12}^* + N_2O \longrightarrow N_2 + O + C_6H_{12} \qquad (16)$$

This suggestion of an energy transfer reaction to nitrous oxide has not been widely supported, and even Holroyd's results can be explained using secondary ionic reactions of nitrous oxide.

Robinson and Freemans' proposal of a minor reaction between an excited oxygen atom and nitrous oxide (55) was included in the mechanism of Takao et al (81).

$$O^* + N_2O \longrightarrow O_2 + N_2 \qquad (33)$$

$$\longrightarrow NO + NO \qquad (34)$$

The latter concluded that $G(N_2)$ from this reaction was 2.6.

Johnson and Warman (3) proposed that as nitrogen was formed from the dissociative capture of electrons by nitrous oxide, then as previously mentioned the O^- ion reacted with nitrous oxide to form more nitrogen. Also an electron with sufficient kinetic energy might react with nitrous oxide according to the following equations (82).

$$e^{-*} + N_2O \longrightarrow N_2 + O + e^- \qquad (35)$$

Since Schulz observed a similar reaction in a mass

spectrometer (83), Sears proposed that like reactions could account for the "excess yield" of nitrogen (48).

Recently interest has been concentrated towards the existence of a long-lived N_2O^- ion. Evidence for this anion was indicated in the gas phase, as the electron capture by nitrous oxide turned out to be a pseudo three-body reaction (5,6).

$$e^- + N_2O + M \longrightarrow N_2O^- \qquad (31)$$

As previously mentioned the lifetime of this ion is about 10^{-4} sec (7), thus it can undergo additional reactions. Warman (67) proposed the following reactions concluding that two molecules of nitrogen are produced for each electron captured.

$$N_2O^- + N_2O \longrightarrow N_2 + N_2O_2^{-*} \qquad (36)$$

$$N_2O_2^{-*} + RH^+ \longrightarrow N_2 + \text{products} \qquad (37)$$

Takao et al (81) suggested a neutralisation reaction between the N_2O^- ion and a hydrocarbon positive ion producing one molecule of nitrogen per electron captured.

$$N_2O^- + RH^+ \longrightarrow N_2 + OH + R \qquad (38)$$

The products of the reactions between nitrous oxide and solvent ions are not well known. Various suggestions have

been made, being dependent upon whether the authors believe that one, or more than one, nitrogen molecule results from each electron scavenged by nitrous oxide. The yield of nitrogen obtained from the radiolysis of a 0.3 M solution of nitrous oxide in an alkane is $G(N_2) \approx 5$ (65,83), whereas the gas phase ionisation yield of the hydrocarbon is only G(ionisation) $\approx$ 4 (84,85). However, the ionisation yield in liquid xenon is three-fold greater than in gaseous xenon (86), so a factor of 1.3 between the liquid and gas phase yields in alkanes appears reasonable. If this is the case, then no "additional yield" of nitrogen would be required.

G. OBJECT OF THE PRESENT WORK

The overall interpretation of results from the radiolysis of pure nitrous oxide and from systems using nitrous oxide as an additive is still rather obtuse. The radiolysis of liquid nitrous oxide was therefore studied and the product yields determined. A mechanism is proposed which is consistent with the results obtained, and includes a novel combination of N_2O^- and N_2O^+ ions in the neutralisation reaction.

To support the mechanism, additives such as electron scavengers were introduced into the nitrous oxide system and the changes in product yields measured. Various other compounds, including alkanes and alkenes, were added to the system and all afforded results consistent with the

mechanism.

An additional study determined $G(H_2O)$ in the nitrous oxide n-butane system, which accounted for the oxygen atoms released during radiolysis.

E X P E R I M E N T A L

A. MATERIALS

(a) Nitrous Oxide

The nitrous oxide used was obtained from the Matheson Company, and the average analysis purity was given as 98.5%. The principal impurity was air, but trace amounts of nitrogen dioxide were detected. Therefore it was essential to remove nitrogen dioxide by bubbling the gas stream through two concentrated potassium hydroxide solutions.

(b) Compounds Used as Gaseous Additives

	Additive	Supplier
	Acetylene	Phillips Petroleum Company
	n-Butane	Phillips Petroleum Company
	1-Butene	Phillips Petroleum Company
	1,3-Butadiene	Phillips Petroleum Company
	Carbon Dioxide	Matheson of Canada Limited
	Cyclopropane	Matheson of Canada Limited
	Ethane	Phillips Petroleum Company
	Ethene	Phillips Petroleum Company
	Methyl Acetylene	Phillips Petroleum Company
1)	Methyl Chloride (Practical Grade)	Eastman Organic Chemicals
1)	Methyl Fluoride	Columbia Organic Chemicals
2)	Nitrogen Dioxide	Matheson of Canada Limited
	Propane	Phillips Petroleum Company

Additive	Supplier
Propene	Phillips Petroleum Company
Sulfur Hexafluoride	Matheson of Canada Limited

All reagents used were of research grade quality and used as supplied, unless otherwise stated.

1) Treated with potassium hydroxide pellets to remove acid impurities.

2) Traces of dinitrogen trioxide removed by trap-to-trap distillation at -78°C using a dry ice and acetone slush bath.

(c) Compounds Used as Liquid Additives

	Additive	Supplier
	Acetone (Spectral Grade)	Baker Chemical Company
1)	Acetaldehyde	Fisher Scientific Company
2)	Carbon Tetrachloride	Eastman Organic Chemicals
2)	Chloroform (Reagent Grade)	McArthur Chemical Co. Ltd.
3)	Cyclopentane	Phillips Petroleum Company
	Cyclopentene	Phillips Petroleum Company
	Ethanol	U.S. Industrial Chemicals Co.
3)	n-Hexane	Phillips Petroleum Company
	1-Hexene	Phillips Petroleum Company
4)	Methanol	Baker Chemical Company
2)	Methyl Bromide (Practical Grade)	Eastman Organic Chemicals

Additive	Supplier
Methyl Iodide (Practical Grade)	Eastman Organic Chemicals
3) Neohexane	Phillips Petroleum Company
2) n-Propyl Bromide (Reagent Grade)	Matheson, Coleman and Bell
Toluene (Reagent Grade)	Fisher Scientific Company

Reagents were of research grade quality and used as supplied, with the following exceptions:-

1) Distilled and middle fraction used.
2) Treated with potassium hydroxide pellets to remove acid impurities.
3) Shaken with an equal amount of concentrated sulphuric acid, dried over anhydrous magnesium sulphate and distilled from lithium aluminium hydride.
4) Refluxed with 1.5 g of 2,4-dinitrophenylhydrazine and 1 ml of concentrated sulphuric acid per litre of methanol and then distilled.

(d) Materials Used in the Gas Chromatographic Units

Compound	Supplier
Molecular Sieve 5A (1/16" pellets)	Union Carbide Corporation
Porapak Q (mesh size 50-80)	Waters Associates Inc.
Porapak Q (mesh size 150-200)	Waters Associates Inc.

Compound	Supplier
Helium	Canadian Liquid Air Ltd.

(e) Miscellaneous

Compound	Supplier
1) Chlorobenzene	Fisher Scientific Company
1) Chloroform	McArthur Chemical Co. Ltd.
Drierite	Hammond Drierite Company
1) Ethanol	U.S. Industrial Chemicals Co.
1) Methanol	McArthur Chemical Co. Ltd.
1-Naphthylamine	Fisher Scientific Company
Potassium Hydroxide	Fisher Scientific Company
Sulphanilic Acid	May and Baker Ltd.
2) Water (doubly-distilled)	
1) m-Xylene	Eastman Organic Chemicals

1) These compounds were used in the preparation of refrigerant slush-baths.

2) First distillation from alkaline potassium permanganate.

B. APPARATUS

(a) The High Vacuum System

The diagram of the main manifold is given in Figure II-1. A Welch duo-seal vacuum pump (Model 1402) coupled with a two-stage mercury diffusion pump ensured working

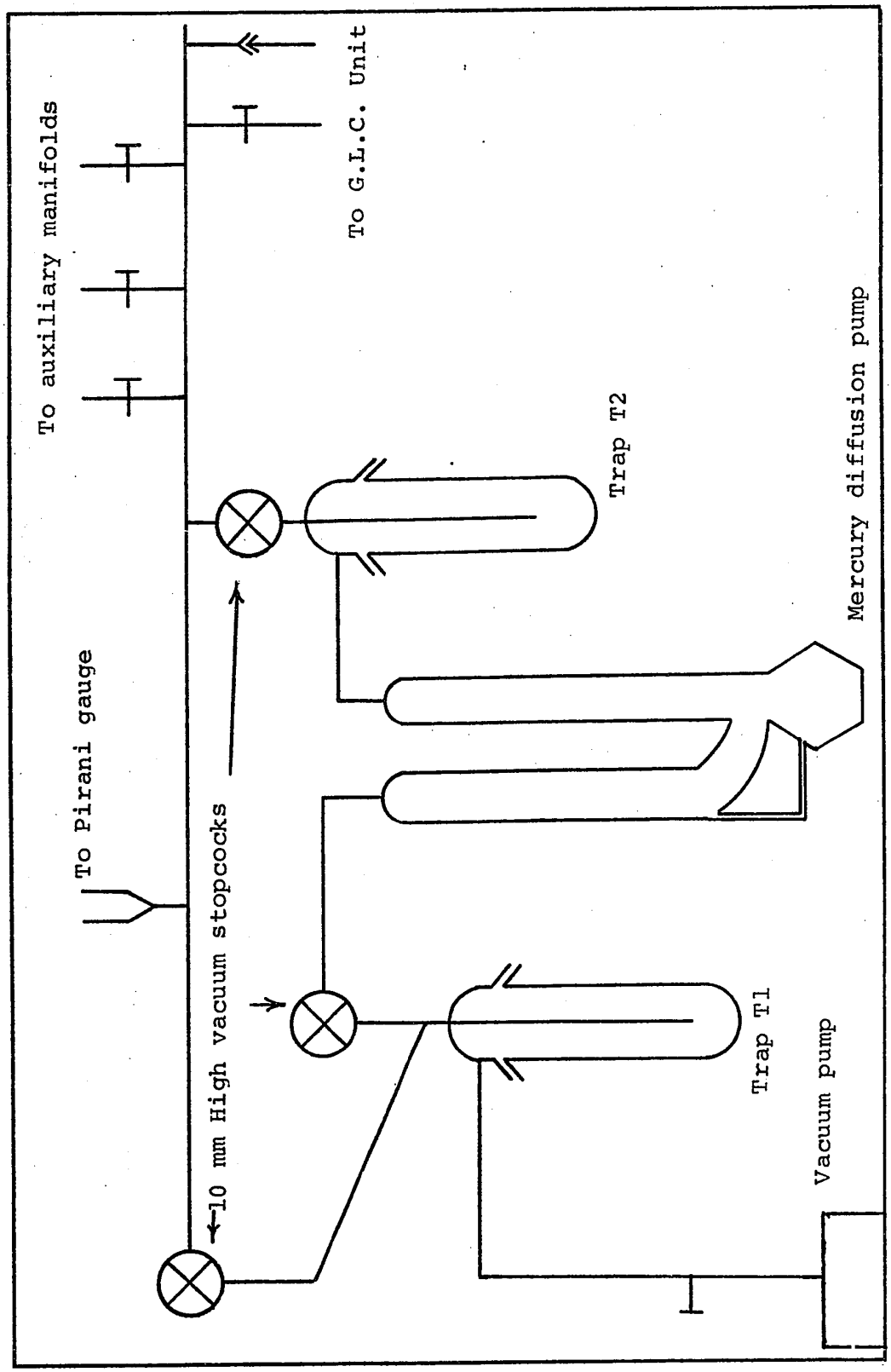

FIGURE II-1 Main Vacuum Manifold

vacuums of one micron or less. Pressure measurement was achieved using a Pirani gauge supplied by Consolidated Electrodynamics (Model GP-110) and the gauge-tube attached to the manifold by means of a Kovar seal.

Pyrex glassware was used in the construction of the high-vacuum system, and clamped to a metal frame, which was supported on a wooden table. All glass used in the assembly of the rack was initially cleaned using soap solution and thoroughly rinsed with distilled water. When in working order, traps T1 and T2 were immersed in liquid nitrogen baths to ensure smooth operation of the pumps.

(i) The Sample Preparation Manifold

The system (as shown in Figure II-2) was used for the preparation of pure nitrous oxide samples and samples containing additives, both liquid and gaseous.

Sample cells (Figure II-3) were constructed from Pyrex glass tubing (15 mm diameter). This tubing was initially cleaned by treating with hot concentrated nitric acid, and then thoroughly washed with distilled water, and finally rinsed with doubly-distilled water. The cells were glass-blown to 10/30 inner ground-glass joints and attached to 10/30 outer ground-glass joints on the manifold.

After testing for leaks, the cells were weighed and the weights recorded. When refitted to the manifold, the vials were flamed quite strongly whilst open to the pump

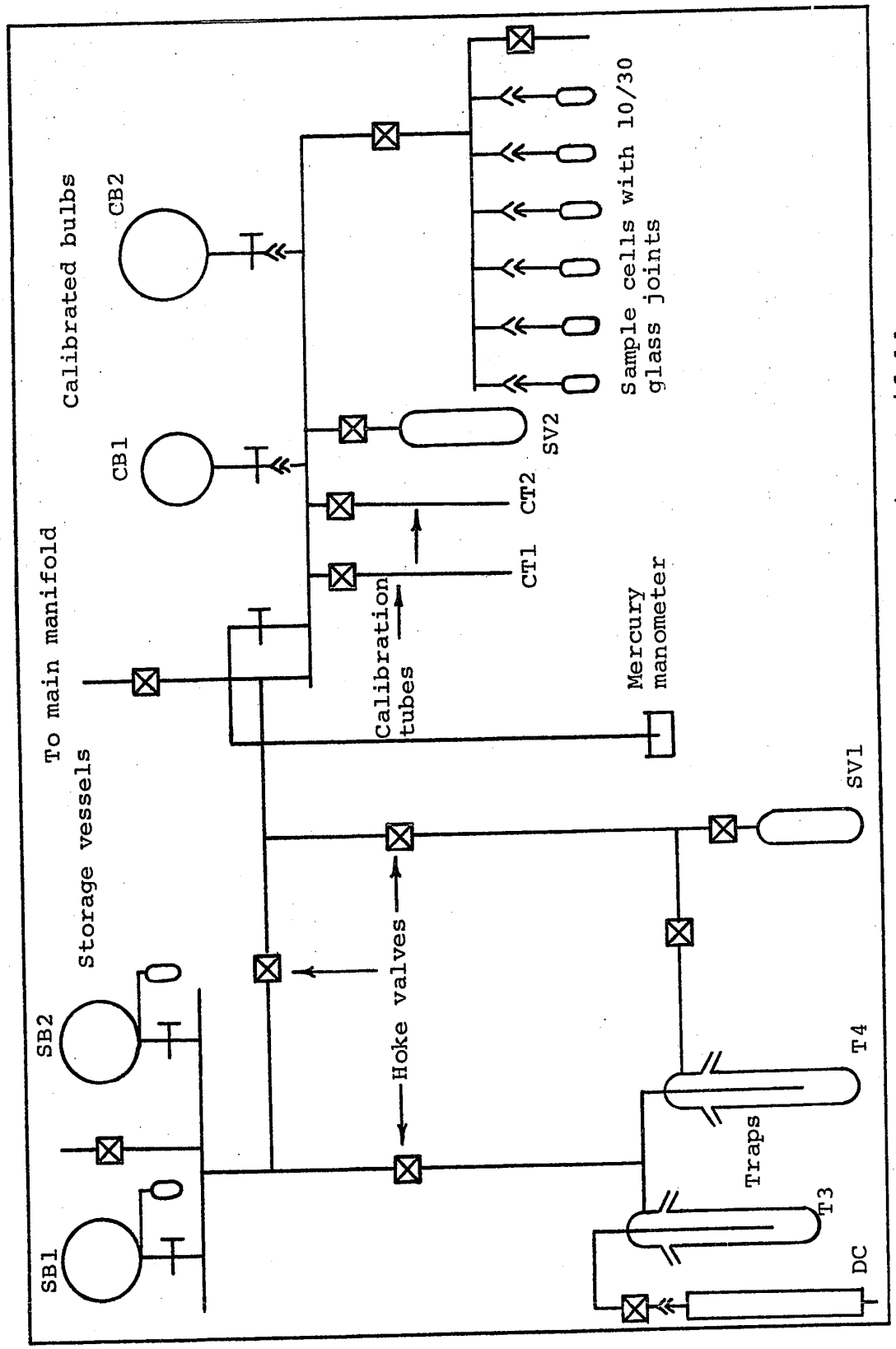

FIGURE II-2 Sample Preparation Manifold

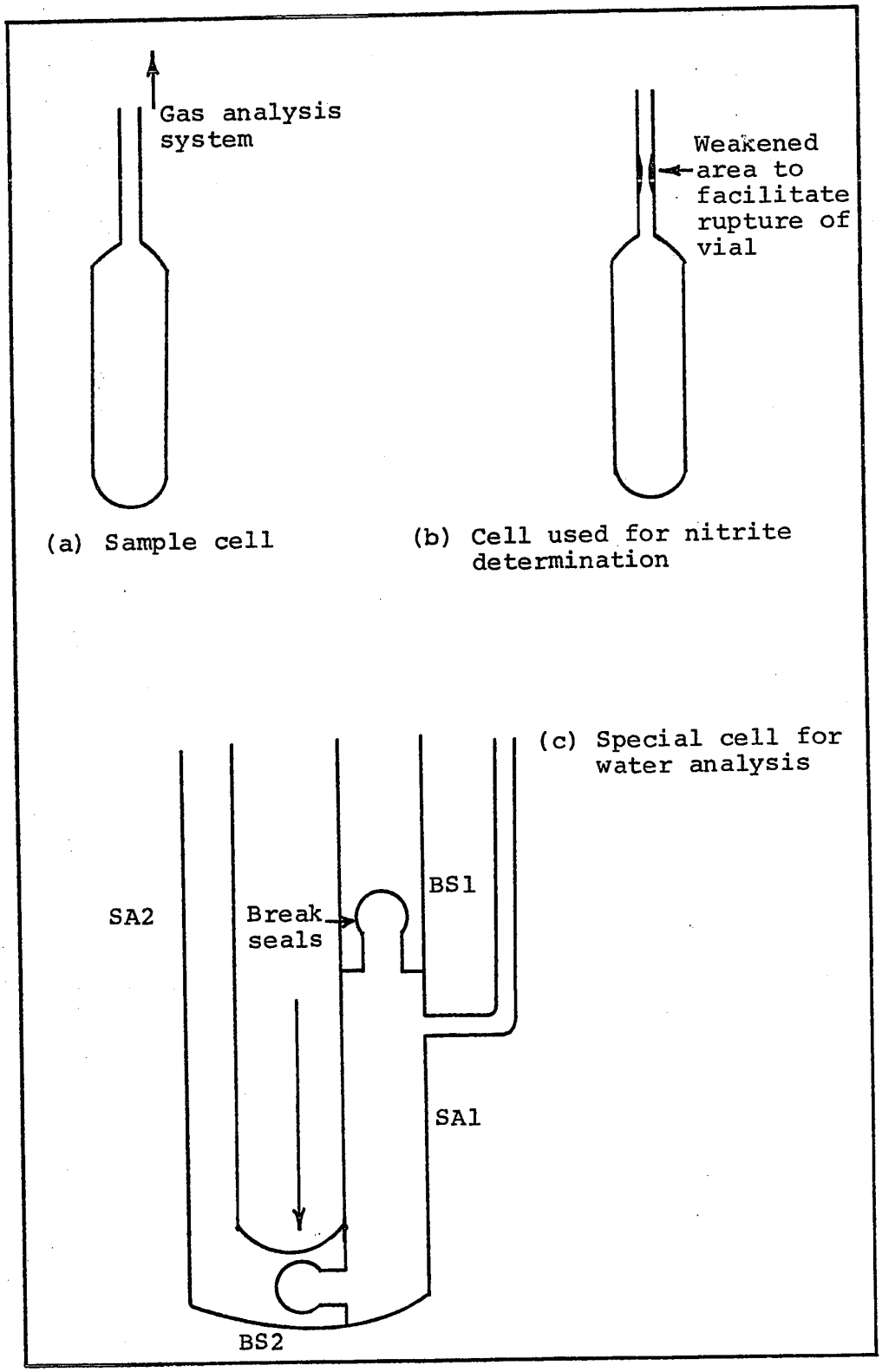

FIGURE II-3 Sample Bulbs

until no deflection on the Pirani gauge was noted. As an added precaution, a drying tube containing Drierite beads was used as a breath filter when glass blowing on the rack.

The cells used for water analysis were cleaned by using equal quantities of ethanol and nitric acid, washed with doubly-distilled water, dried, and kept in a desiccator until used. The use of greased stopcocks was kept to a minimum, and preference was given to the stainless-steel and Teflon Hoke valves. Where the use of grease (Apiezon N) was unavoidable, such as in the case of ground-glass joints, then frugal application of the grease was essential.

Several calibration bulbs were used, depending on the quantity of gaseous additive required. These were attached to the manifold by means of 12/30 ground-glass joints. The magnitudes of the calibrated volumes, using water as the determinant, are given below.

Calibrated Bulb	1	153.4 $\pm$ 0.2 ml at 25°C
	2	271.0 $\pm$ 0.3 ml at 26°C
	3	518.0 $\pm$ 0.5 ml at 27°C
	4	1051 $\pm$ 1 ml at 29°C

The two calibrated tubes used CT1 and CT2 were of 1 and 10 ml maximum capacity, respectively, and were used to measure the volume of liquid additive at the required

temperature (Figure II-2).

The storage vessels SV1 and SV2 were constructed from thick-walled glass, and were of 300 ml capacity. SV2 was used to store the purified nitrous oxide.

(ii) The Sample Analysis Manifold

The block diagram of this manifold is shown in Figure II-4. An auxiliary pump (Welch duo-seal) was used to operate the mercury float valve and to assist in evacuating the Toepler-McLeod gauge. A breaker device in the sample breaker unit, SCA, was constructed from a solid glass stopcock and incorporated a hole at one end. The stem of the sample cell was fitted into this orifice and broken with a twist of the stopcock. Cold traps T5 and T6 were maintained at -196°C when an analysis was performed. The Toepler pump efficiently carried over the non-condensable gases into the McLeod gauge. The storage bulbs SB3, SB4 and SB5 held various gases used for calibration purposes; these gases were introduced into the manifold through the inlet mercury valve IV.

(b) The Gas Chromatographic Unit

Helium carrier gas flowed through the detector cell and column. Its flow rate was determined by a bubble flowmeter. Both the detector, Model TRIIB (containing W2

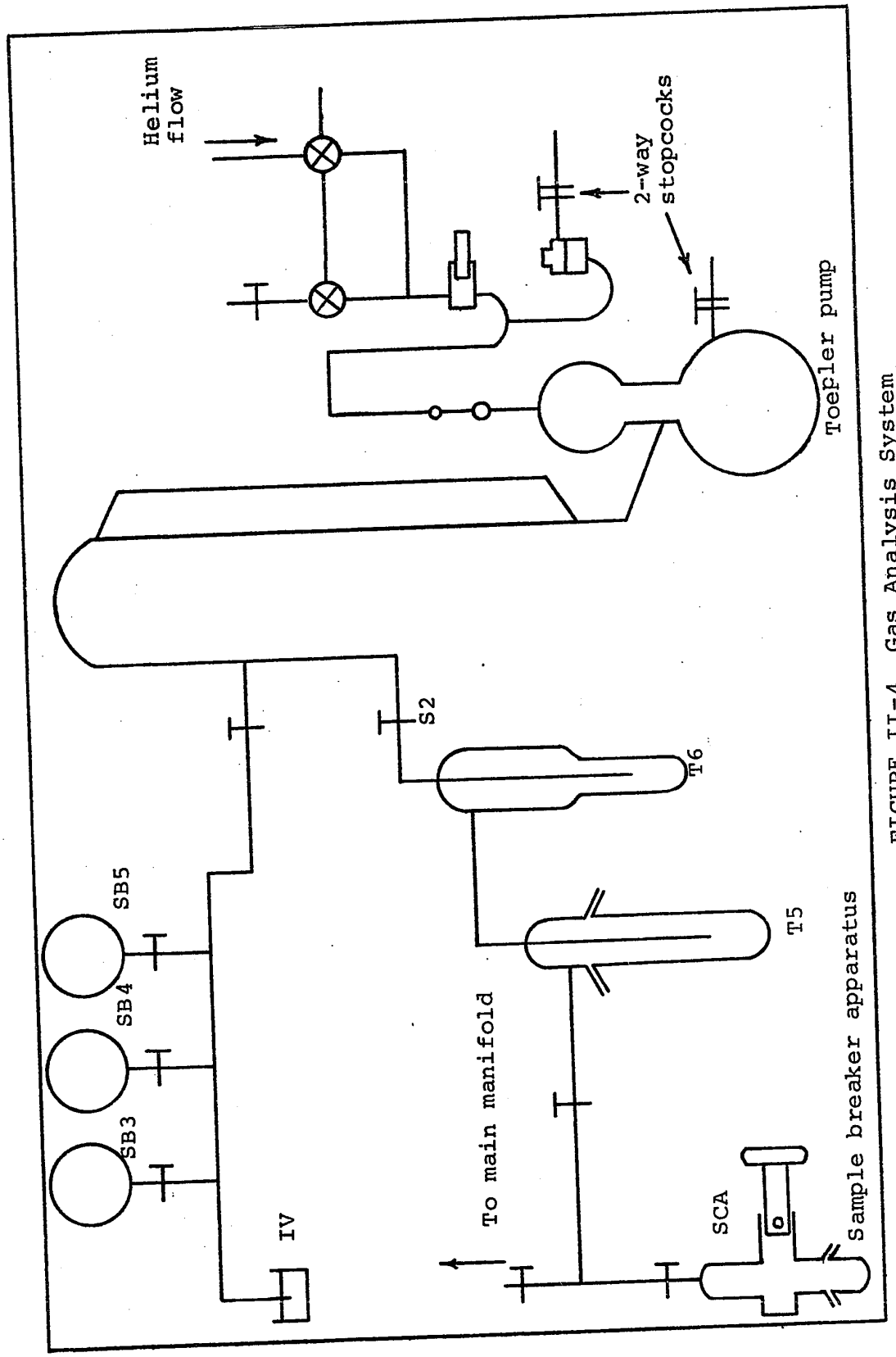

FIGURE II-4 Gas Analysis System

replaceable filaments), and the power supply (Model 405-C1) were manufactured by the Gow-Mac Instrument Company. The recorder was supplied by E. H. Sargent and Company (Cat. No. S-72180). When in use the detector was maintained at a temperature of 129°C and the current used was 250 mA. A 10' Molecular Sieve (5A) column in the form of a U-tube was operated at room temperature.

(i) Water Analysis

The sample analysis manifold was modified so as to incorporate the special cells used for the water analysis (Figure II-5). When the cell was glass-blown to the unit, each side-arm, SA1 and SA2, could be evacuated independently. A Hoke valve H3 with a metal side-arm connected this cell to the column; this distance was kept as short as possible. An injection unit SI fitted with a septum cap was attached to SA2 and used to inject alcohol chasers into the unit. Under final analysis conditions the whole apparatus was wrapped in heating-tape (supplied by Glass-Col Ltd.) and maintained at 190°C by means of variable voltage power supplies (Superior Electrical Company).

The column used for water analysis was a 6' x 3/16" copper tubing containing Porapak Q. For the alcohol determinations, a 9" x 3/16" column afforded the optimum results. These columns were contained in a heating mantle

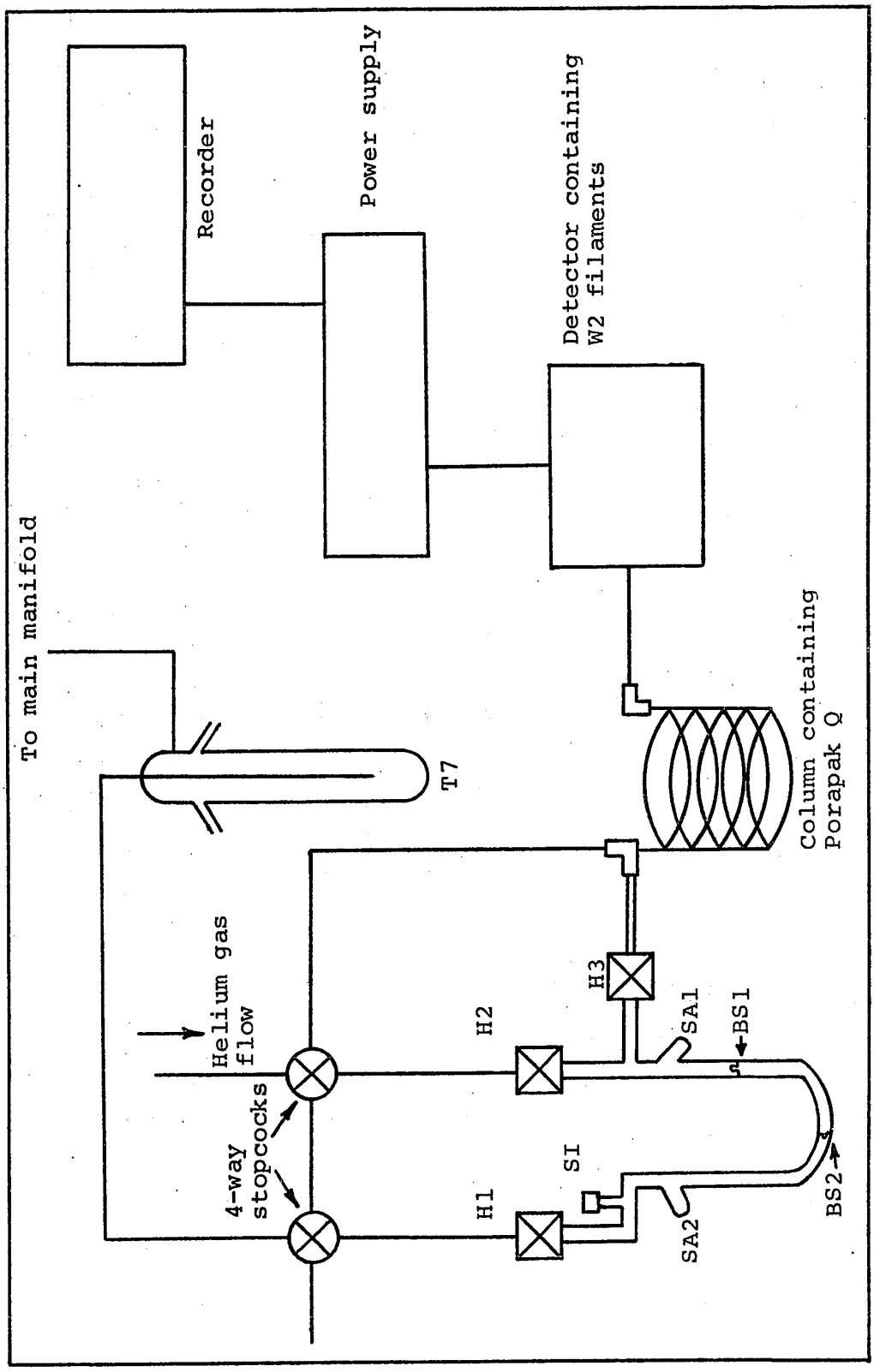

FIGURE II-5 Water Analysis System

at 210°C and insulated with glass wool. The detector cell and power supply were supplied by the Gow-Mac Instrument Company, and the cell operated at 150 mA at a temperature of 129°C. The recorder was supplied by Hewlett-Packard (Model 7127A).

Helium gas was dried in a drying tube containing Molecular Sieve (type 5A) and no water could be detected in the carrier gas stream.

(c) Spectrophotometric Analysis

A Beckmann DU spectrophotometer incorporating a hydrogen lamp was used at a wavelength of 304 mμ to determine the concentration of ferric ions in the Fricke dosimeter. The dosimetry is described later.

The same instrument, when operated at 540 mμ using a tungsten lamp, gave the quantity of nitrite in the irradiated samples. By means of a calibration curve obtained with standard solutions, the yield of nitrogen dioxide was calculated.

C. TECHNIQUES

(a) Preparation of Pure Nitrous Oxide

Nitrous oxide was purified by bubbling the gas through sintered glass discs in gas scrubber bottles containing concentrated potassium hydroxide solution. This procedure was essential as it removed impurities such as

nitrogen dioxide and carbon dioxide from the gas stream. An empty bottle was employed as a safety precaution to prevent back-flushing into the nitrous oxide cylinder (Figure II-6). The gas then passed through a column (50 cm x 0.25 cm) containing Drierite beads, and into a flowmeter which regulated the quantity of gas from the cylinder. After further drying through three columns of Drierite (50 cm x 0.15 cm), the nitrous oxide now purified and dried, entered the auxiliary manifold through stopcock S1. The gas was allowed to flush out the system and escaped through a mercury bubbler (MB) to a line leading to the fume-hood. After five minutes, the appropriate stopcocks were turned and the gas frozen in the storage bulb (SV3) which was immersed in a liquid nitrogen bath. When sufficient material was collected, usually after half an hour, the frozen nitrous oxide was warmed up, and approximately a third allowed to distill off. Then the remaining gas was subjected to several degassing processes consisting of freeze-pump-thaw cycles and trap-to-trap distillations (T8 and T9). This nitrous oxide was collected in the storage vessel (SV2) and kept at liquid nitrogen temperature until used (Figure II-2).

Samples were prepared in batches and fresh nitrous oxide used for each series. Distillation of the liquid nitrous oxide was effected by cooling the sample cell to methanol slush temperature at -90°C. When sufficient liquid

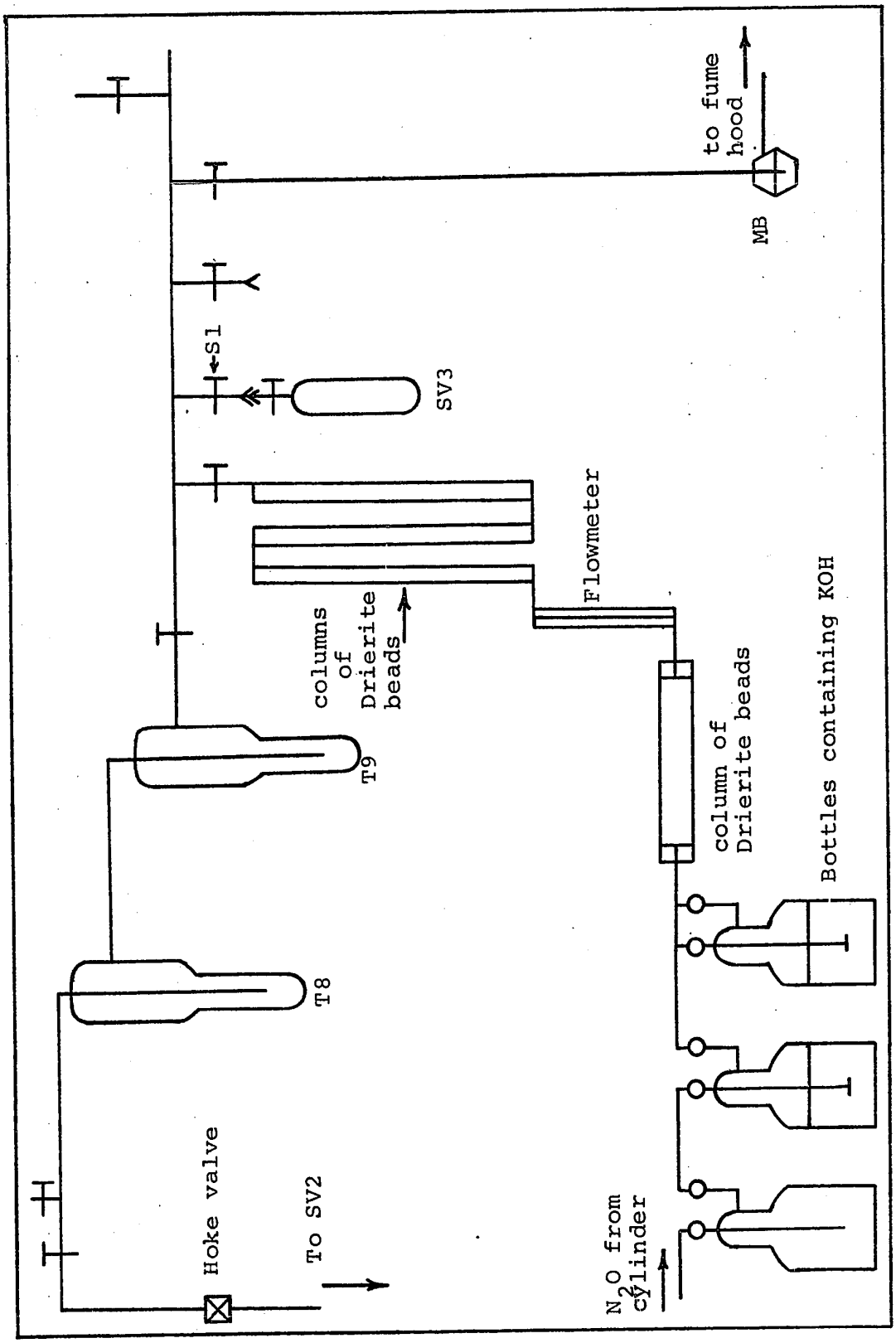

FIGURE II-6 Nitrous Oxide Preparation System

was collected, usually 2 g, the cell was frozen and thoroughly degassed. The vial was then sealed off with a flame, quickly washed in methanol to remove frozen methanol, dried, and weighed. This procedure was repeated to constant weight. The remaining stem containing the 10/30 ground-glass joint was cleaned of grease and weighed. Hence the weight of nitrous oxide was determined.

The sample cell containing nitrous oxide was placed in a holder and lowered into the irradiation vessel, which was maintained at a temperature of -90°C by means of methanol slush. When liquified, the nitrous oxide was irradiated in a Gamma-220 Cell.

For each batch of samples prepared, an unirradiated sample was set aside and used as the blank.

(b) Gaseous Additives

A list of the gaseous additives used in given on page 21.

For the non-halogenated compounds, the additives were first passed through a column containing Drierite (DC) degassed using the cold-traps T3 and T4, and then collected in the storage bulbs SB1 or SB2. When needed for use, further degassing by freeze-pump-thaw cycles in the side-finger of the bulb were performed until no deflection on the Pirani gauge was observed (Figure II-2).

When addition to the sample cell was required, the gas

was allowed to expand into a calibrated bulb CB1 or CB2 until the required number of moles was obtained. The excess gas was pumped off, and the additive was introduced from the calibrated bulb into the sample cell containing nitrous oxide; frozen in a bath of liquid nitrogen. For high concentrations of additives, the calibrated tubes CT1 and CT2 were preferred for measurement, and various temperatures were used to measure the required volume (Table II-1).

After five minutes the system was opened to the pump, and the cell sealed off with a flame. The vial and cell were weighed taking the same precautions as previously described. Hence the mole percentage of additive was calculated.

For the halogenated compounds, an additional column containing potassium hydroxide pellets was placed before the drying column, and the additives passed through it.

Care was used to ensure that the liquid nitrous oxide and the additive were completely mixed at the temperature of irradiation. A list of the additives and their irradiation temperatures is given in Table II-2. These temperatures were achieved through selection of suitable slush-baths.

(c) Liquid Additives

The liquid additives used are listed on page 22.

TABLE II-1

Densities of Additives at Selected Temperatures

(i) Gaseous Additives

Compound	Slush Bath Used	Density
n-Butane	Chloroform	0.676 at -63°C
1-Butene	Chloroform	0.687 at -63°C
1,3-Butadiene	o-Xylene	1.430 at -23°C
Cyclopropane	Chloroform	0.706 at -63°C
Propane	Chloroform	0.606 at -63°C
Propene	Ethanol	0.698 at -116°C

All other gaseous additives measured using calibrated bulbs.

(ii) Liquid Additives

Compound	Slush Bath Used	Density
Acetaldehyde	Ice-bath	0.808 at 0°C
Methyl Bromide	o-Xylene	1.796 at -23°C

Other liquid additives measured at room temperature.

TABLE II-2

Various Irradiation Temperatures Used

(i) Gaseous Additives

Compound	Irradiation Temperature °C	Slush Bath
Carbon Dioxide	-47	m-Xylene
Nitrogen Dioxide	-45	Chlorobenzene
Sulphur Hexafluoride	-45	Chlorobenzene

(ii) Liquid Additives

Compound	Irradiation Temperature °C	Slush Bath
Carbon Tetrachloride	-23	o-Xylene
Chloroform	-63	Chloroform
Methyl Iodide	-63	Chloroform

All other additives were irradiated at -90°C using a methanol slush bath.

These additives were first introduced into a 1 litre flask through a side-arm, then attached to the manifold, and preliminarily degassed. After subsequent degassing cycles through traps T3 and T4, the purified liquid was distilled into the storage vessel SV1. Calibrated tubes CT1 and CT2 of 1 and 10 ml capacity, respectively, were used to measure the volume of liquid required. Various slush baths were used depending on the particular additive, these temperatures are given in Table II-1. The liquid was then distilled into the sample cell containing the nitrous oxide, using the same technique as described above, sealed off and weighed. The sample cells were vigorously shaken in the irradiation vessel to achieve a homogeneous solution. All liquid additives were irradiated at -90°C in methanol slush unless otherwise stated (Table II-2).

The halogenated compounds were initially passed as vapor through a column of potassium hydroxide pellets before the degassing procedure.

(d) Gas Analysis

The irradiated sample cell containing the products to be analysed was initially washed free of frozen methanol and then placed in the sample breaker apparatus (Figure II-4). The cell was kept at liquid nitrogen temperature whilst the unit was evacuated until the Pirani

gauge read less than one micron. Further evacuation was done with the Toepler pump and the pressure now determined by the McLeod gauge. When the system was completely evacuated, traps T5 and T6 were enclosed in liquid nitrogen baths. As a safety precaution, the stopcock (S2) leading to the Toepler-McLeod apparatus was closed temporarily as the neck of the sample cell was broken.

The gases non-condensable at -196°C were pumped off and collected in the McLeod gauge. When three consecutive constant readings were obtained, usually after fifteen separate pumping cycles, the volume, pressure and temperature were recorded.

These gases were then transferred through the mercury float valve, passed the Teflon valve, and finally injected into the carrier gas stream. The flow-rate of helium was 78 ml/min, and maintained to within 2% of this value by a mercury flow control system. The g.c. column separated the gases and their peaks displayed on the recorder-chart, using the peak height times the width at half-height methanol to measure the areas.

(i) Calibration Gases

Nitrogen, oxygen, air, hydrogen, carbon monoxide and methane were used as the calibration gases. A known concentration of the required gas was injected into the chromatographic unit and the peak area measured. This procedure

was repeated until sufficient data were collected. A linear response was obtained for a plot of concentration of gas versus peak area. For hydrogen, the peak height was measured, as the peak area gave a non-linear plot. This peak height plot was linear in the concentration range required. These calibration curves were checked at monthly intervals. The retention times of the calibration gases were noted and therefore the identification of the product gases could be determined.

(e) Nitrogen Dioxide Determination as Nitrite

The sample cells were prepared and irradiated using the same techniques as previously described. A file-mark was scratched around the stem of the cell, since this procedure facilitated rupture of the vial. The cell containing frozen nitrous oxide was quickly dropped into a 1 litre bottle containing 20 ml of 0.025 M sodium hydroxide solution. A rubber bung equipped with a two-way stopcock was fitted to the bottle, which was then partially evacuated. For safety reasons, the bottle was placed in a fume-cupboard (with safety-glass windows) and the cell allowed to explode.

After the explosion, the bottle was shaken vigorously for a few minutes, and then agitated on a mechanical shaker for half an hour to ensure complete conversion of nitrogen dioxide to nitrite. The resultant solution was

filtered through a sintered-glass crucible (10-20 μ porosity). Great care was taken in washing out the bottle with small quantities of distilled water. The clear filtrate was transferred to a 100 ml volumetric flask and 10 ml of sulphanilic acid (8 g of acid in 1 litre) then 10 ml of α-naphthylamine reagent (5 g of α-naphthylamine in 1 litre) were added; the solution mixed and set aside. After half an hour, aliquots were pipetted into 1 cm optical cells and measured spectrophotometrically at 520 mμ using a Beckman D.U. Spectrophotometer (87).

An unirradiated sample was used as the blank, this being carried through all the above stages.

A calibration curve of known concentrations of nitrite versus optical density was constructed. Hence the amount of nitrite in the irradiated sample could be determined and therefore the $G(NO_2)$ in the sample calculated.

(f) Water Analysis

The special cell was glass-blown to the sample breaker unit and evacuated whilst maintained at -196°C by means of a liquid nitrogen bath. Hot air from a heat-gun was played around the break-seal BS1 to facilitate the pumping-off process. When the side-arm was completely evacuated, trap T7 was immersed in a bath of liquid nitrogen, then the break-seal (BS1) was broken and the non-condensable gases pumped off. A methanol slush bath was substituted for the

liquid nitrogen one and the distillation of nitrous oxide plus additive into cold trap T7 followed.

After the distillation was complete, the Hoke valve H2 was closed and the side-arm SA2 evacuated, again assisted by using a heat gun. Valve H1 was now closed and the second break-seal broken.

A novel method of breaking 'unbreakable' seals was perfected, and will be described briefly here. The side-arm under test was opened to the air, and the glass tubing around the break-seal carefully heated. This procedure forced the seal to collapse somewhat and after re-evacuating the side-arm the break-seal was easily shattered.

Heating tape was carefully wrapped around the side-arms and Hoke valve H3 leading to the column; this heated the unit to 190°C. A 1 µl of pure ethanol was injected into the heated unit through the injection cap SI and acted as a chaser to the water. By manipulating the four-way stopcocks, the helium gas flowed through the unit and out through Hoke valve H3 into the column The water peak obtained was displayed on the Hewlett-Packard recorder.

(i) Calibrations

Known volumes of water were injected into the Poropak Q column, the peak height measured, and hence a calibration curve plotted. In the detection of alcohols, a shorter Poropak Q column (9" x 3/16") was used, and the pure alco-

hols injected straight into the column. Thus plots of concentration of alcohols versus peak heights were constructed, and their respective retention times recorded.

D. IRRADIATION

(a) The γ-ray Source

A ^{60}Co Gammacell 220 Irradiation Unit supplied by Atomic Energy of Canada Ltd. was used throughout the project. It contained 12,000 curies of ^{60}Co. The sample cells were contained in a metal sample holder and immersed in a Dewar vessel containing a slush at the irradiation temperature desired.

(b) Dosimetry

Fricke dosimetry was used. The Fricke solution consisted of 1 mM $Fe(NH_4)_2(SO_4)_2$, 1 mM NaCl and 0.4 M H_2SO_4 in doubly-distilled water. Ferrous ions were converted into ferric ions by irradiation. The concentration of ferric ions was measured at a wavelength of 304 mμ using a Beckmann DU Spectrophotometer. $G(Fe^{+++})$ was 15.6 and the molar extinction coefficient was 2201 at 25°C (88). A set of samples containing Fricke solution was irradiated for various time intervals in the Dewar vessel containing water as this closely approximated the density of methanol slush (the usual slush bath used).

Dose rates for all systems were calculated using the appropriate electron densities, and corrected for the

radioactive decay of ^{60}Co (half-life of 5.28 years).

RESULTS

A. DEFINITIONS OF TERMS USED

(a) G Value

The G value in this study is defined as the number of molecules of product formed per 100 eV of energy absorbed by the system. It is based on the total energy absorbed by the solution.

(b) g Value

A g value is based upon the energy absorbed by the solvent only. Thus in a system containing nitrous oxide and ethane, $g(H_2)$ is determined using the energy initially absorbed by the ethane.

$$g(H_2) = \frac{G(H_2)}{\varepsilon_E}$$

where ε_E is the electron fraction of ethane in the solution.

(c) Electron Fraction ε_X

$$\varepsilon_X = \frac{E_X W_X}{E_X W_X + E_N W_N}$$

where E_X and E_N are the number of electrons per gram of additive and nitrous oxide respectively, and W_X and W_N are their respective weights in the sample.

(d) Nitrogen Yields

Electrons generated in the additive can be scavenged by the nitrous oxide.

Hence $$G(N_2) = \varepsilon_N g(N_2)_N + \varepsilon_X G(N_2)_X$$

and $$g(N_2)_N = \frac{G(N_2)}{\varepsilon_N} - \frac{\varepsilon_X G(N_2)_X}{\varepsilon_N}$$

where ε_X and ε_N are the electron fractions of the additive and nitrous oxide respectively. The true value of $G(N_2)_X$ is uncertain, so $g(N_2)_N$ was calculated using $G(N_2)_X$ = 0,1 2,3,4 and 5 giving $g(N_2)_N^0$, $g(N_2)_N^1$, $g(N_2)_N^2$ etc. With some additives, such as the halo-compounds, the high correction factors of 4 and 5 afforded negative values at high concentrations of the additives, meaning that $g(N_2)_N$ was less than 4. Therefore the lower values of $G(N_2)_X$ of 2 and 3 yielding $g(N_2)_N^2$ and $g(N_2)_N^3$ were calculated. The corrected curve referred to in the survey of the results is hence the one which gives the flattest curve along most of the concentration range. The $g(N_2)_N^0$ values, in most cases, are used for comparison purposes, as the corrected curves lower the uncorrected $g(N_2)_N^0$ curves.

B. THE RADIOLYSIS OF LIQUID NITROUS OXIDE

2 g samples of liquid nitrous oxide were contained in 2.5 ml Pyrex bulbs and irradiated to a dose of 2.5×10^{18} eV/g. The products were nitrogen, oxygen and nitrogen dioxide, and their respective G values are given in Table III-1. These results are in good agreement with a previous study (55).

C. ADDITIVE STUDIES

Over thirty compounds were used as additives, so it

TABLE III-1

G Values for the Radiolysis of Liquid Nitrous Oxide at -90°C

Product	G Value
Nitrogen	13.1 ± 0.2
Oxygen	2.7 ± 0.1
Nitrogen Dioxide	5.6 ± 0.2

is convenient to classify the compounds into groups, as far as possible, according to their common properties. Great care was taken during the additive studies to select suitable irradiation temperatures, thus ensuring homogeneous solutions during radiolysis. The dose used was in the range 2-4 x 10^{18} eV/g, being dependent upon the electron density of the particular additive, and took into account the decay of ^{60}Co.

Three additives namely n-propyl bromide, methyl bromide and methyl iodide, as they contained relatively heavy atoms, were further corrected for dosimetry using the factors calculated by Robinson and Freeman (86).

(a) High Electron Affinity Compounds

Sulphur hexafluoride, carbon dioxide and nitrogen dioxide. Pure nitrogen dioxide was also irradiated to determine the yields of nitrogen and oxygen from that additive.

(b) Alkanes

n-hexane, n-butane, propane and ethane.

(c) Alkenes

1-hexene, 1-butene, propene and ethene.

(d) Halo-compounds

Methyl fluoride, methyl chloride, methyl bromide, methyl iodide, n-propyl bromide, chloroform and carbon tetrachloride.

(e) Oxygen-containing Compounds

Acetone, acetaldehyde, methanol and ethanol.

(f) Alkynes

Acetylene and methyl acetylene.

(g) Cyclo-compounds

Cyclopentane, cyclopentene and cyclopropane.

(h) Miscellaneous

Toluene, 1,3-butadiene and neopentane.

All results are presented in tabular and graphical form, and the temperature recorded is the irradiation temperature.

D. PRODUCT YIELDS

(a) High Electron Affinity Compounds

(i) Sulphur Hexafluoride

The results are presented in Table III-2 and Figure III-1.

In Figure III-1A, the $G(N_2)$ curve decreases steadily with increasing additive concentration. $G(O_2)$ decreases to zero at 0.11 mole fraction of additive. Several samples were irradiated at -45°C, and it is concluded that elevation of temperature has little effect on the product yields.

The $g(N_2)^4_N$ curve decreases initially by about 1 g unit, and then levels out around a value of 10.5 units. The overall decrease is due to preferential scavenging of the electron generated in the nitrous oxide by sulphur hexa-

TABLE III-2

G Values Using Sulphur Hexafluoride as the Additive at -90°C and -45°C

Mole Fraction of Additive	$G(N_2)$	$G(O_2)$	$g(N_2)_N^0$	$g(N_2)_N^4$	$g(N_2)_N^5$
0.007	12.8	1.6	13.1	13.0	13.0
0.03	10.9	0.85	12.0	11.6	11.5
0.039	10.0	0.76	11.3	10.8	10.7
0.114	8.6	0.0	12.1	10.5	10.1
0.169	7.7	0.0	12.7	10.1	9.5
0.238	7.6	0.0	15.2	11.2	10.2
0.365	6.1	0.0	17.3	9.9	8.1
*0.031	12.6	1.8	13.9	13.5	13.4
*0.073	9.8	0.70	12.3	11.3	11.0
*0.117	8.9	0.48	12.7	11.0	10.6
*0.179	7.4	0.0	12.5	9.7	9.0

* Irradiated at -45°C.

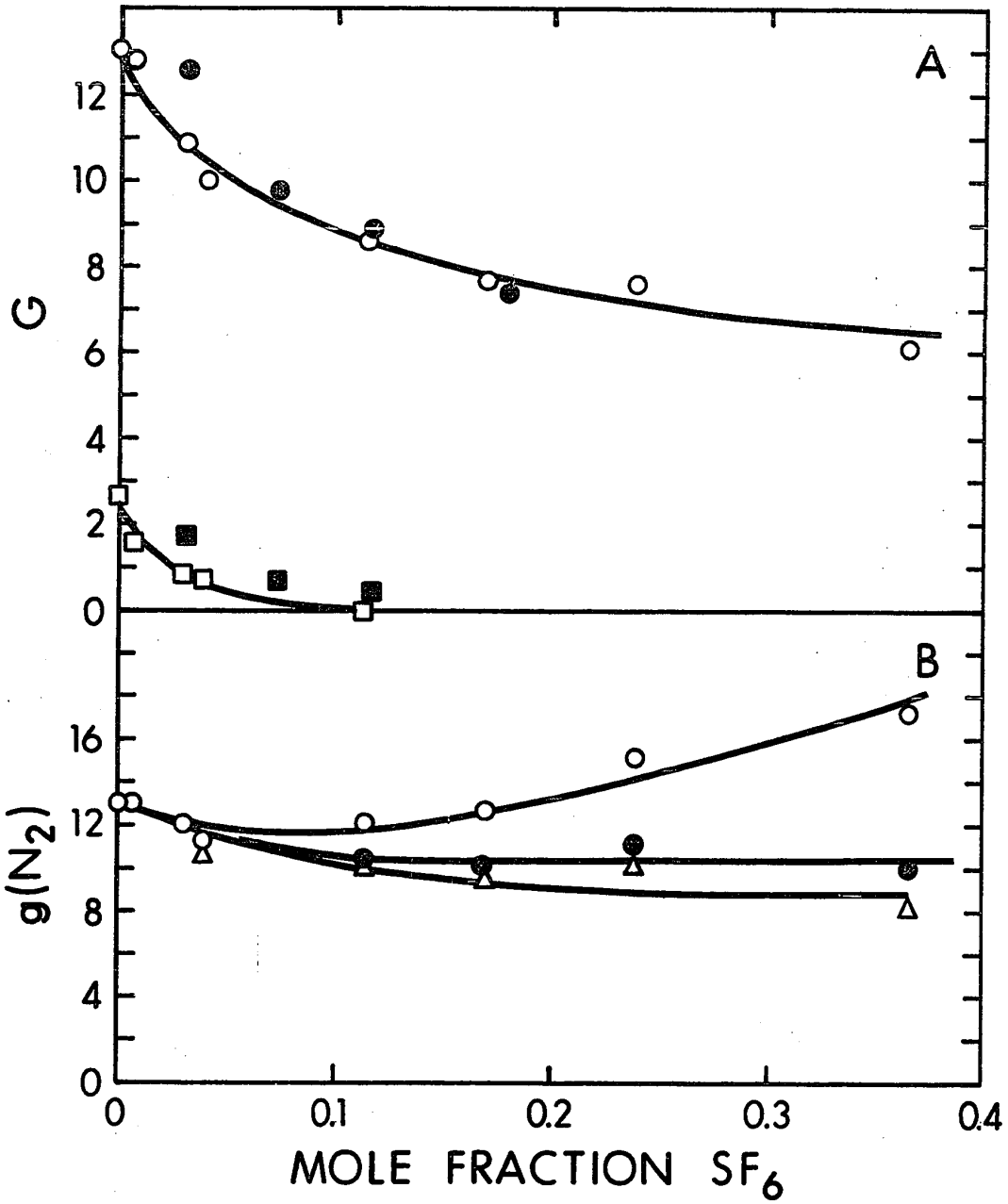

FIGURE III-1 Product Yields Using Sulphur Hexafluoride as the Additive at -90°C and -45°C.

A ○ Nitrogen (at -90°C), ● Nitrogen (at -45°C).
□ Oxygen (at -90°C), ■ Oxygen (at -45°C).

B ○ $g(N_2)^0_N$, ● $g(N_2)^4_N$, Δ $g(N_2)^5_N$.

fluoride, then subsequent neutralisation reactions yielding the observed decrease of 2.6 g units. By employing the correction factors $g(N_2)_N^4$ and $g(N_2)_N^5$, the original values of $g(N_2)_N^0$ are decreased (Figure III-1B).

Nitrogen dioxide was determined using this additive, and the results are expressed in Table III-3 and Figure III-2. The $G(NO_2)$ curve decreases along the concentration range studied.

(ii) Carbon Dioxide

The results are recorded in Table III-4 and Figure III-3, and are comparable with the results obtained using sulphur hexafluoride. In Figure III-3B, the $g(N_2)_N^4$ curve decreases by about 1.5 g units, but the $g(O_2)$ values remain constant over the concentration range used.

(iii) Nitrogen Dioxide

Considerable difficulty was first encountered in removing the impurity, nitrous anhydride N_2O_3, from the nitrogen dioxide gas stream. However, a method was perfected and has been described in the Experimental Section. The results are given in Table III-5 and Figure III-4.

Referring to Figure III-4A, the $G(N_2)$ and $G(O_2)$ values decrease with increasing nitrogen dioxide.

In Figure III-4B, the $g(N_2)_N^0$ curve levels out around a value of 7, showing considerable deviation from the two previous additives. The phenomenum can be rationalised in terms of a lower ionisation potential and higher electron affinity as compared to nitrous oxide. To measure the extent

TABLE III-3

$G(NO_2)$ Using Sulphur Hexafluoride as the Additive at -90°C

Mole Fraction of Additive	$G(NO_2)$	$g(NO_2)$
0.098	5.5	5.6
0.028	4.2	4.6
0.044	3.8	4.4
0.069	3.2	4.0
0.097	2.8	3.8
0.11	2.7	3.8
0.148	2.2	3.4
0.174	2.0	3.3
0.192	1.8	3.2
0.203	1.7	3.1
0.218	1.6	3.0
0.240	1.5	3.0
0.302	1.1	2.6
0.355	0.8	2.2
0.386	0.7	2.1

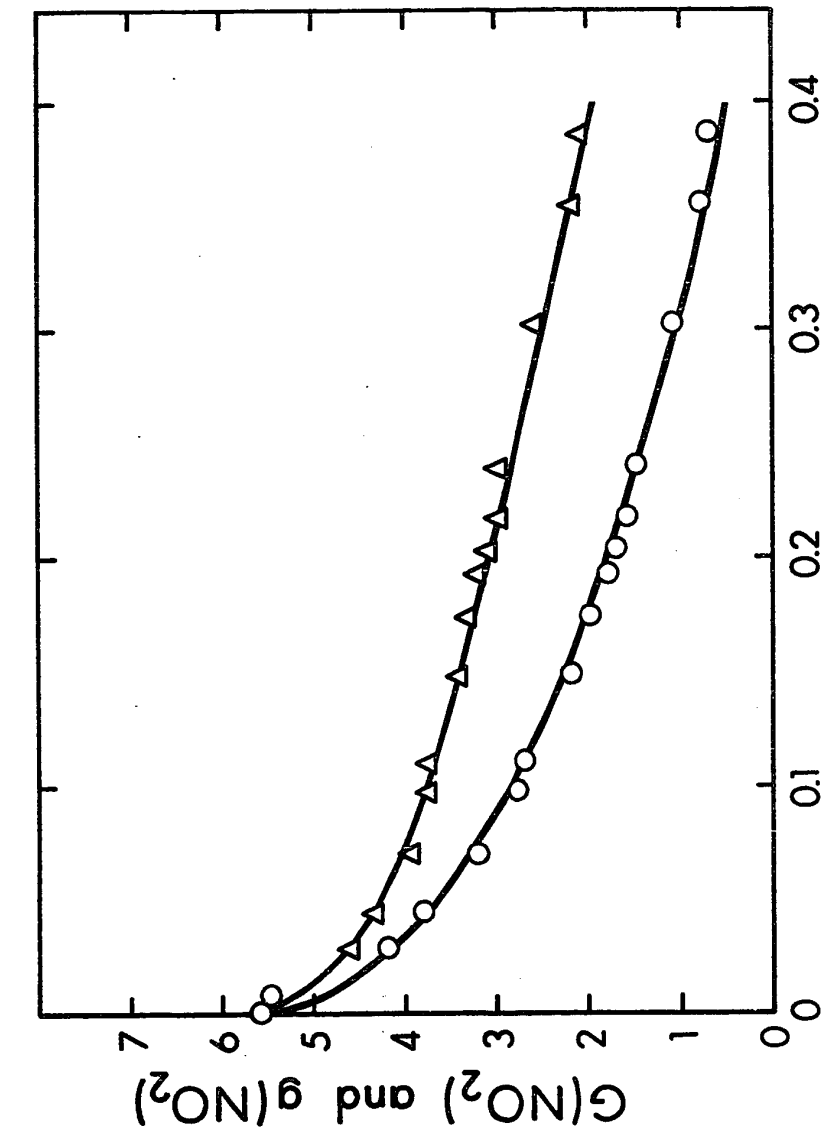

FIGURE III-2 Effect of Sulphur Hexafluoride on the $G(NO_2)$ Yield at -90°C.

O $G(NO_2)$, Δ $g(NO_2)$.

TABLE III-4

G Values Using Carbon Dioxide as the Additive at -47°C

Mole Fraction of Additive	$G(N_2)$	$G(O_2)$	$g(N_2)_N^0$	$g(N_2)_N^4$	$g(N_2)_N^5$	$g(O_2)$
0.020	12.7	2.6	13.0	12.9	12.9	2.6
0.115	10.4	2.3	11.8	11.3	11.1	2.6
0.169	10.7	1.9	12.9	12.1	11.8	2.3
0.233	9.8	1.8	12.8	11.6	11.3	2.4
0.272	9.1	1.6	12.5	11.0	10.6	2.2
0.364	9.3	1.7	14.6	12.3	11.8	2.7

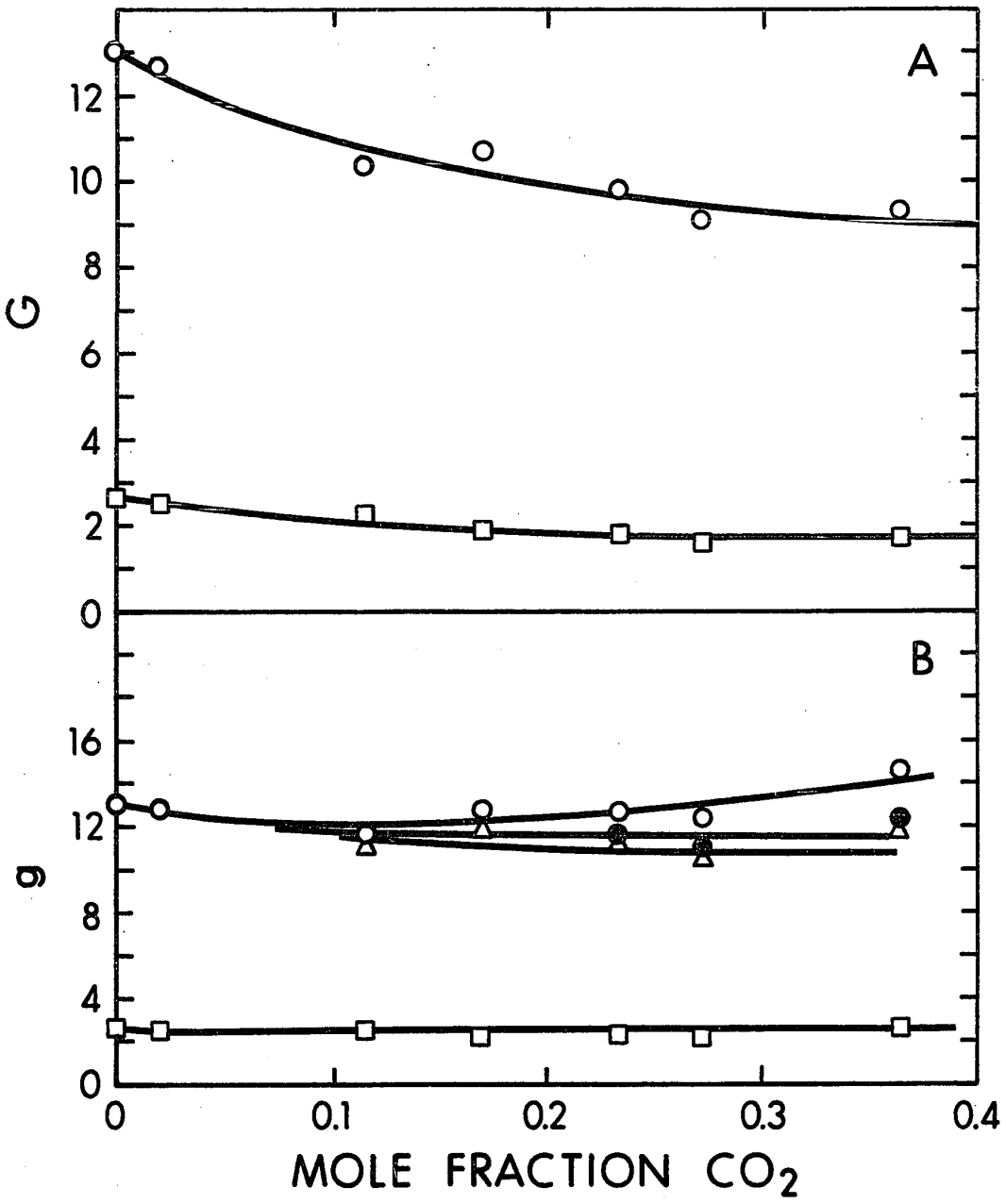

FIGURE III-3 Product Yields with Carbon Dioxide as the Additive at -47°C.

A ○ Nitrogen, □ Oxygen.

B ○ $g(N_2)_N^0$, ● $g(N_2)_N^4$, Δ $g(N_2)_N^5$, □ Oxygen.

TABLE III-5

G Values Using Nitrogen Dioxide as the Additive at -45°C

Mole Fraction of Additive	$G(N_2)$	$G(O_2)$	$g(N_2)_N^0$	$g(N_2)_N^4$	$g(N_2)_N^5$
0.029	10.7	0.66	11.0	10.9	10.9
0.031	9.7	0.60	10.0	9.8	9.8
0.061	8.8	0.45	9.4	9.1	9.0
0.077	7.9	0.25	8.6	8.2	8.1
0.095	7.1	0.0	7.9	7.4	7.3
0.117	7.0	0.0	8.0	7.4	7.3
0.146	6.6	0.0	7.8	7.0	6.9
0.153	6.2	0.0	7.4	6.6	6.3
0.182	5.6	0.0	6.9	6.0	5.7

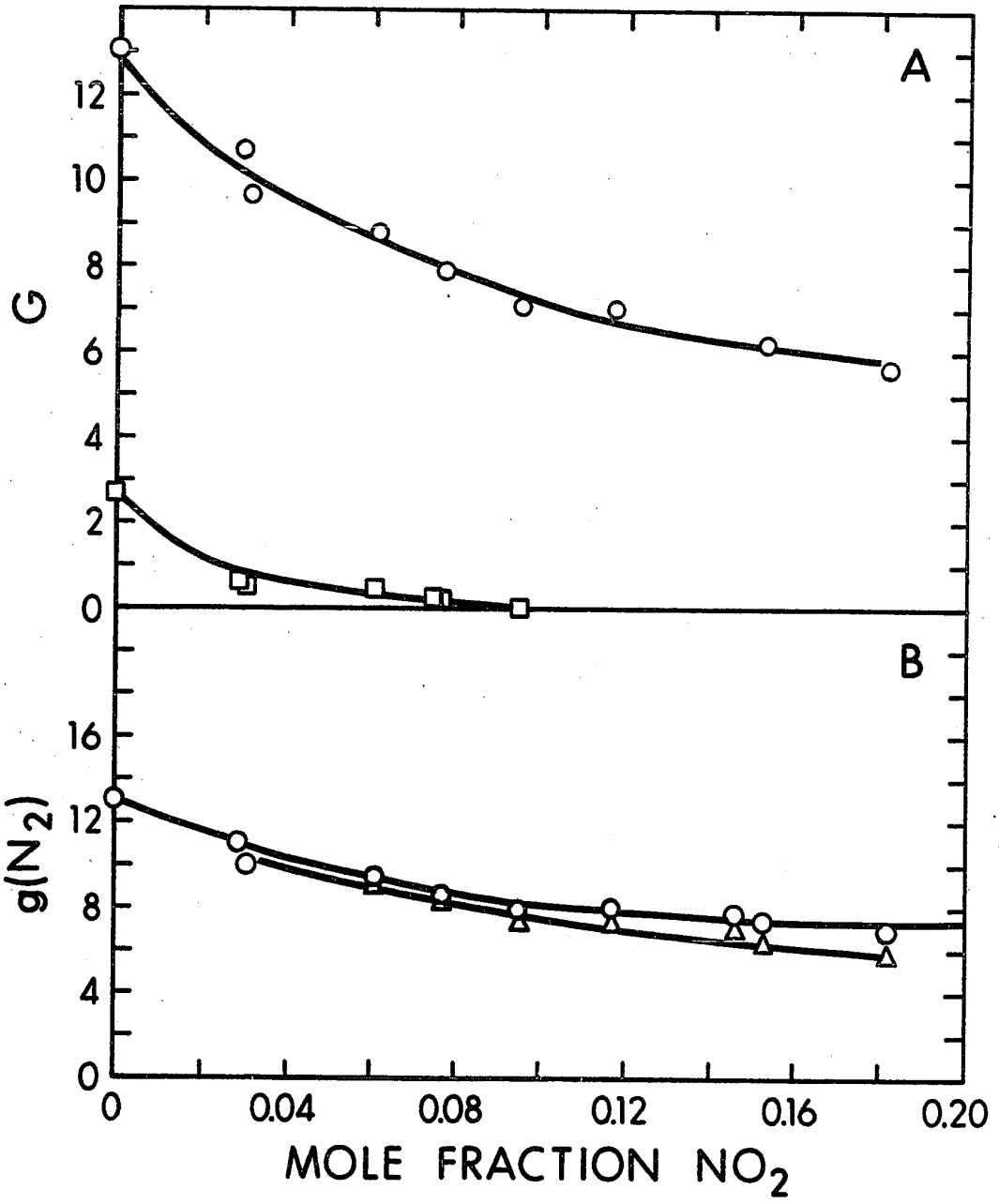

FIGURE III-4 Product Yields with Nitrogen Dioxide as the Additive at -45°C.

A ○ Nitrogen, □ Oxygen.

B ○ $g(N_2)_N^0$, △ $g(N_2)_N^5$.

of the nitrogen contribution from pure nitrogen dioxide it was necessary to carry out the radiolysis of pure nitrogen dioxide. Only extremely small yields of nitrogen and oxygen were obtained, $G(N_2) < 0.1$ and $G(O_2) < 0.1$, so a self-perpetuating reaction is thought to occur. These results concur with those obtained by photochemical studies (89,90).

(b) Alkanes

(i) n-Hexane

The results are presented in Table III-6 and Figure III-5.

In Figure III-5A, $G(O_2)$ decreases to zero at 0.07 mole fraction of additive. $G(H_2)$ decreases rapidly with increasing nitrous oxide concentration. This is due to the electron released by the hexane during radiolysis being scavenged by the nitrous oxide (75). Referring to Figure III-5B, the $g(N_2)_N^5$ curve remains fairly constant over the concentration range.

The $g(H_2)$ value for pure n-hexane is 5.0, and the $g(H_2)$ curve levels off around a value of 1.4. This plateau is due to residual unscavengeable hydrogen (91). No nitrogen dioxide was observed after a 0.06 mole fraction addition of n-hexane. These results are displayed in Table III-7 and Figure III-6A.

(ii) n-Butane

The results are recorded in Table III-8 and Figure III-7,

TABLE III-6

G Values Using n-Hexane as the Additive at -90°C

Mole Fraction of Additive	$G(N_2)$	$G(O_2)$	$G(H_2)$	$g(N_2)_N^0$	$g(N_2)_N^4$	$g(N_2)_N^5$	$g(H_2)$
0.010	13.0	1.9	0.0	13.3	13.2	13.2	0.0
0.019	12.1	0.57	0.0	12.6	12.5	12.4	0.0
0.029	11.5	0.50	0.0	12.3	12.0	11.9	0.0
0.058	11.0	0.0	0.0	12.5	12.0	11.8	0.0
0.099	10.4	0.0	0.0	12.9	11.9	11.7	0.0
0.200	8.8	0.0	0.0	13.6	11.4	10.9	0.0
0.221	8.7	0.0	0.54	14.1	11.6	11.0	1.4
0.359	7.8	0.0	0.67	17.2	12.3	11.1	1.2
0.473	6.9	0.0	0.92	20.4	12.6	10.6	1.4
0.588	6.9	0.0	1.3	28.	15.8	12.7	1.6
0.901	5.6	0.0	1.5	116.	36.	16.5	1.6
0.948	5.2	0.0	1.9	212.	53.	13.6	1.9
0.990	4.6	0.0	2.7	996.	132.	(-84.)	2.7
1.000	0.0	0.0	5.0	0.0	0.0	0.0	5.0

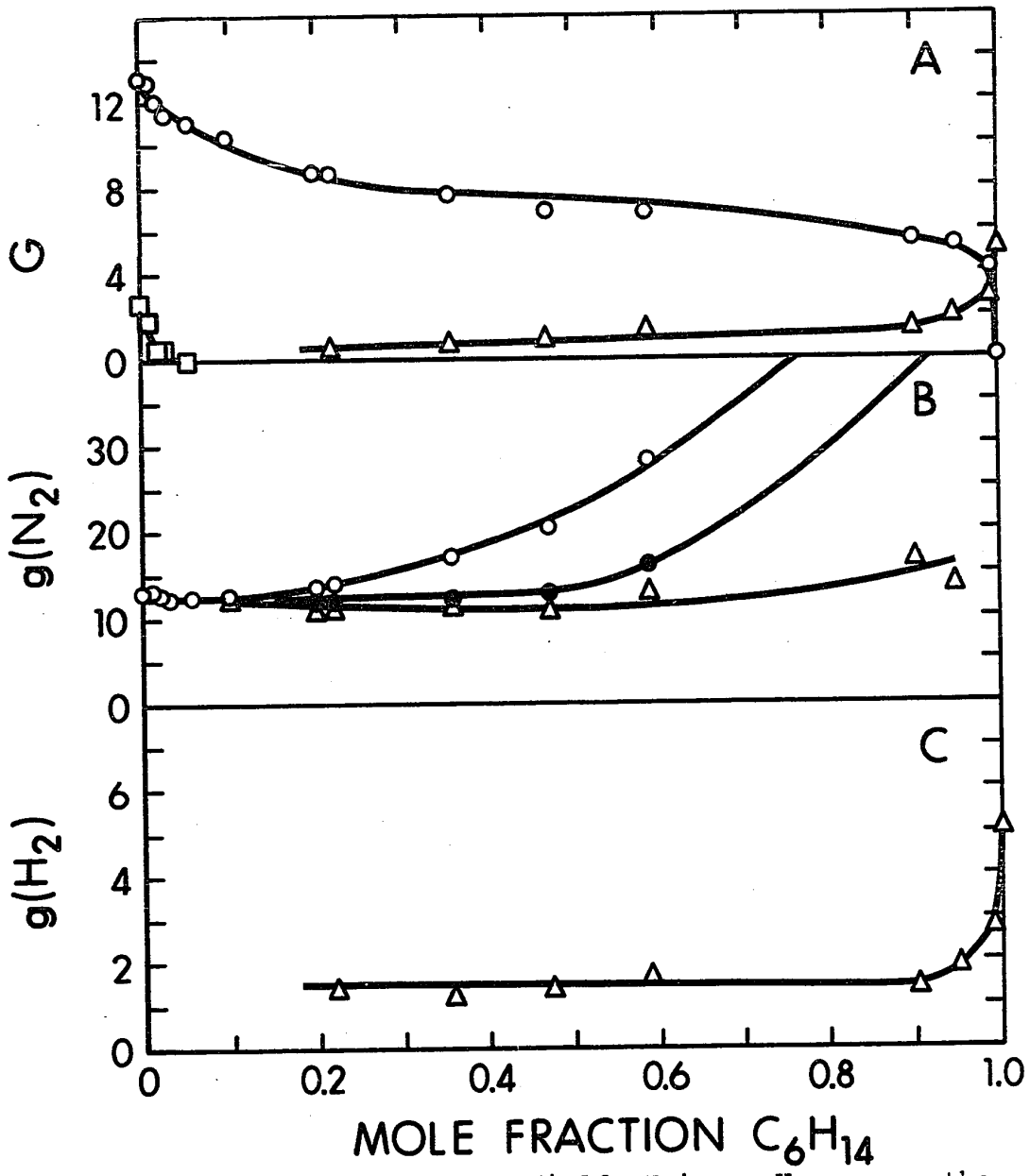

FIGURE III-5 Product Yields Using n-Hexane as the Additive at -90°C.

A	O Nitrogen,	□ Oxygen,		Δ Hydrogen.
B	O $g(N_2)_N^0$,	● $g(N_2)_N^4$,		Δ $g(N_2)_N^5$.
C	Δ Hydrogen.			

TABLE III-7

G Values of Nitrogen Dixoide Using Alkanes as the Additives at -90°C

Mole Fraction of n-Hexane	$G(NO_2)$	Mole Fraction of n-Butane	$G(NO_2)$	Mole Fraction of Ethane	$G(NO_2)$
0.000	5.6	0.000	5.6	0.000	5.6
0.005	3.9	0.015	1.6	0.040	0.7
0.008	1.9	0.035	0.9	0.073	0.0
0.013	1.4	0.083	0.0		
0.042	0.6				
0.061	0.0				

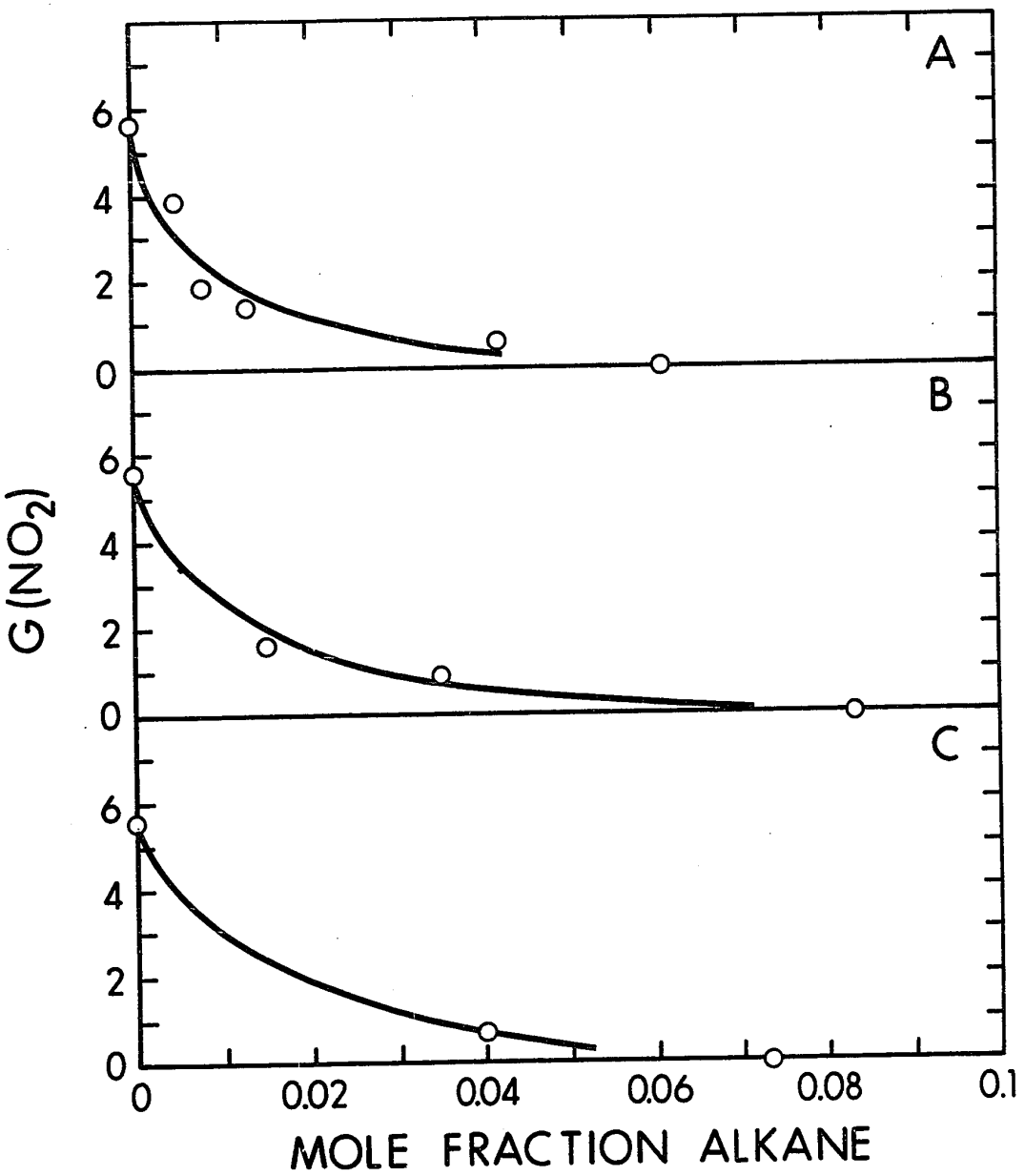

FIGURE III-6 Effect of the Alkanes on the $G(NO_2)$ Yield at -90°C.

A Using n-hexane , O Nitrogen Dioxide .

B Using n-butane , O Nitrogen Dioxide .

C Using ethane , O Nitrogen Dioxide .

TABLE III-8

G Values Using n-Butane as the Additive at -90°C

Mole Fraction of Additive	$G(N_2)$	$G(O_2)$	$G(H_2)$	$g(N_2)_N^0$	$g(N_2)_N^4$	$g(N_2)_N^5$	$g(H_2)$
0.018	13.0	1.5	0.0	13.4	13.3	13.3	0.0
0.067	11.3	0.0	0.0	12.5	12.1	12.0	0.0
0.187	9.7	0.0	0.0	13.2	11.8	11.4	0.0
0.208	9.6	0.0	0.20	13.5	11.9	11.5	0.69
0.229	8.5	0.0	0.30	12.4	10.6	10.1	0.95
0.451	8.0	0.0	0.60	18.0	13.0	11.7	1.1
0.538	7.1	0.0	1.0	20.0	12.8	11.0	1.6
0.599	7.3	0.0	0.94	24.	14.8	12.5	1.3
0.704	7.5	0.0	1.5	35.	20.4	16.7	1.9
0.800	5.9	0.0	1.3	42.	17.7	11.5	1.5
0.897	5.7	0.0	1.8	83.	29.	15.3	1.9
0.947	5.0	0.0	2.7	143.	33.	5.3	2.8
0.984	4.4	0.0	3.3	425.	44.	(-5.1)	3.3
1.000	0.0	0.0	5.4	0.0	0.0	0.0	5.4

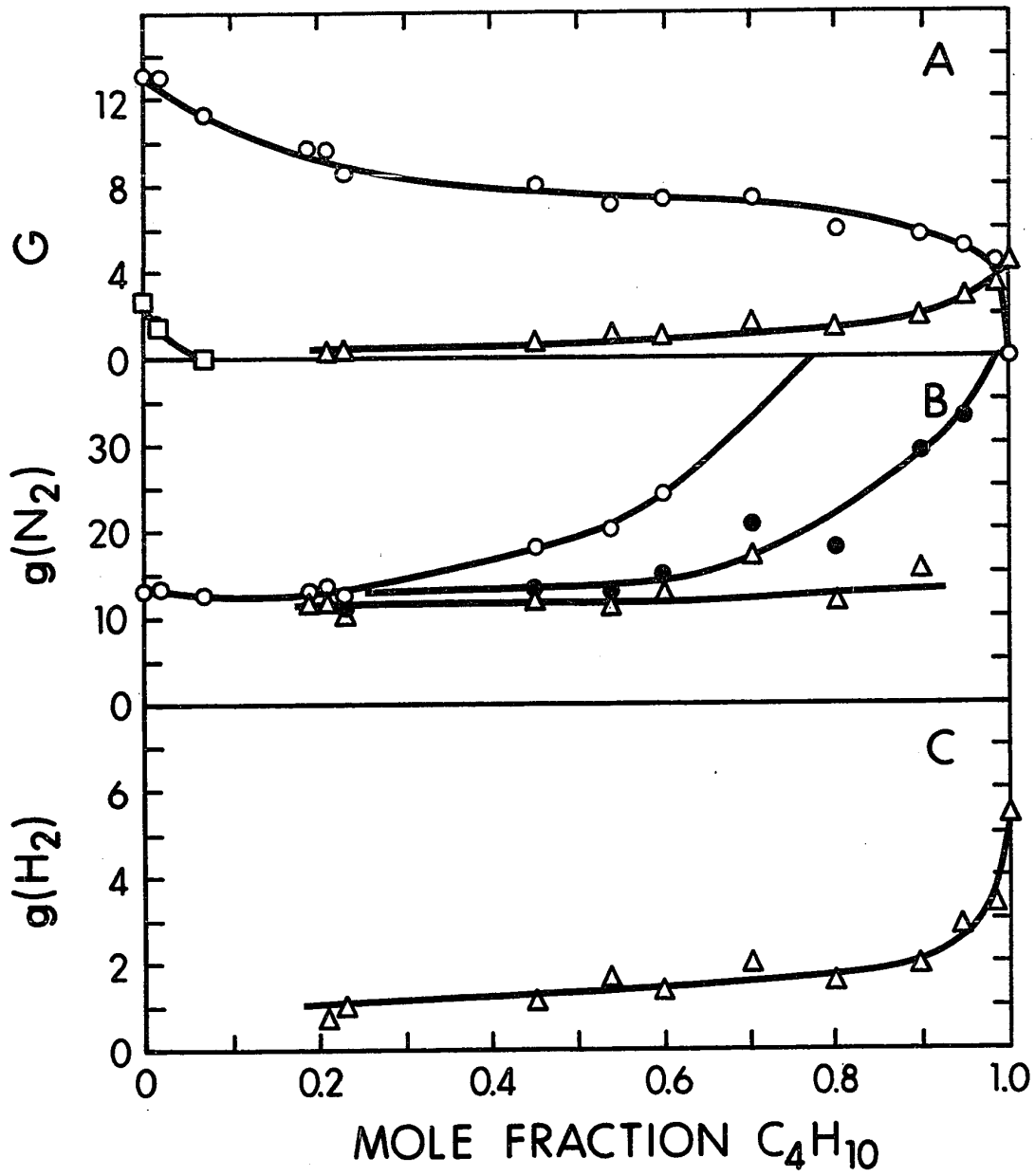

FIGURE III-7 Product Yields with n-Butane as the Additive at -90°C.

A ○ Nitrogen, □ Oxygen, △ Hydrogen.

B ○ $g(N_2)^0_N$, ● $g(N_2)^4_N$, △ $g(N_2)^5_N$.

C △ Hydrogen .

and the trends are similar to those of n-hexane.

$G(O_2)$ decreases to zero at 0.08 mole fraction of additive (Figure III-7A).

The $g(N_2)^5_N$ curve again remains quite constant up to 0.90 mole fraction (Figure III-7B).

In Figure III-7C, the $g(H_2)$ curve shows a plateau around 1.5 and equals 5.4 for the pure n-butane.

The $G(NO_2)$ curve decreases rapidly with small additions of n-butane (Figure III-6B).

(iii) Propane

The results are given in Table III-9 and Figure III-8.

In Figure III-8A, the $G(N_2)$ and $G(O_2)$ curves are similar to those of the other alkanes. At a propane concentration of 0.90 mole fraction, methane was detected.

The g values of hydrogen and methane for the pure additive are 4.3 and 0.47 respectively (Figure III-8C).

(iv) Ethane

The results are displayed in Table III-10 and Figure III-9.

In Figure III-9A, the $G(N_2)$ curve differs from those for the previous alkanes in that even at a high ethane value of 0.99 mole fraction, the $G(N_2)$ result is 5.2, which is unusually high. Methane was observed at a concentration of 0.77 mole fraction of ethane.

The $g(N_2)^5_N$ curve is uniform along the concentration range (Figure III-9B).

TABLE III-9

G Values Using Propane as the Additive at -90°C

Mole Fraction of Additive	$G(N_2)$	$G(O_2)$	$G(H_2)$	$G(CH_4)$	$g(N_2)_N^0$	$g(N_2)_N^4$	$g(N_2)_N^5$	$g(H_2)$	$g(CH_4)$
0.019	12.9	1.1	0.0	0.0	13.2	13.1	13.1	0.0	0.0
0.087	11.2	0.0	0.0	0.0	12.5	12.0	11.9	0.0	0.0
0.105	10.8	0.0	0.0	0.0	12.3	11.7	11.6	0.0	0.0
0.255	9.8	0.0	0.20	0.0	13.7	12.1	11.7	0.69	0.0
0.277	9.3	0.0	0.50	0.0	13.4	11.6	11.2	1.6	0.0
0.329	9.2	0.0	0.40	0.0	14.6	12.2	11.7	1.1	0.0
0.613	7.3	0.0	1.1	0.0	21.1	13.6	11.7	1.7	0.0
0.715	7.0	0.0	0.98	0.0	28.	16.0	13.0	1.3	0.0
0.800	7.0	0.0	1.1	0.0	40.	21.0	16.2	1.3	0.0
0.849	6.8	0.0	1.4	0.0	52.	25.	18.5	1.6	0.0
0.898	6.5	0.0	1.5	0.12	74.	33.	22.2	1.6	0.13
0.949	5.5	0.0	1.8	0.20	127.	39.	17.4	1.9	0.21
0.988	4.8	0.0	2.2	0.30	472.	83.	(-14.7)	2.2	0.30
1.000	0.0	0.0	4.3	0.47	0.0	0.0	0.0	4.3	0.47

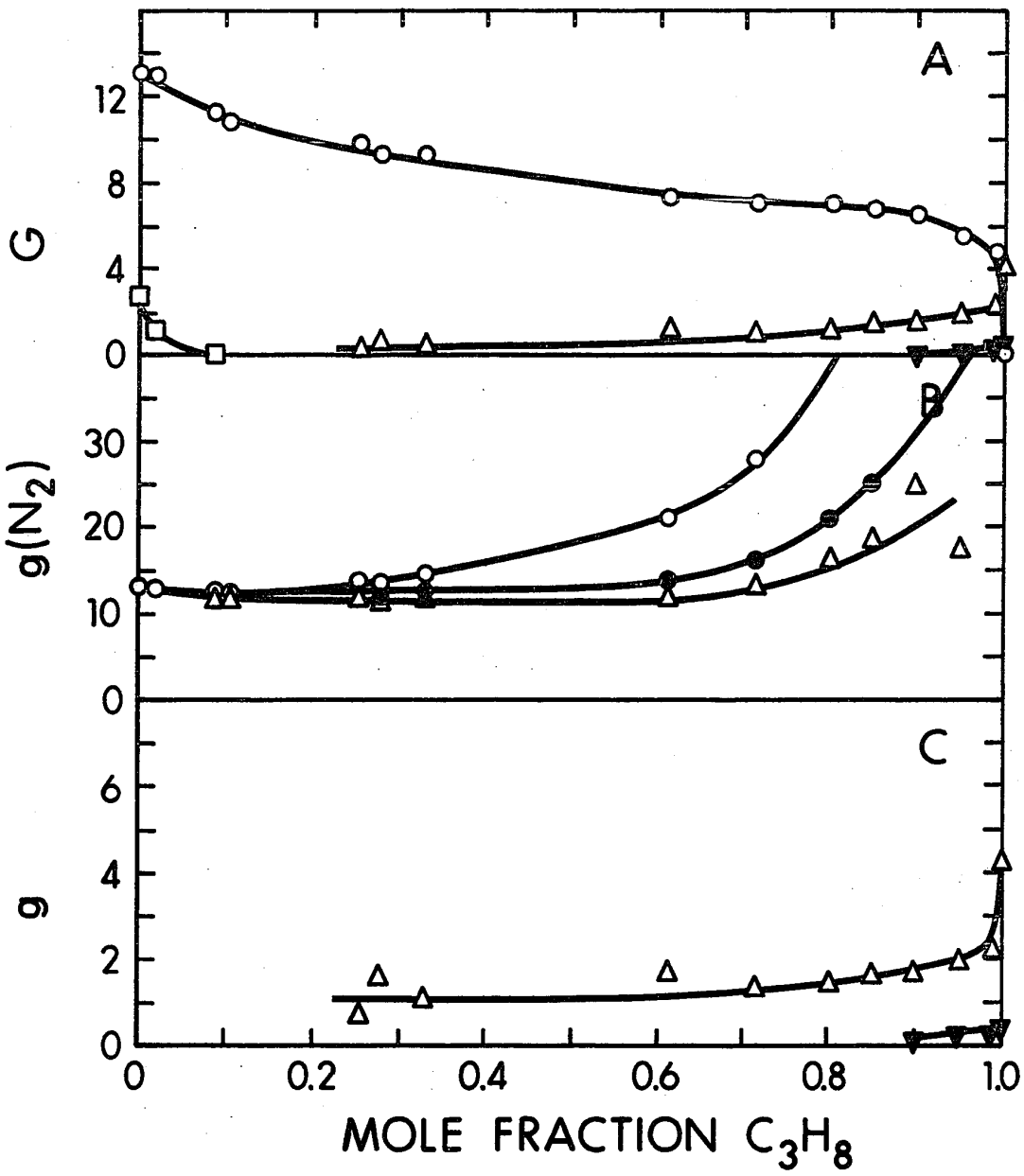

FIGURE III-8 Product Yields with Propane as the Additive at -90°C.

A ○ Nitrogen, □ Oxygen, Δ Hydrogen, ▼ Methane.

B ○ $g(N_2)_N^0$, ● $g(N_2)_N^4$, Δ $g(N_2)_N^5$.

C Δ Hydrogen, ▼ Methane.

TABLE III-10

G Values Using Ethane as the Additive at -90°C

Mole Fraction of Additive	$G(N_2)$	$G(O_2)$	$G(H_2)$	$G(CH_4)$	$g(N_2)_N^0$	$g(N_2)_N^4$	$g(N_2)_N^5$	$g(H_2)$	$g(CH_4)$
0.016	12.9	1.4	0.0	0.0	13.1	13.0	13.0	0.0	0.0
0.045	11.8	0.50	0.0	0.0	12.3	12.1	12.1	0.0	0.0
0.064	11.8	0.0	0.0	0.0	12.4	12.2	12.2	0.0	0.0
0.118	10.9	0.0	0.0	0.0	12.1	11.7	11.6	0.0	0.0
0.162	10.1	0.0	0.30	0.0	11.6	11.0	10.8	2.2	0.0
0.210	8.9	0.0	0.45	0.0	10.8	10.0	9.8	2.5	0.0
0.377	7.7	0.0	0.70	0.0	11.5	9.5	9.0	2.1	0.0
0.635	6.8	0.0	1.0	0.0	16.4	10.7	9.3	1.7	0.0
0.771	6.8	0.0	1.5	0.15	25.	14.4	11.6	2.1	0.20
0.808	6.2	0.0	1.8	0.20	28.	13.7	10.3	2.3	0.26
0.853	5.6	0.0	1.5	0.28	32.	12.9	8.2	1.8	0.34
0.906	5.4	0.0	1.9	0.40	48.	16.4	8.6	2.2	0.45
0.953	5.3	0.0	2.5	0.35	93.	26.	9.6	2.7	0.37
0.992	5.2	0.0	3.2	0.40	534.	128.	27.	3.2	0.40
1.000	0.0	0.0	4.8	0.35	0.0	0.0	0.0	4.8	0.35

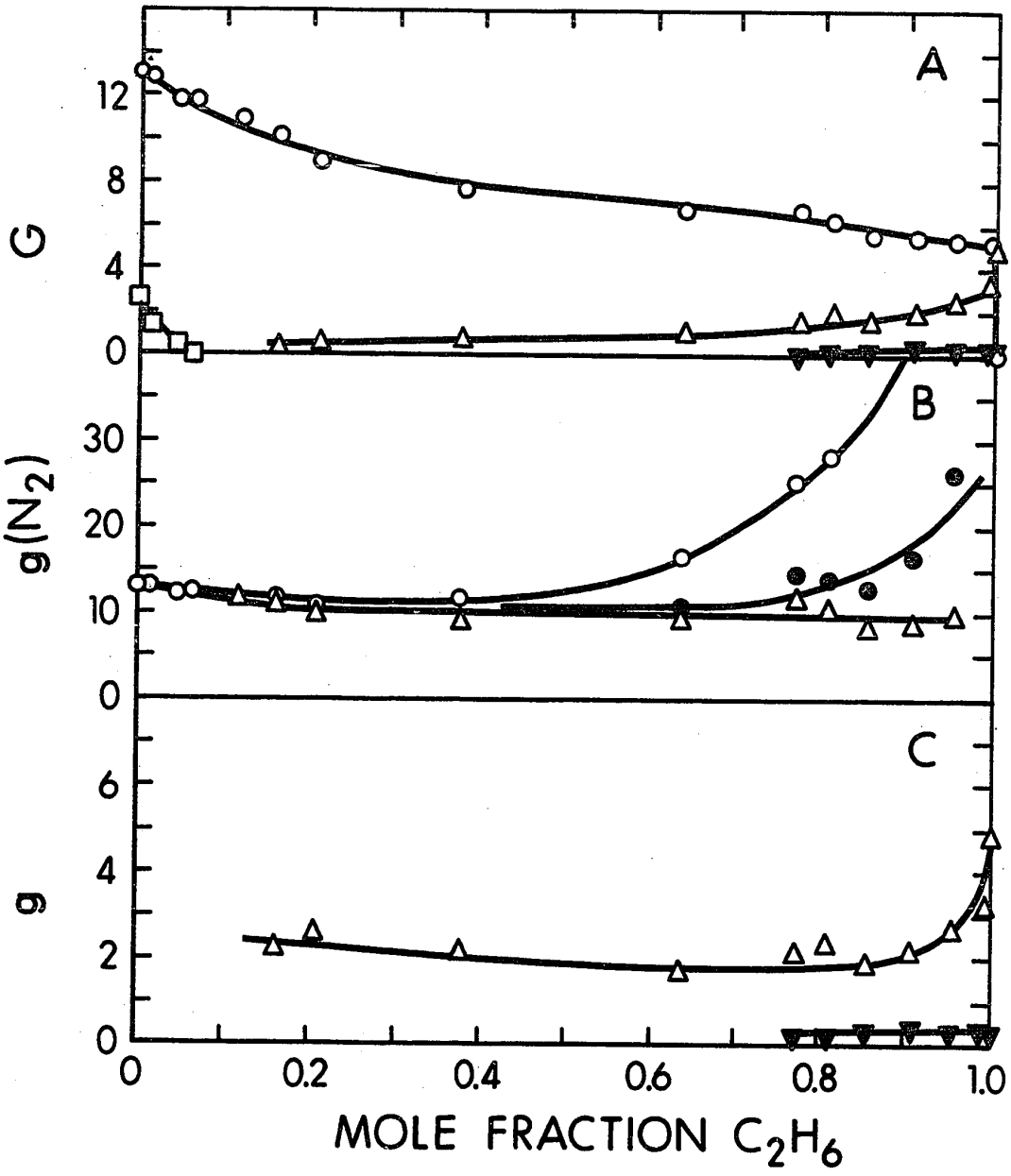

FIGURE III-9 Product Yields with Ethane as the Additive at -90°C.

A O Nitrogen, □ Oxygen, Δ Hydrogen, ▼ Methane.

B O $g(N_2)_N^0$, ● $g(N_2)_N^4$, Δ $g(N_2)_N^5$.

C Δ Hydrogen, ▼ Methane.

In Figure III-9C, the $g(H_2)$ curve increases sharply at high ethane concentrations giving a value of 4.8 for pure ethane. $g(CH_4)$ for the pure compound is 0.35.

The $G(NO_2)$ results (Figure III-6C) concur with those for the other alkanes, and no nitrogen dioxide was detected at 0.07 mole fraction addition of ethane.

(c) Alkenes

(i) 1-Hexene

The results are given in Table III-11 and Figure III-10.

It is generally accepted that the nitrous oxide scavenging efficiency for electrons is lower in alkenes than in alkanes (65). Therefore, the $G(N_2)$ curves for the alkenes are expected to be lower than those for the corresponding alkanes. The results obtained confirm these observations.

In Figure III-10B, the $g(N_2)_N^5$ curve remains constant, whilst the $g(N_2)_N^4$ curve increases at high concentrations of 1-hexene.

Referring to Figure III-10C, the $g(H_2)$ curve is constant along the concentration range, and equalling 0.8 for pure 1-hexene.

Nitrogen dioxide was determined, and the results are given in Table III-12 and Figure III-11A. A rapid decrease in the $G(NO_2)$ curve occurs upon the addition of a few mole % of the additive.

TABLE III-11

G Values Using 1-Hexene as the Additive at -90°C

Mole Fraction of Additive	$G(N_2)$	$G(O_2)$	$G(H_2)$	$g(N_2)_N^0$	$g(N_2)_N^4$	$g(N_2)_N^5$	$g(H_2)$
0.009	11.7	1.1	0.0	11.9	11.8	11.8	0.0
0.050	10.1	0.1	0.0	11.2	10.7	10.6	0.0
0.100	9.1	0.0	0.0	11.2	10.3	10.1	0.0
0.145	8.6	0.0	0.0	11.7	10.3	9.9	0.0
0.269	6.3	0.0	0.43	11.1	8.0	7.2	0.99
0.450	6.2	0.0	0.42	16.9	10.1	8.4	0.67
0.700	5.8	0.0	0.60	34.	14.6	9.7	0.72
0.805	5.3	0.0	0.64	51.	16.7	8.1	0.71
0.902	4.8	0.0	0.74	97.	19.6	0.34	0.78
0.949	3.8	0.0	0.76	153.	(-2.8)	(-42.)	0.78
0.989	2.9	0.0	0.75	546.	(-212.)	(-402.)	0.75
1.000	0.0	0.0	0.80	0.0	0.0	0.0	0.80

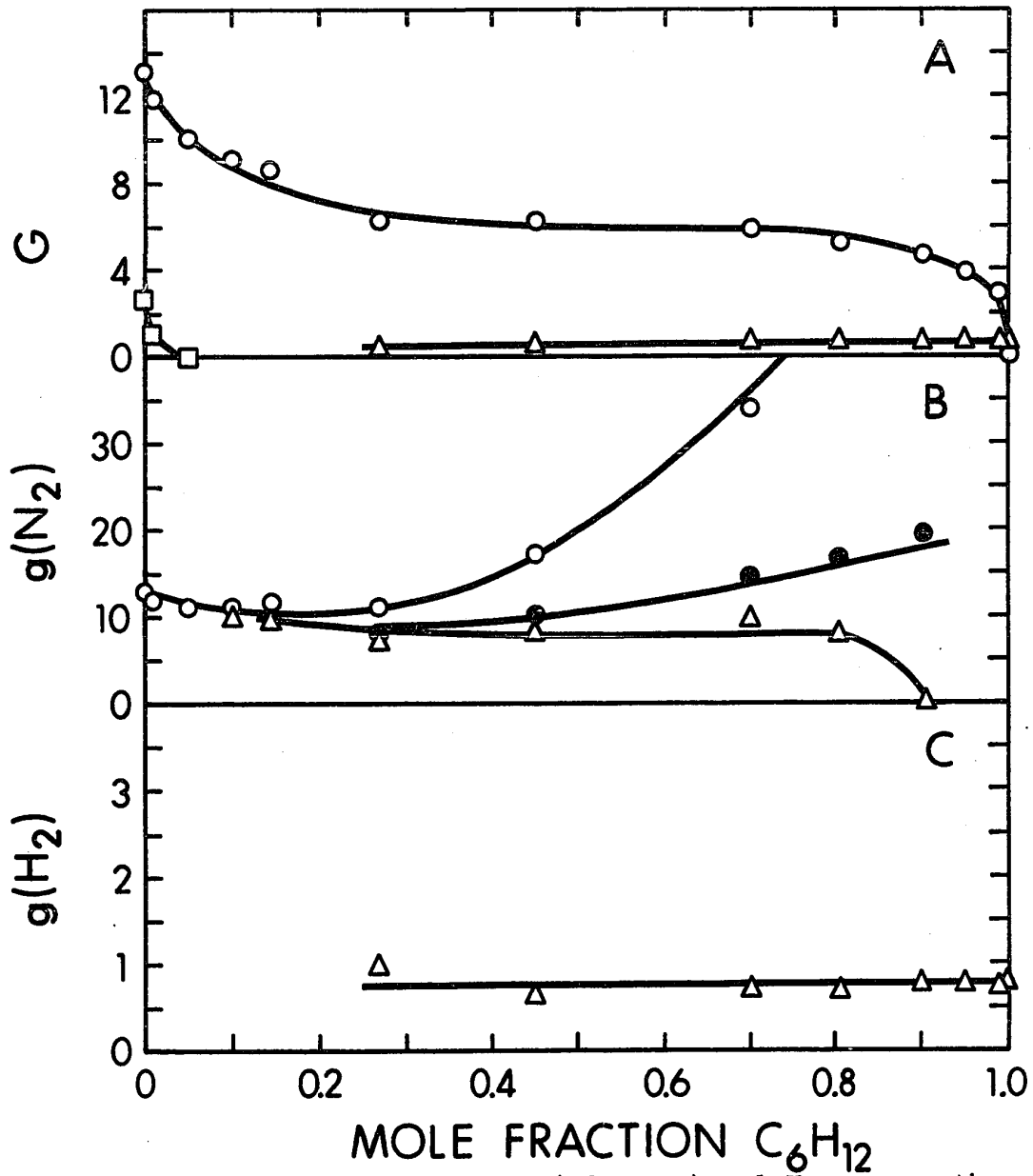

FIGURE III-10 Product Yields Using 1-Hexene as the Additive at -90°C.

A ○ Nitrogen, □ Oxygen, △ Hydrogen.

B ○ $g(N_2)_N^0$, ● $g(N_2)_N^4$, △ $g(N_2)_N^5$.

C △ Hydrogen.

TABLE III-12

G Values of Nitrogen Dioxide Using Alkenes as the Additives at -90°C

Mole Fraction of 1-Hexene	$G(NO_2)$	Mole Fraction of 1-Butene	$G(NO_2)$	Mole Fraction of Ethene	$G(NO_2)$
0.000	5.6	0.000	5.6	0.000	5.6
0.007	2.5	0.017	0.9	0.020	0.6
0.011	1.1	0.041	0.0	0.056	0.0
0.039	0.4				
0.068	0.0				

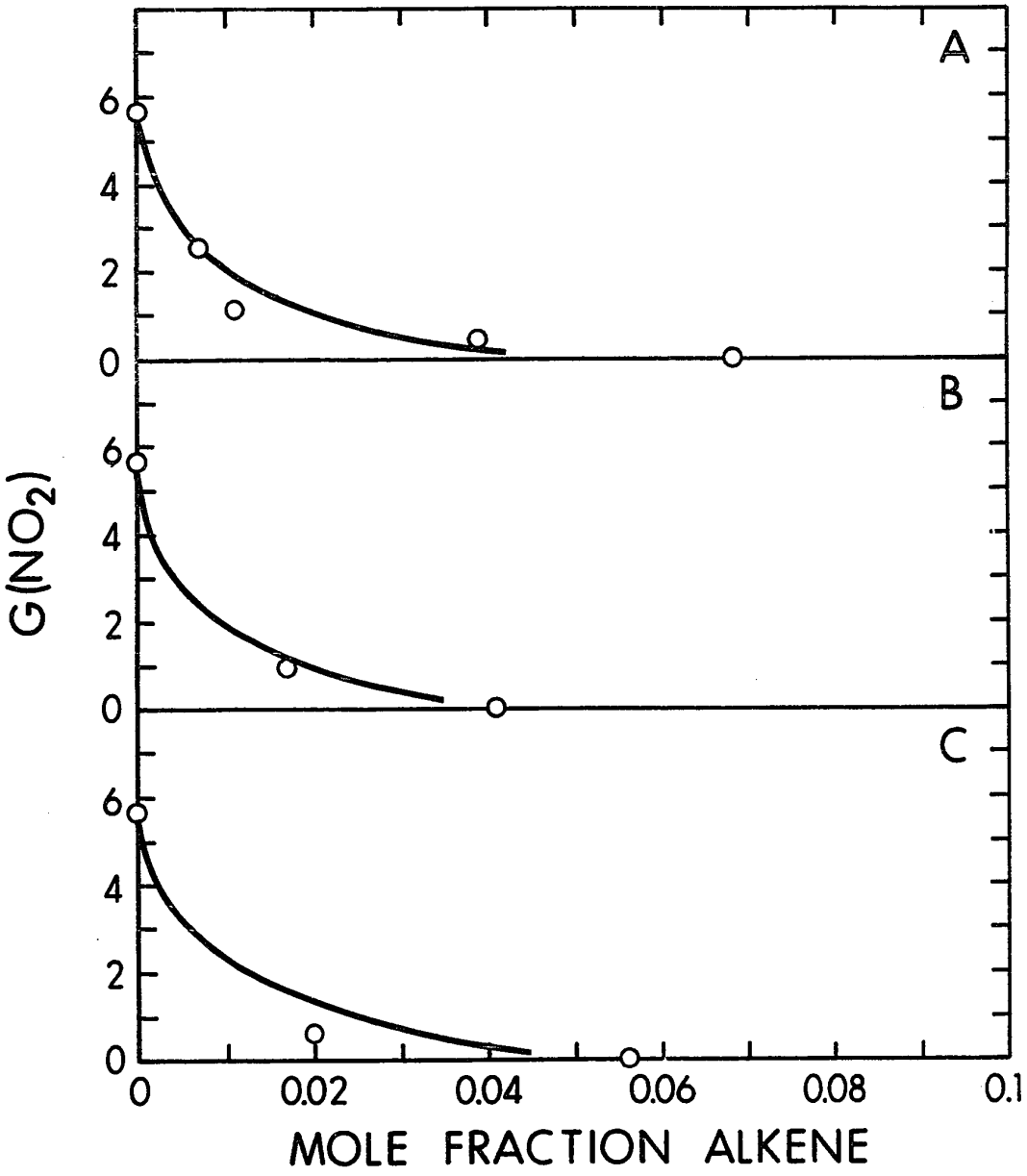

FIGURE III-11 Effect of the Alkenes on the $G(NO_2)$ Yield at -90°C.

A Using 1-hexene, O Nitrogen Dioxide.

B Using 1-butene, O Nitrogen Dioxide.

C Using ethene, O Nitrogen Dioxide.

(ii) 1-Butene

The results are presented in Table III-13 and Figure III-12, and are similar to those obtained for 1-hexene.

$G(O_2)$ in Figure III-12A, decreases to zero at a 0.06 mole fraction addition, and no nitrogen dioxide was detected after a 1-butene addition of 0.04 mole fraction. In Figure III-12B the $g(N_2)_N^4$ curve remains fairly constant along the concentration range. The $g(H_2)$ curve (Figure III-12C) shows little change with increasing additive concentration, yielding a value of 0.90 for the pure 1-butene.

(iii) Propene

The results are reported in Table III-14 and Figure III-13. The $G(N_2)$ curve decreases with increasing concentration of propene (Figure III-13A). In Figure III-13B, both correction curves decrease at high concentrations of additive. Referring to Figure III-13C, the $g(H_2)$ value for pure propene is 0.1

(iv) Ethene

The results are given in Table III-15 and Figure III-14. In Figure III-14B, the $g(N_2)_N^4$ curve affords the best plateau. In Figure III-14C, $g(H_2)$ for pure ethene is 1.2.

(d) Halo-compounds

(i) Methyl fluoride

The results are presented in Table III-16 and Figure III-15.

The $G(N_2)$ curve in Figure III-15A decreases slowly

TABLE III-13

G Values Using 1-Butene as the Additive at -90°C

Mole Fraction of Additive	$G(N_2)$	$G(O_2)$	$G(H_2)$	$g(N_2)^0_N$	$g(N_2)^4_N$	$g(N_2)^5_N$	$g(H_2)$
0.015	13.0	0.54	0.0	13.3	13.2	13.2	0.0
0.061	10.7	0.0	0.0	11.7	11.3	11.2	0.0
0.163	9.0	0.0	0.0	11.6	10.5	10.2	0.0
0.198	8.4	0.0	0.0	11.4	10.0	9.7	0.0
0.206	9.1	0.0	0.0	12.5	11.0	10.6	0.0
0.272	8.2	0.0	0.38	12.7	10.5	9.9	1.1
0.574	6.5	0.0	0.50	19.2	11.3	9.4	0.76
0.721	5.6	0.0	0.59	26.	11.4	7.7	0.75
0.804	5.7	0.0	0.52	39.	15.6	9.6	0.61
0.860	5.0	0.0	0.62	49.	13.4	4.5	0.69
0.906	5.0	0.0	0.70	75.	18.9	4.9	0.75
0.952	3.4	0.0	0.80	103.	(-12.7)	(-42.)	0.83
0.985	2.7	0.0	0.76	261.	(-122.)	(-217.)	0.77
1.000	0.0	0.0	0.90	0.0	0.0	0.0	0.90

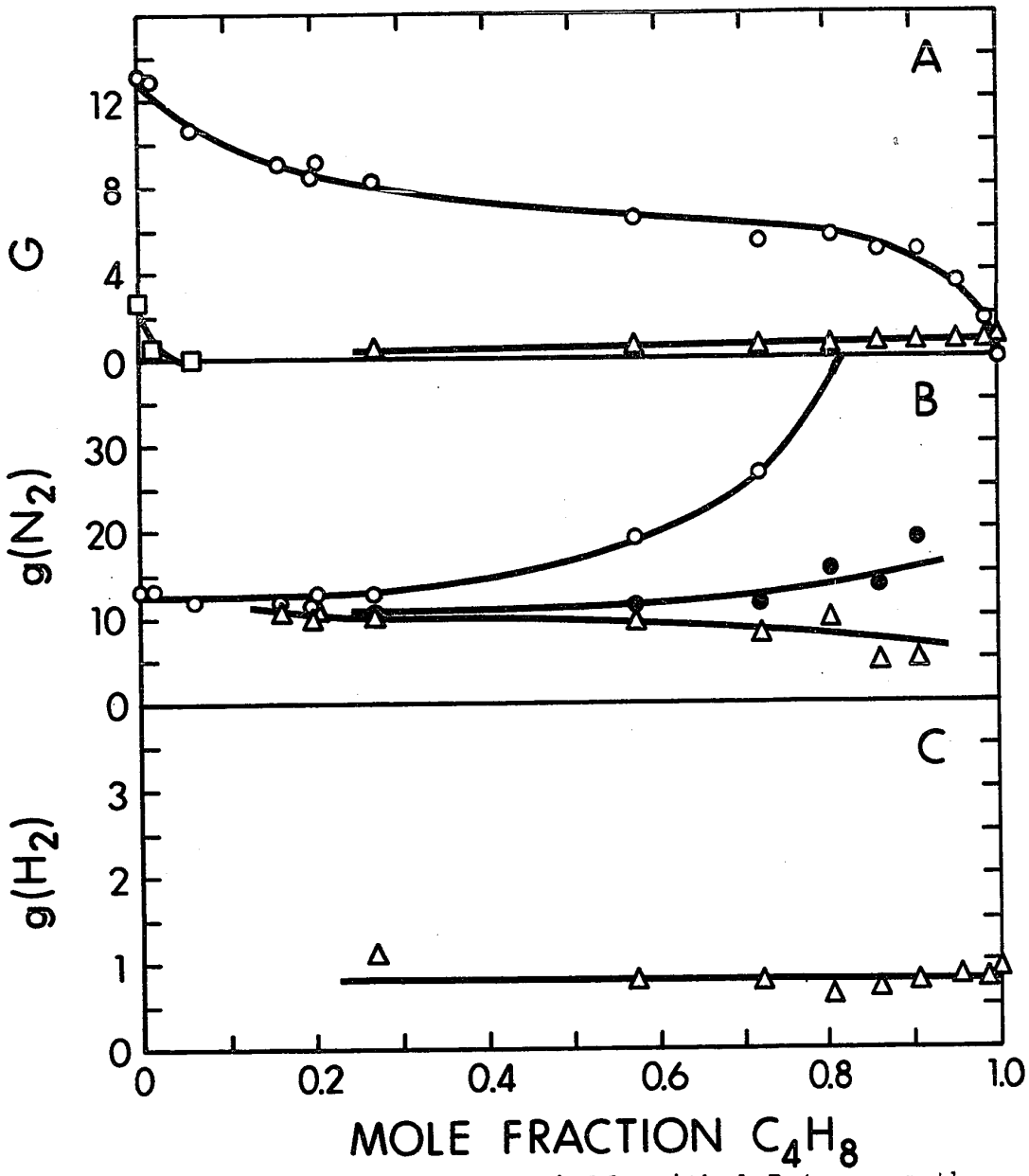

FIGURE III-12 Product Yields with 1-Butene as the Additive at -90°C.

A ○ Nitrogen, □ Oxygen, △ Hydrogen.

B ○ $g(N_2)_N^0$, ● $g(N_2)_N^4$, △ $g(N_2)_N^5$.

C △ Hydrogen.

TABLE III-14

G Values Using Propene as the Additive at -90°C

Mole Fraction of Additive	$G(N_2)$	$G(O_2)$	$G(H_2)$	$g(N_2)_N^0$	$g(N_2)_N^4$	$g(N_2)_N^5$	$g(H_2)$
0.009	11.6	1.0	0.0	11.7	11.7	11.7	0.0
0.028	10.7	0.0	0.0	11.1	10.9	10.9	0.0
0.031	11.5	0.0	0.0	11.9	11.7	11.7	0.0
0.129	9.9	0.0	0.0	11.5	10.9	10.7	0.0
0.173	9.3	0.0	0.0	11.4	10.5	10.2	0.0
0.479	6.8	0.0	0.50	13.6	9.6	8.6	1.0
0.685	5.8	0.0	0.60	19.4	9.9	7.5	0.92
0.791	5.6	0.0	0.70	29.	12.0	7.9	0.87
0.843	4.5	0.0	0.74	31.	7.4	1.6	0.87
0.890	4.3	0.0	0.84	42.	7.0	(-1.9)	0.93
0.949	3.2	0.0	0.71	68.	(-13.0)	(-33.)	0.75
0.988	2.8	0.0	0.84	254.	(-105.)	(-195.)	0.85
1.000	0.0	0.0	1.0	0.0	0.0	0.0	1.0

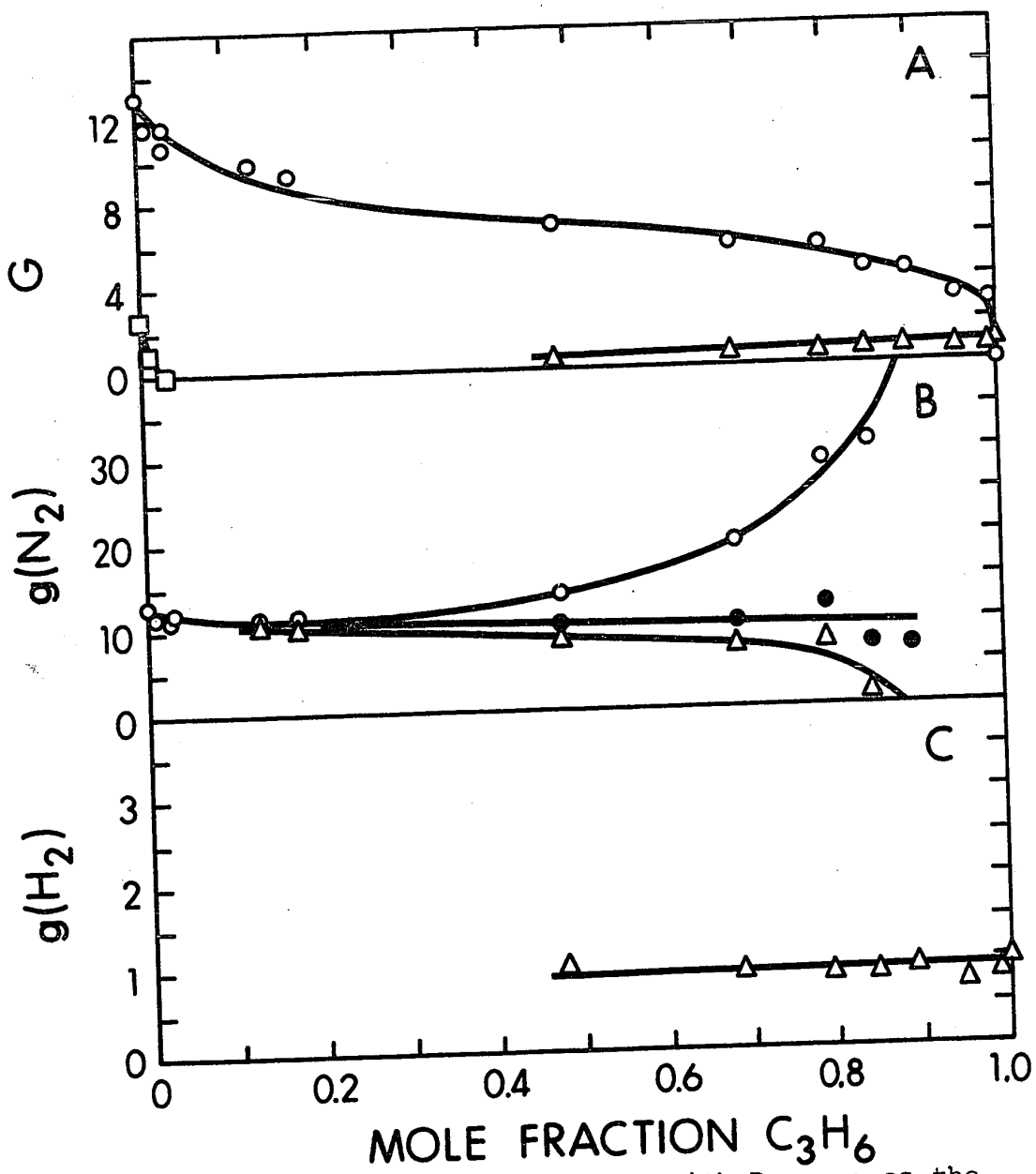

FIGURE III-13 Product Yields with Propene as the Additive at -90°C.

A ○ Nitrogen, □ Oxygen, △ Hydrogen.

B ○ $g(N_2)_N^0$, ● $g(N_2)_N^4$, △ $g(N_2)_N^5$.

C △ Hydrogen.

TABLE III-15

G Values Using Ethene as the Additive at -90°C

Mole Fraction of Additive	$G(N_2)$	$G(O_2)$	$G(H_2)$	$g(N_2)_N^0$	$g(N_2)_N^4$	$g(N_2)_N^5$	$g(H_2)$
0.009	13.2	1.1	0.0	13.3	13.2	13.2	0.0
0.033	12.3	0.76	0.0	12.6	12.5	12.5	0.0
0.071	11.7	0.0	0.0	12.4	12.1	12.1	0.0
0.128	10.4	0.0	0.0	11.5	11.1	11.0	0.0
0.153	10.2	0.0	0.0	11.5	11.0	10.9	0.0
0.207	9.3	0.0	0.0	11.1	10.3	10.1	0.0
0.648	6.7	0.0	0.70	15.7	10.3	9.0	1.2
0.718	5.8	0.0	0.60	16.6	9.2	7.4	0.93
0.849	5.6	0.0	0.78	29.	12.4	8.3	0.97
0.900	4.5	0.0	0.72	34.	8.0	1.5	0.83
0.938	4.4	0.0	0.89	53.	8.9	(-2.1)	0.97
0.953	3.9	0.0	1.1	61.	2.3	(-12.5)	1.2
0.991	2.0	0.0	1.3	158.	(-162.)	(-242.)	1.3
1.000	0.0	0.0	1.2	0.0	0.0	0.0	1.2

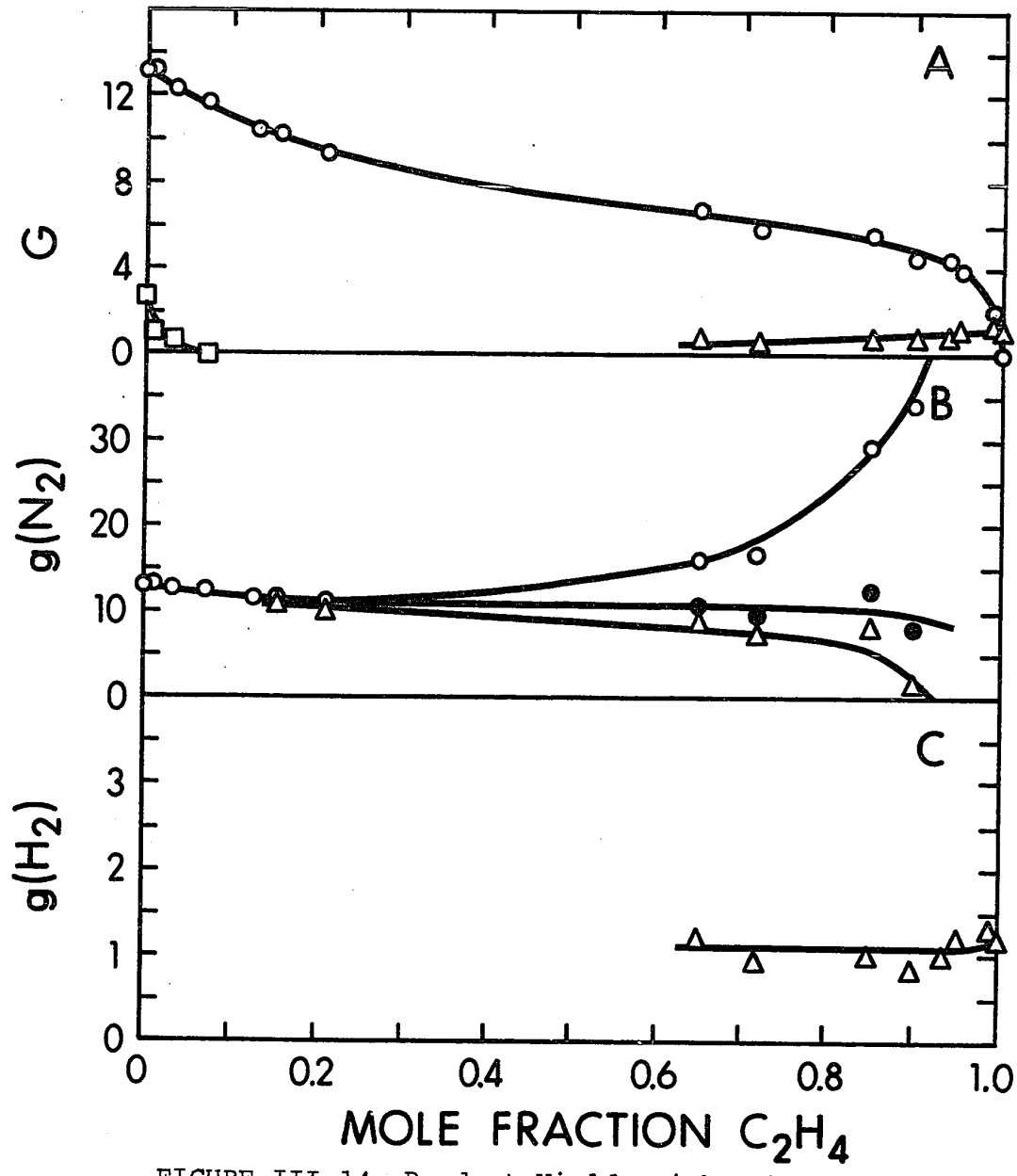

FIGURE III-14 Product Yields with Ethene as the Additive at -90°C.

A ○ Nitrogen, □ Oxygen, △ Hydrogen.

B ○ $g(N_2)_N^0$, ● $g(N_2)_N^4$, △ $g(N_2)_N^5$.

C △ Hydrogen.

TABLE III-16

G Values Using Methyl Fluoride as the Additive at -90°C

Mole Fraction of Additive	$G(N_2)$	$G(O_2)$	$G(H_2)$	$g(N_2)_N^0$	$g(N_2)_N^3$	$g(N_2)_N^4$	$g(H_2)$
0.021	13.0	1.0	0.0	13.2	13.2	13.2	0.0
0.061	12.6	0.13	0.0	13.3	13.2	13.1	0.0
0.097	12.1	0.0	0.0	13.2	12.9	12.8	0.0
0.172	10.9	0.0	0.0	12.8	12.3	12.1	0.0
0.264	10.5	0.0	0.0	13.5	12.6	12.3	0.0
0.327	9.8	0.0	0.50	13.7	12.5	12.1	1.8
0.666	7.0	0.0	0.83	18.3	13.4	11.8	1.3
0.697	6.5	0.0	0.78	18.6	12.9	11.1	1.2
0.858	5.4	0.0	1.1	32.	17.2	12.1	1.4
0.943	4.2	0.0	1.5	62.	21.0	7.3	1.6
0.986	3.0	0.0	1.4	176.	(-4.0)	(-55.)	1.4
1.000	0.0	0.0	1.3	0.0	0.0	0.0	1.3

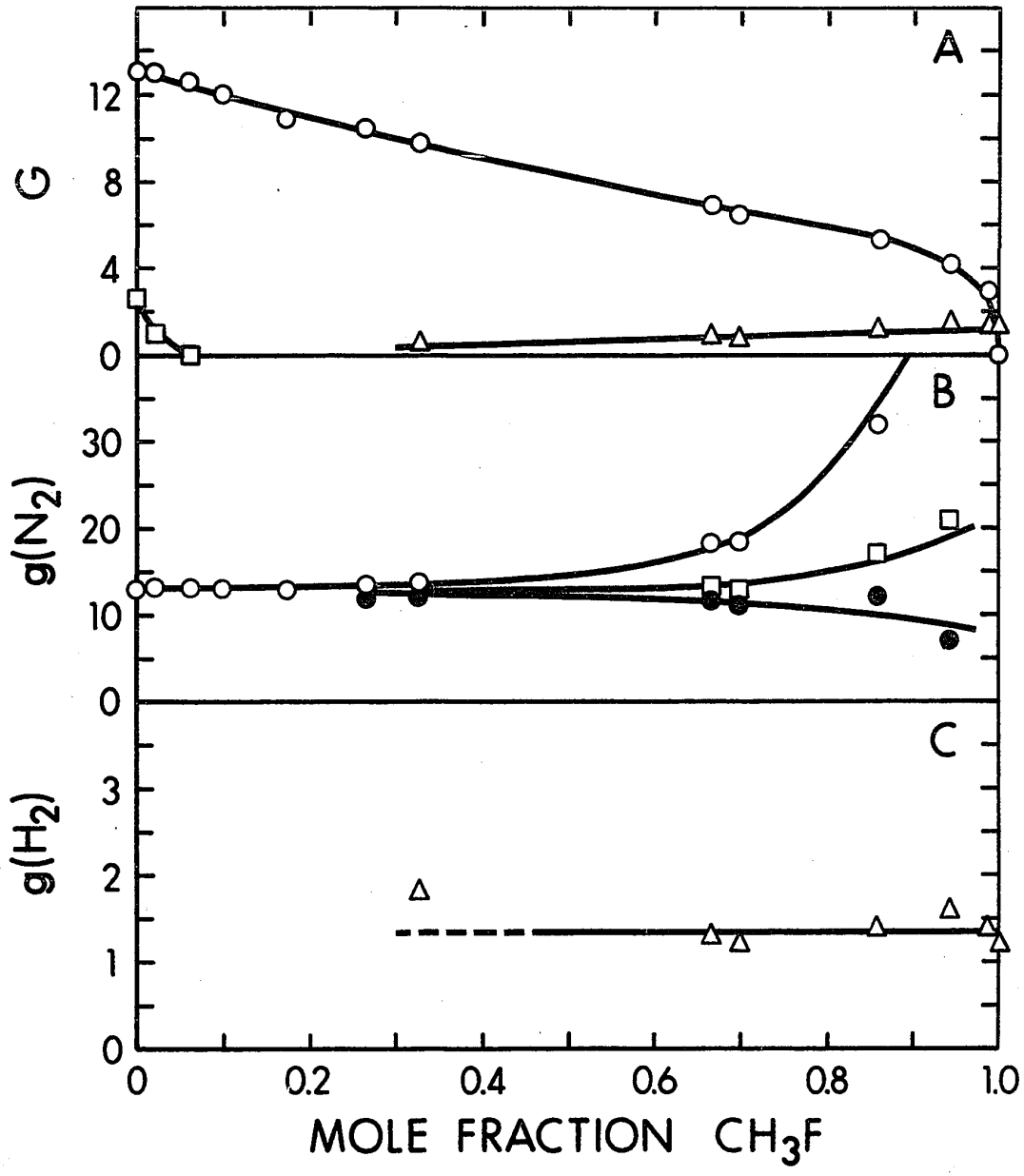

FIGURE III-15 Product Yields Using Methyl Fluoride as the Additive at -90°C.

A ○ Nitrogen, □ Oxygen, △ Hydrogen.

B ○ $g(N_2)_N^0$, □ $g(N_2)_N^3$, ● $g(N_2)_N^4$.

C △ Hydrogen.

with increasing methyl fluoride concentration. No oxygen was detected at a concentration of 0.097 mole fraction of methyl fluoride. $G(H_2)$ increases slowly, giving a value of 1.3 for the pure compound. No methane was detected. The $G(N_2)$ value at 0.99 mole fraction is 3.0, this value being considerably higher than the G values obtained for other halo-compounds at the same concentration.

In Figure III-15B, the $g(N_2)_N^4$ curve initially displays a plateau around a value of 13, then decreases slowly at higher concentrations of the additive.

(ii) Methyl Chloride

The results are reported in Table III-17 and Figure III-16.

Competition for the electron between methyl chloride and nitrous oxide becomes more apparent, as the $G(N_2)$ curve is steeper and the $G(N_2)$ value at 0.99 mole fraction of methyl chloride is 0.99. A value of 0.70 for $G(H_2)$ is obtained for the pure additive (Figure III-16A).

The $g(N_2)_N^3$ curve (Figure III-16B) defects from its plateau level at high concentrations of methyl chloride yielding negative values. This is indicative of an efficient electron scavenger.

In Figure III-16C, the $g(CH_4)$ curve remains fairly constant around a value of 0.70 up to a concentration of 0.87 mole fraction, then increases to 2.5, the g value for pure methyl chloride.

Nitrogen dioxide was not detected after a 0.094 mole

TABLE III-17

G Values Using Methyl Chloride as the Additive at -90°C

Mole Fraction of Additive	$G(N_2)$	$G(O_2)$	$G(H_2)$	$G(CH_4)$	$g(N_2)_N^0$	$g(N_2)_N^3$	$g(N_2)_N^4$	$g(H_2)$	$g(CH_4)$
0.024	12.2	0.88	0.0	0.0	12.6	12.5	12.4	0.0	0.0
0.067	11.9	0.18	0.0	0.0	12.9	12.7	12.6	0.0	0.0
0.209	10.8	0.0	0.0	0.0	14.2	13.3	12.9	0.0	0.0
0.245	9.7	0.0	0.20	0.20	13.5	12.3	11.9	0.72	0.72
0.403	9.1	0.0	0.30	0.28	16.4	14.0	13.2	0.67	0.63
0.508	8.5	0.0	0.38	0.27	18.9	15.2	14.0	0.69	0.49
0.599	6.8	0.0	0.40	0.50	18.9	13.6	11.8	0.63	0.79
0.722	6.0	0.0	0.40	0.45	25.	15.8	12.2	0.53	0.60
0.800	4.6	0.0	0.41	0.75	26.	11.8	7.5	0.50	0.91
0.873	4.0	0.0	0.50	1.1	36.	11.6	3.5	0.56	1.2
0.900	3.3	0.0	0.39	0.94	38.	6.1	(-4.4)	0.43	1.0
0.950	1.9	0.0	0.40	1.7	45.	(-22.)	(-45.)	0.42	1.7
0.991	0.99	0.0	0.47	2.4	130.	(-260.)	(-391.)	0.48	2.4
1.000	0.0	0.0	0.70	2.5	0.0	0.0	0.0	0.70	2.5

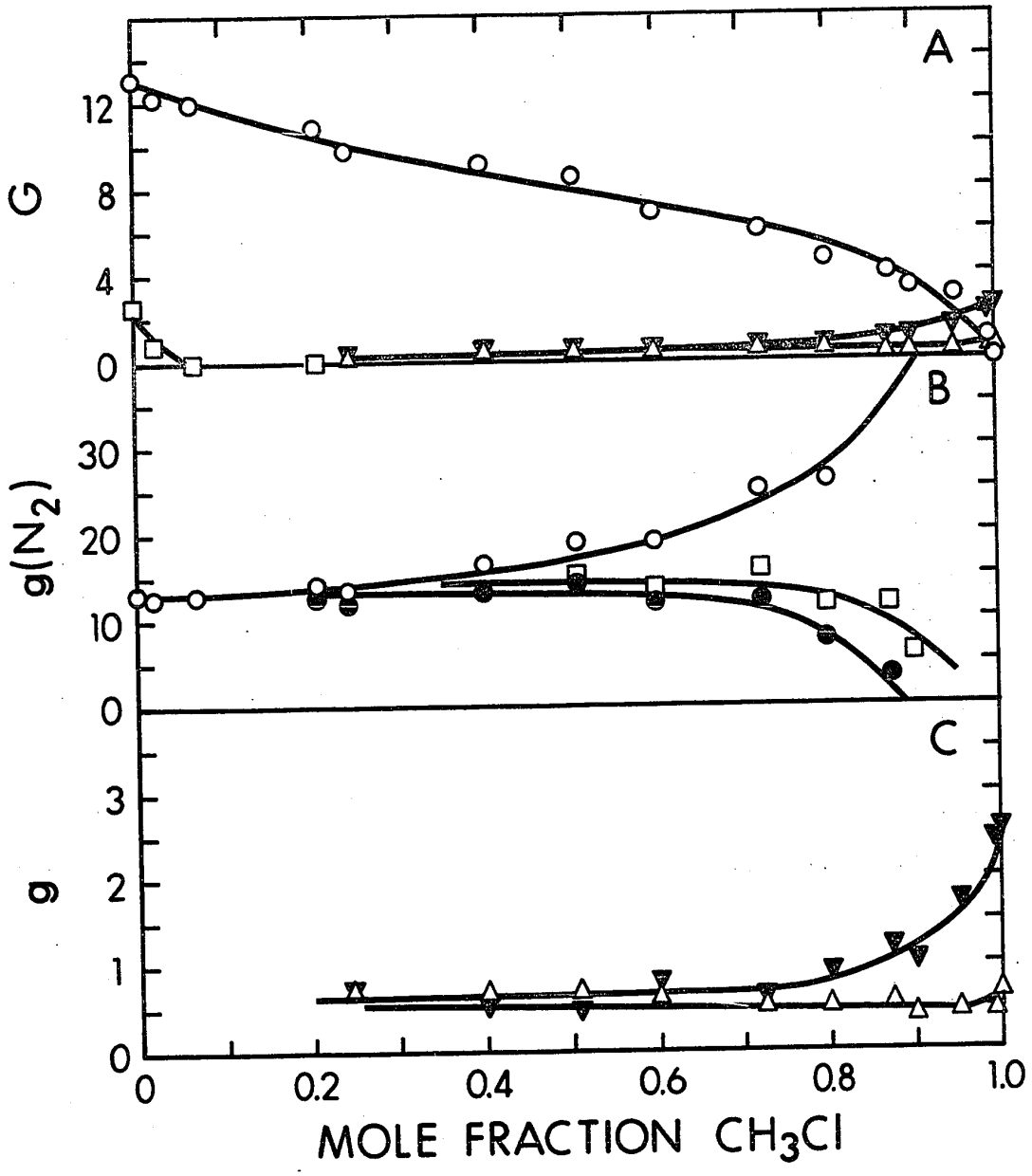

FIGURE III-16 Product Yields with Methyl Chloride as the Additive at -90°C.

A ○ Nitrogen, □ Oxygen, Δ Hydrogen, ▼ Methane.

B ○ $g(N_2)^0_N$, □ $g(N_2)^3_N$, ● $g(N_2)^4_N$.

C Δ Hydrogen, ▼ Methane.

fraction addition of the additive, and the decrease in $G(NO_2)$ with concentration is slower if compared to the $G(NO_2)$ curve for the alkanes (Table III-18 and Figure III-17A).

(iii) Methyl Bromide

The results are presented in Table III-19 and Figure III-18.

Referring to Figure III-18A, the $G(N_2)$ curve is noticeably steeper than that of its predecessor (Figure III-16A), yielding a value at 0.99 mole fraction of 0.24. Methane and hydrogen had much lower yields than those obtained from methyl chloride.

The $g(N_2)_N^2$ curve in Figure III-18B remains constant over most of the concentration range, giving negative values after 0.96 mole fraction of additive.

In Figure III-18C, the g values of hydrogen and methane in pure methyl bromide are 0.18 and 0.13 respectively.

$G(NO_2)$ in Figure III-17B decreases to zero at a 0.09 mole fraction addition of the halo-compound.

(iv) Methyl Iodide

The results are given in Table III-20 and Figure III-19.

In Figure III-19A, no oxygen was observed after a 0.04 mole fraction addition and the $G(N_2)$ curve decreases rapidly giving a value of 0.15 at 0.99 mole fraction.

TABLE III-18

G Values of Nitrogen Dioxide Using Methyl Chloride and Methyl Bromide as the Additives at -90°C

Mole Fraction of Methyl Chloride	$G(NO_2)$	Mole Fraction of Methyl Bromide	$G(NO_2)$
0.000	5.6	0.000	5.6
0.012	4.5	0.020	3.7
0.025	3.4	0.033	3.0
0.059	0.5	0.066	0.3
0.094	0.0	0.089	0.0

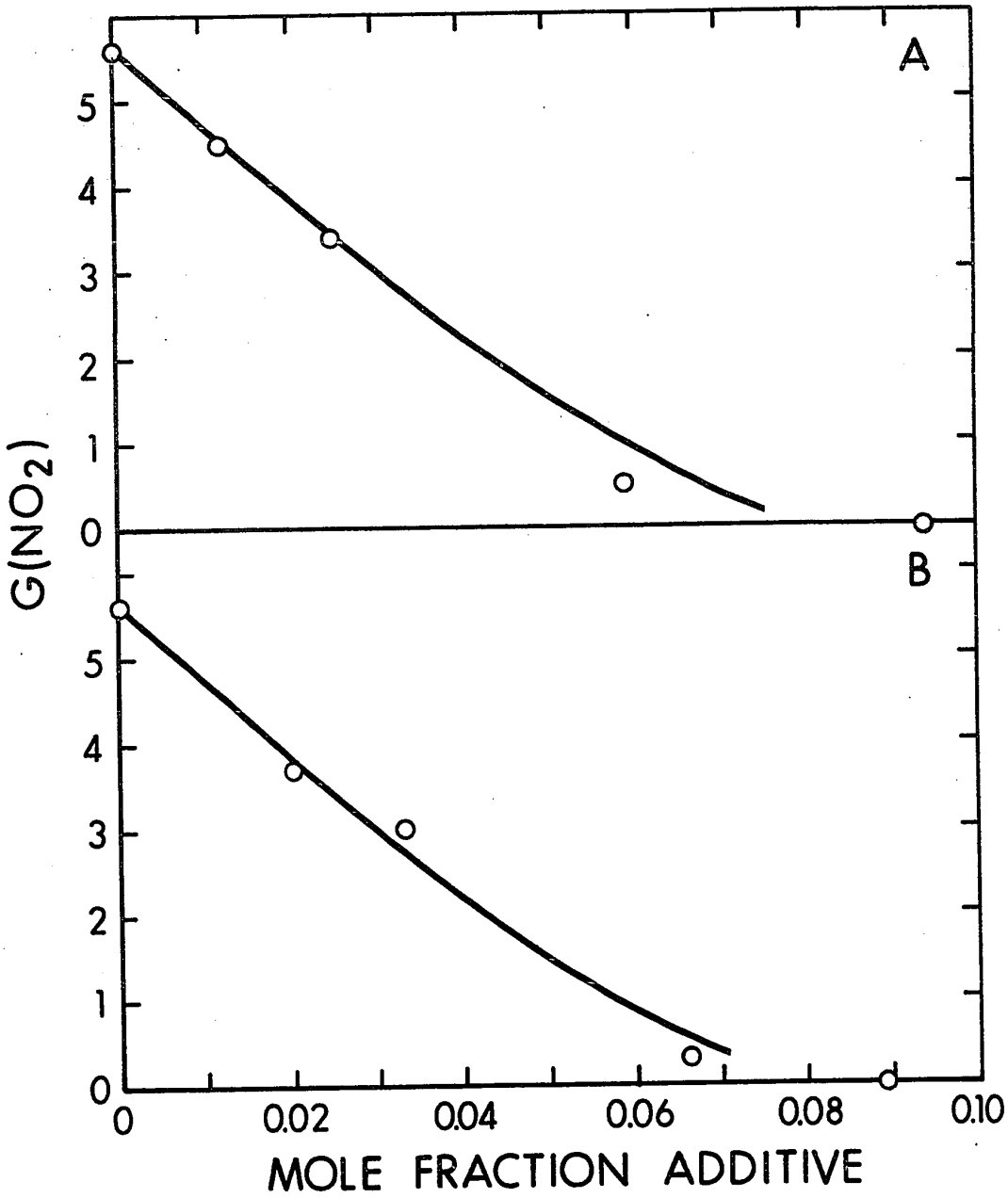

FIGURE III-17 Effect of the Halo-compounds on the $G(NO_2)$ Yield at -90°C.

A Using methyl chloride, O Nitrogen Dioxide.

B Using methyl bromide, O Nitrogen Dioxide.

TABLE III-19

G Values Using Methyl Bromide as the Additive at -90°C

Mole Fraction of Additive	$G(N_2)$	$G(O_2)$	$G(H_2)$	$G(CH_4)$	$g(N_2)_N^0$	$g(N_2)_N^2$	$g(N_2)_N^3$	$g(H_2)$	$g(CH_4)$
0.018	12.2	1.0	0.0	0.0	12.7	12.6	12.6	0.0	0.0
0.102	10.5	0.0	0.0	0.0	12.9	12.4	12.2	0.0	0.0
0.150	10.4	0.0	0.0	0.0	14.1	13.4	13.0	0.0	0.0
0.419	7.7	0.0	0.31	0.09	18.8	15.9	14.5	0.53	0.15
0.576	6.3	0.0	0.17	0.13	23.5	18.1	15.3	0.23	0.18
0.597	6.5	0.0	0.25	0.16	26.	20.1	17.1	0.33	0.21
0.689	4.9	0.0	0.30	0.21	27.	18.1	13.7	0.37	0.26
0.805	3.3	0.0	0.21	0.13	31.	14.5	6.0	0.24	0.15
0.838	2.8	0.0	0.25	0.10	32.	11.3	1.0	0.27	0.11
0.906	2.1	0.0	0.28	0.32	42.	3.5	(-16.)	0.30	0.34
0.963	1.0	0.0	0.19	0.09	54.	(-51.)	(-103.)	0.19	0.09
0.987	0.21	0.0	0.20	0.10	32.	(-267.)	(-417.)	0.20	0.10
1.000	0.0	0.0	0.18	0.13	0.0	0.0	0.0	0.18	0.13

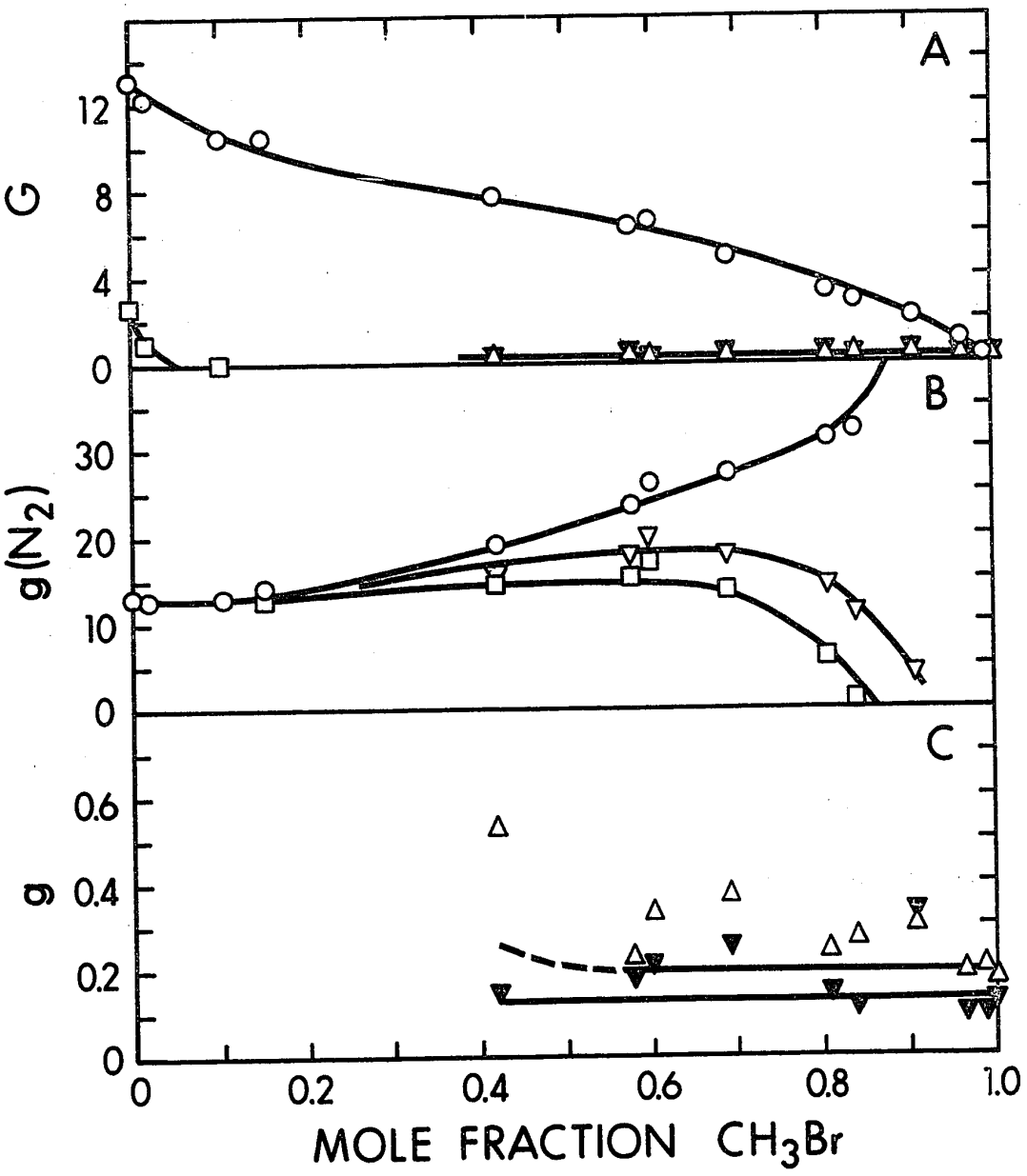

FIGURE III-18 Product Yields with Methyl Bromide as the Additive at -90°C.

A ○ Nitrogen, □ Oxygen, △ Hydrogen, ▼ Methane.

B ○ $g(N_2)_N^0$, ▽ $g(N_2)_N^2$, □ $g(N_2)_N^3$.

C △ Hydrogen, ▼ Methane.

TABLE III-20

G Values Using Methyl Iodide as the Additive at -63°C

Mole Fraction of Additive	$G(N_2)$	$G(O_2)$	$G(H_2)$	$G(CH_4)$	$g(N_2)_N^0$	$g(N_2)_N^2$	$g(N_2)_N^3$	$g(H_2)$	$g(CH_4)$
0.014	11.1	0.8	0.0	0.0	11.6	11.5	11.5	0.0	0.0
0.043	10.4	0.0	0.0	0.0	11.7	11.4	11.3	0.0	0.0
0.130	9.3	0.0	0.0	0.0	13.2	12.4	11.9	0.0	0.0
0.213	7.8	0.0	0.12	0.17	13.8	12.3	11.5	0.28	0.39
0.383	6.4	0.0	0.17	0.27	17.6	14.1	12.3	0.27	0.42
0.420	4.9	0.0	0.14	0.32	14.9	10.8	8.8	0.21	0.48
0.545	4.0	0.0	0.19	0.40	17.5	10.7	7.4	0.25	0.52
0.711	3.4	0.0	0.16	0.12	27.	13.1	6.2	0.18	0.14
0.790	2.3	0.0	0.15	0.26	27.	5.8	(-5.0)	0.16	0.28
0.848	1.1	0.0	0.14	0.13	18.4	(-13.6)	(-29.)	0.15	0.14
0.898	1.1	0.0	0.14	0.12	29.	(-21.)	(-46.)	0.15	0.13
0.950	0.84	0.0	0.18	0.10	46.	(-61.)	(-115.)	0.18	0.10
0.988	0.15	0.0	0.17	0.17	36.	(-435.)	(-671.)	0.17	0.17
1.000	0.0	0.0	0.28	0.29	0.0	0.0	0.0	0.28	0.29

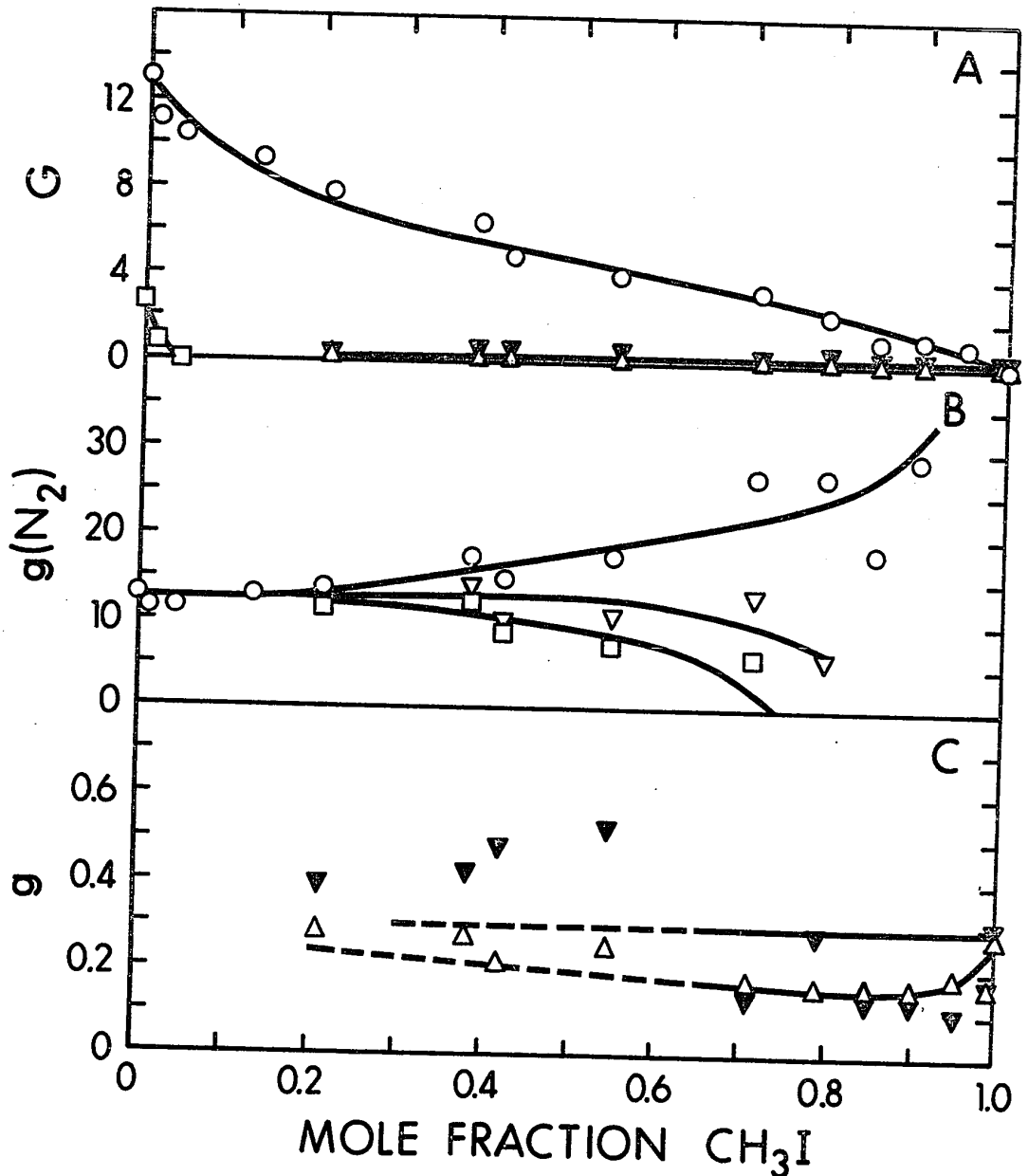

FIGURE III-19 Product Yields with Methyl Iodide as the Additive at -63°C.

A ○ Nitrogen, □ Oxygen, △ Hydrogen, ▼ Methane.

B ○ $g(N_2)^0_N$, ▽ $g(N_2)^2_N$, □ $g(N_2)^3_N$.

C △ Hydrogen, ▼ Methane.

Referring to the $G(N_2)$ curves mentioned in this series, it becomes clear that methyl iodide is the most efficient electron scavenger when compared to the above mentioned halo-compounds, and that these differences in efficiency are expressed in the slopes of their respective curves.

The $g(N_2)^2_N$ curve in Figure III-19B remains constant only up to 0.60 mole fraction then decreases slowly. The $g(H_2)$ and $g(CH_4)$ curves show similar behaviour along the concentration range yielding values of 0.28 and 0.29 respectively for the pure compound.

(v) n-Propyl Bromide

The results are presented in Table III-21 and Figure III-20.

Referring to Figure III-20A, $G(O_2)$ decreases to zero at 0.11 mole fraction addition, and the $G(N_2)$ curve decreases sharply with increasing concentration of the halo-compound. The $g(N_2)^2_N$ curve in Figure III-20B is similar to those for other halo-compounds giving negative values after 0.86 mole fraction.

In Figure III-20C, the $g(H_2)$ curve remains constant along the concentration range equalling 0.50 for pure n-propyl bromide.

(vi) Chloroform

The results are reported in Table III-22 and Figure III-21.

TABLE III-21

G Values using n-Propyl Bromide as the Additive at -90°C

Mole Fraction of Additive	$G(N_2)$	$G(O_2)$	$G(H_2)$	$g(N_2)_N^0$	$g(N_2)_N^2$	$g(N_2)_N^3$	$g(H_2)$
0.022	12.2	1.1	0.0	12.9	12.8	12.7	0.0
0.111	9.9	0.0	0.0	13.3	12.6	12.3	0.0
0.183	9.1	0.0	0.0	14.7	13.5	12.9	0.0
0.291	8.7	0.0	0.10	18.4	16.2	15.0	0.19
0.331	7.3	0.0	0.12	17.2	14.5	13.2	0.21
0.567	5.1	0.0	0.30	23.3	16.2	12.6	0.38
0.578	5.3	0.0	0.41	25.	17.5	13.8	0.52
0.679	4.4	0.0	0.43	30.	18.5	12.7	0.51
0.856	2.4	0.0	0.37	39.	6.6	(-10.0)	0.39
0.913	1.8	0.0	0.47	53.	(-4.4)	(-33.)	0.49
0.955	1.6	0.0	0.54	91.	(-24.)	(-83.)	0.55
0.988	0.16	0.0	0.51	36.	(-413.)	(-638.)	0.51
1.000	0.0	0.0	0.50	0.0	0.0	0.0	0.50

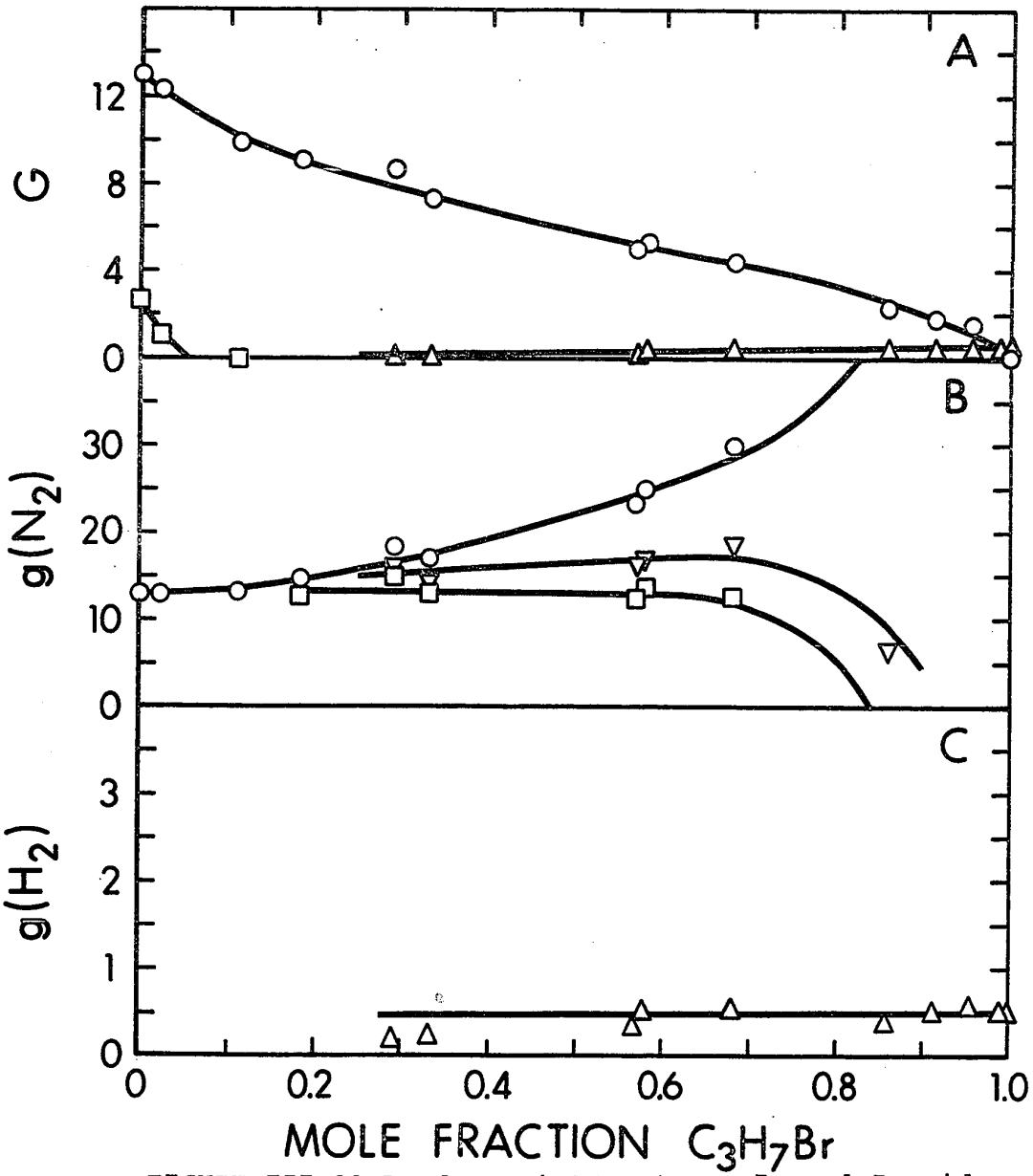

FIGURE III-20 Product Yields with n-Propyl Bromide as the Additive at -90°C.

A ○ Nitrogen, □ Oxygen, △ Hydrogen.

B ○ $g(N_2)^0_N$, ▽ $g(N_2)^2_N$, □ $g(N_2)^3_N$.

C △ Hydrogen.

TABLE III-22

G Values Using Chloroform as the Additive at -63°C

Mole Fraction of Additive	$G(N_2)$	$G(O_2)$	$g(N_2)_N^0$	$g(N_2)_N^1$	$g(N_2)_N^2$
0.011	12.0	1.7	12.3	12.3	12.2
0.028	9.8	0.15	10.5	10.4	10.4
0.071	9.2	0.0	11.1	10.9	10.7
0.136	7.2	0.0	10.2	9.8	9.4
0.269	4.3	0.0	8.5	7.4	6.6
0.383	2.6	0.0	6.8	5.2	3.5
0.468	2.5	0.0	8.3	6.0	3.7
0.593	1.4	0.0	6.7	2.9	(-1.0)
0.713	1.1	0.0	8.3	1.7	(-4.8)
0.813	0.33	0.0	4.1	(-7.4)	(-18.9)
0.829	0.65	0.0	9.0	(-12.8)	(-17.0)
0.948	0.42	0.0	20.6	(-27.)	(-75.)
0.993	0.16	0.0	60.	(-314.)	(-688.)
1.000	0.0	0.0	0.0	0.0	0.0

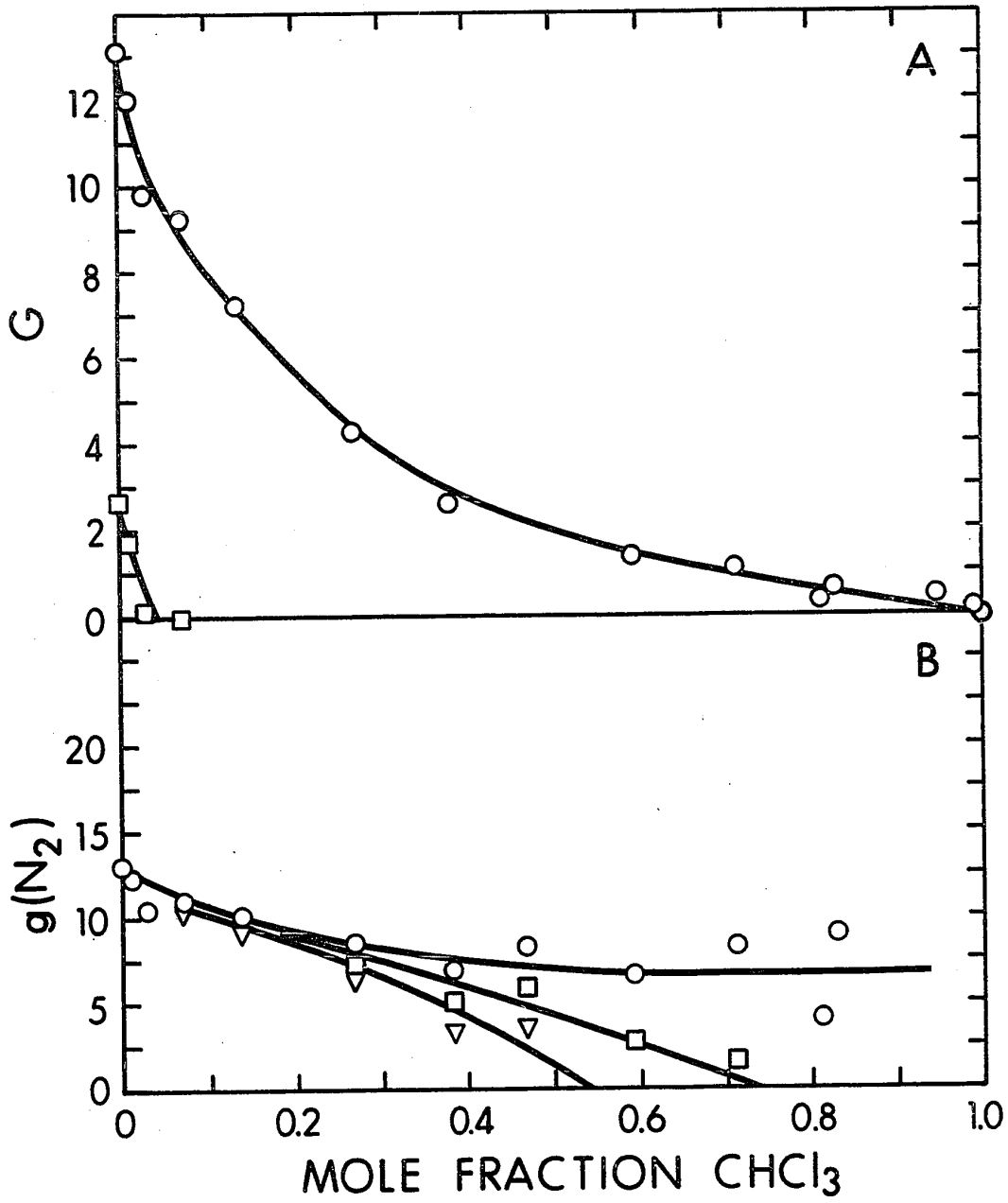

FIGURE III-21 Product Yields with Chloroform as the Additive at -63°C.

A ○ Nitrogen, □ Oxygen.

B ○ $g(N_2)^0_N$, ▽ $g(N_2)^2_N$, □ $g(N_2)^3_N$.

In Figure III-21A, the $G(N_2)$ curve drops quickly with the addition of a few mole percentage of chloroform. No oxygen was detected after a 0.07 mole fraction addition.

The uncorrected curve $g(N_2)_N^0$ in Figure III-21B decreases slowly then levels out around a value of 8 over most of the concentration range. This result is consistent with the behaviour of a compound having a lower ionisation potential but higher electron affinity when compared to nitrous oxide. The corrected curves incorporating $g(N_2)_N^1$ and $g(N_2)_N^2$ gave negative values at high concentrations of chloroform.

(vii) Carbon Tetrachloride

The results are given in Table III-23 and Figure III-22.

Only the higher concentrations of the additive were used, due to the high pressures of nitrous oxide involved at -23°C, the freezing point of carbon tetrachloride. The $G(N_2)$ values are lower than those for chloroform at the corresponding concentrations. No oxygen was observed (Figure III-22A).

The values for $g(N_2)_N^0$ are quite scattered, however the curve levels out around 8.

(e) Oxygen-containing Compounds

(i) Acetone

The results are presented in Table III-24 and Figure

TABLE III-23

G Values Using Carbon Tetrachloride as the Additive at -23°C

Mole Fraction of Additive	$G(N_2)$	$G(O_2)$	$g(N_2)_N^0$	$g(N_2)_N^1$	$g(N_2)_N^2$
0.571	1.6	0.0	8.9	4.4	0.1
0.666	0.78	0.0	6.0	0.7	(-7.4)
0.752	0.44	0.0	4.9	(-5.3)	(-15.5)
0.878	0.40	0.0	10.1	(-14.1)	(-39.)
0.930	0.25	0.0	11.4	(-34.)	(-78.)
0.995	0.05	0.0	34.	(-635.)	(-1305.)
1.000	0.0	0.0	0.0	0.0	0.0

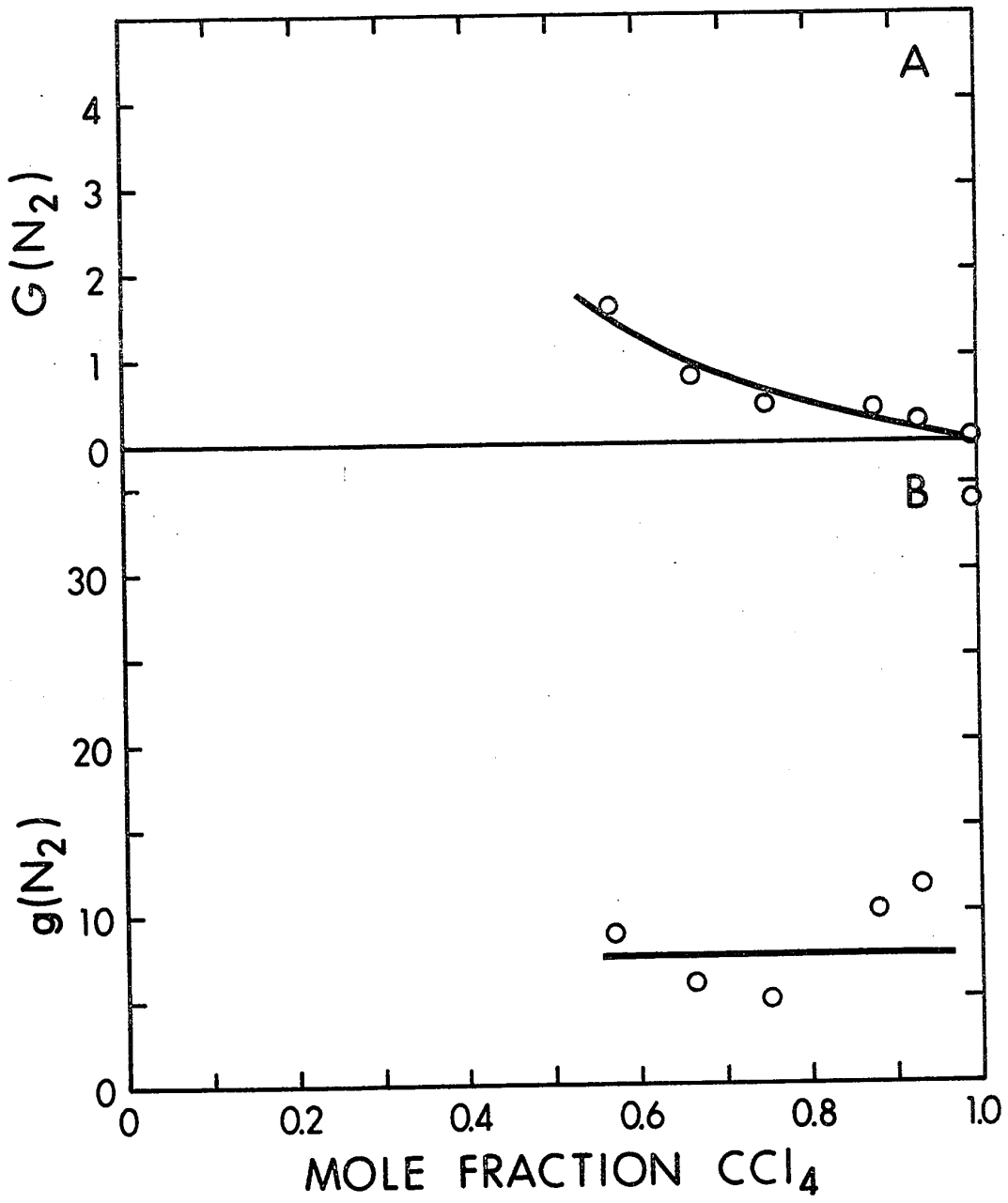

FIGURE III-22 Product Yields with Carbon Tetrachloride as the Additive at -23°C.

A O Nitrogen .

B O Nitrogen .

TABLE III-24

G Values Using Acetone as the Additive at -90°C

Mole Fraction of Additive	$G(N_2)$	$G(O_2)$	$G(H_2)$	$G(CH_4)$	$g(N_2)_N^0$	$g(N_2)_N^3$	$g(N_2)_N^4$	$g(H_2)$	$g(CH_4)$
0.019	13.0	0.51	0.0	0.0	13.3	13.2	13.2	0.0	0.0
0.069	11.8	0.0	0.0	0.0	13.1	12.8	12.6	0.0	0.0
0.099	11.8	0.0	0.0	0.0	13.7	13.2	13.1	0.0	0.0
0.143	11.0	0.0	0.0	0.0	13.7	13.0	12.7	0.0	0.0
0.181	9.9	0.0	0.0	0.0	13.1	12.1	11.8	0.0	0.0
0.362	8.0	0.0	0.30	0.40	14.6	12.1	11.3	0.66	0.89
0.558	6.2	0.0	0.47	0.42	17.6	12.1	10.3	0.73	0.65
0.610	5.7	0.0	0.52	0.52	18.7	11.9	9.6	0.75	0.75
0.697	5.5	0.0	0.47	0.45	23.9	13.9	10.5	0.61	0.59
0.767	5.0	0.0	0.47	0.60	29.	14.6	10.0	0.57	0.73
0.889	3.5	0.0	0.55	0.80	44.	9.0	(-2.5)	0.60	0.87
0.954	2.0	0.0	0.75	0.79	64.	(-27.)	(-57.)	0.77	0.82
0.992	1.1	0.0	0.95	0.65	194.	(-347.)	(-527.)	0.96	0.66
1.000	0.0	0.0	0.95	0.70	0.0	0.0	0.0	0.95	0.70

III-23.

In Figure III-23A, the $G(N_2)$ curve decreases steadily with increasing concentration of additive. $G(O_2)$ decreases to zero at 0.07 mole fraction of acetone.

The $g(N_2)_N^3$ curve in Figure III-23B shows a plateau throughout most of the concentration range.

Referring to Figure III-23C, the $g(H_2)$ value for pure acetone is 0.95 and $g(H_4)$ is 0.70.

$G(NO_2)$ in Figure III-24B and Table III-25 decreases rapidly with increasing acetone concentration.

(ii) Acetaldehyde

The results are given in Table III-26 and Figure III-25.

The $G(N_2)$ curve in Figure III-25A is lower than the corresponding one for acetone. Carbon monoxide, hydrogen and methane were detected, and these all three products increase with increasing acetaldehyde concentration.

In Figure III-25B, the $g(N_2)_N^2$ curve decreases from its plateau level at high aldehyde concentrations.

The g values for the pure acetaldehyde in Figure III-25C are 1.3 for hydrogen, 1.0 for methane and 1.3 for carbon monoxide.

(iii) Methanol

The results are reported in Table III-27 and Figure III-26.

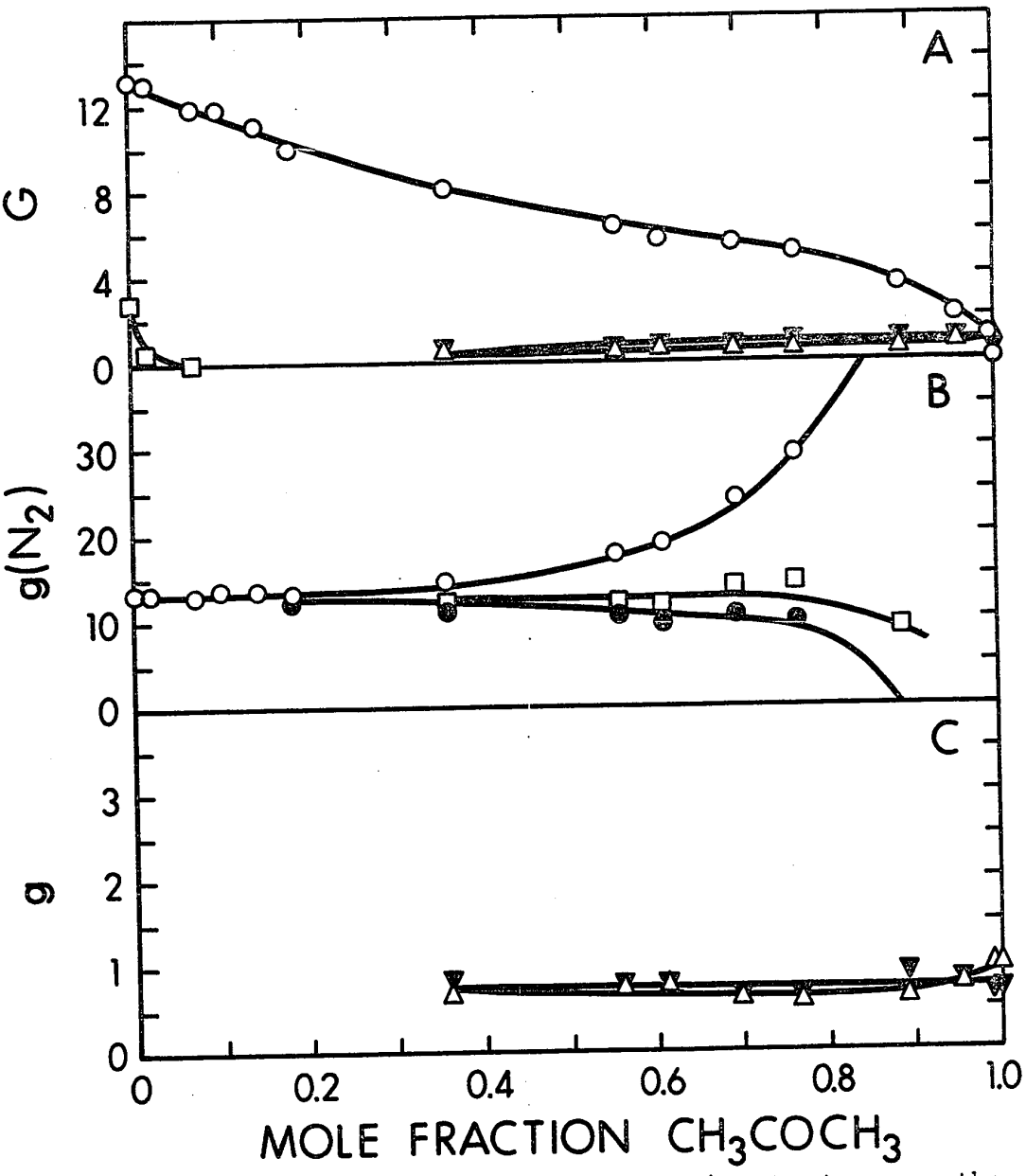

FIGURE III-23 Product Yields Using Acetone as the Additive at -90°C.

A ○ Nitrogen, □ Oxygen, △ Hydrogen, ▼ Methane.

B ○ $g(N_2)_N^0$, □ $g(N_2)_N^3$, ● $g(N_2)_N^4$.

C △ Hydrogen, ▼ Methane.

TABLE III-25

G Values of Nitrogen Dioxide Using Methanol and Acetone as Additives at -90°C

Mole Fraction of Methanol	$G(NO_2)$	Mole Fraction of Acetone	$G(NO_2)$
0.000	5.6	0.000	5.6
0.009	1.6	0.010	0.8
0.015	0.7	0.023	0.2
0.025	0.3	0.069	0.0
0.057	0.0		

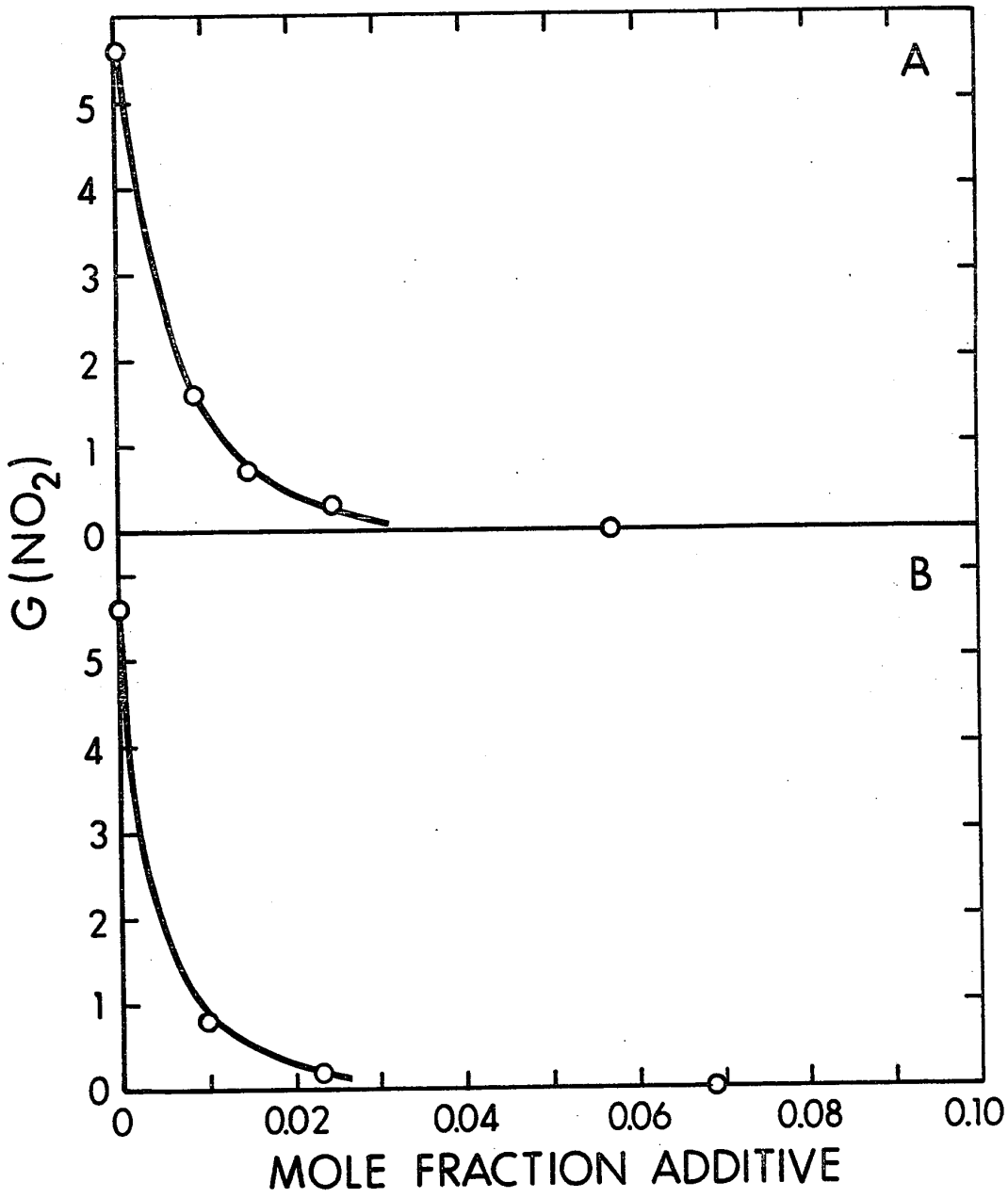

FIGURE III-24 Effect of the Oxygen-containing Compounds on the $G(NO_2)$ Yield at -90°C.

A Using methanol, O Nitrogen Dioxide.

B Using acetone, O Nitrogen Dioxide.

TABLE III-26

G Values Using Acetaldehyde as the Additive at -90°C

Mole Fraction of Additive	$g(N_2)$	$G(O_2)$	$G(H_2)$	$G(CH_4)$	$G(CO)$	$g(N_2)_N^0$	$g(N_2)_N^2$	$g(N_2)_N^3$	$g(H_2)$	$g(H_4)$	$g(CO)$
0.057	11.9	0.32	0.0	0.0	0.0	12.7	12.6	12.5	0.0	0.0	0.0
0.108	10.7	0.0	0.0	0.0	0.0	12.1	11.8	11.7	0.0	0.0	0.0
0.192	9.8	0.0	0.35	0.48	0.51	12.4	11.9	11.6	1.7	2.3	2.5
0.344	7.4	0.0	0.76	0.73	0.71	11.7	10.6	10.0	2.1	2.0	1.9
0.556	4.8	0.0	0.89	0.84	1.1	11.4	8.7	7.3	1.5	1.5	1.9
0.621	5.1	0.0	1.1	0.61	1.0	14.3	10.7	8.9	1.7	0.95	1.6
0.691	3.9	0.0	1.2	1.0	1.3	13.5	8.6	6.2	1.7	1.4	1.8
0.907	3.0	0.0	1.2	0.85	0.95	35.	13.8	3.0	1.3	0.93	1.0
0.952	2.1	0.0	1.1	0.97	1.1	48.	5.0	(-17.0)	1.2	1.0	1.2
0.988	0.35	0.0	1.3	1.2	1.4	32.	(-148.)	(-238.)	1.3	1.2	1.4
1.000	0.0	0.0	1.3	1.0	1.4	0.0	0.0	0.0	1.3	1.0	1.4

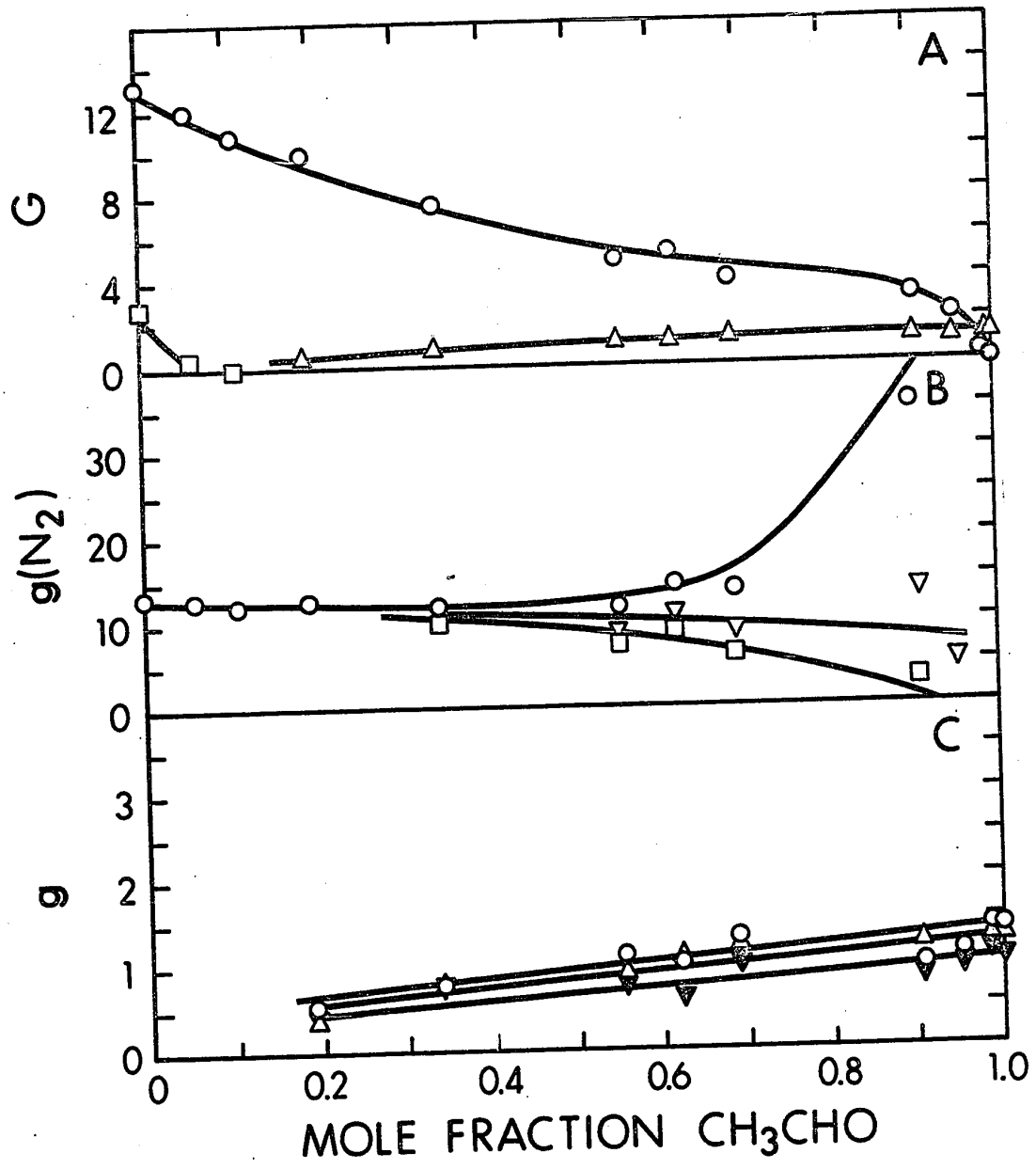

FIGURE III-25 Product Yields with Acetaldehyde as the Additive at -90°C.

A ○ Nitrogen, □ Oxygen, △ Hydrogen (▼ Methane, ● Carbon monoxide).

B ○ $g(N_2)_N^0$, ▽ $g(N_2)_N^2$, □ $g(N_2)_N^3$.

C △ Hydrogen, ▼ Methane, ○ Carbon monoxide.

TABLE III-27

G Values Using Methanol as the Additive at -90°C

Mole Fraction of Additive	$G(N_2)$	$G(O_2)$	$G(H_2)$	$g(N_2)^0_N$	$g(N_2)^4_N$	$g(N_2)^5_N$	$g(H_2)$
0.024	12.2	0.53	0.0	12.4	12.3	12.3	0.0
0.067	11.5	0.0	0.0	12.2	12.0	11.9	0.0
0.119	10.2	0.0	0.0	11.3	10.9	10.8	0.0
0.147	10.4	0.0	0.0	11.9	11.3	11.2	0.0
0.226	8.8	0.0	0.45	10.9	9.9	9.7	2.3
0.243	8.8	0.0	0.43	11.1	10.1	9.8	2.1
0.314	9.0	0.0	0.55	12.4	10.9	10.5	2.0
0.493	7.4	0.0	0.80	13.3	10.1	9.3	1.8
0.551	7.6	0.0	0.84	15.3	11.3	10.3	1.7
0.638	7.3	0.0	1.1	17.9	12.1	10.7	1.9
0.795	5.7	0.0	1.2	23.6	10.9	7.8	1.6
0.900	5.6	0.0	1.5	46.	17.0	9.6	1.7
0.952	4.4	0.0	1.9	77.	11.6	(-4.7)	2.0
0.993	3.7	0.0	2.8	435.	(-29.)	(-145.)	2.8
1.000	0.0	0.0	4.0	0.0	0.0	0.0	4.0

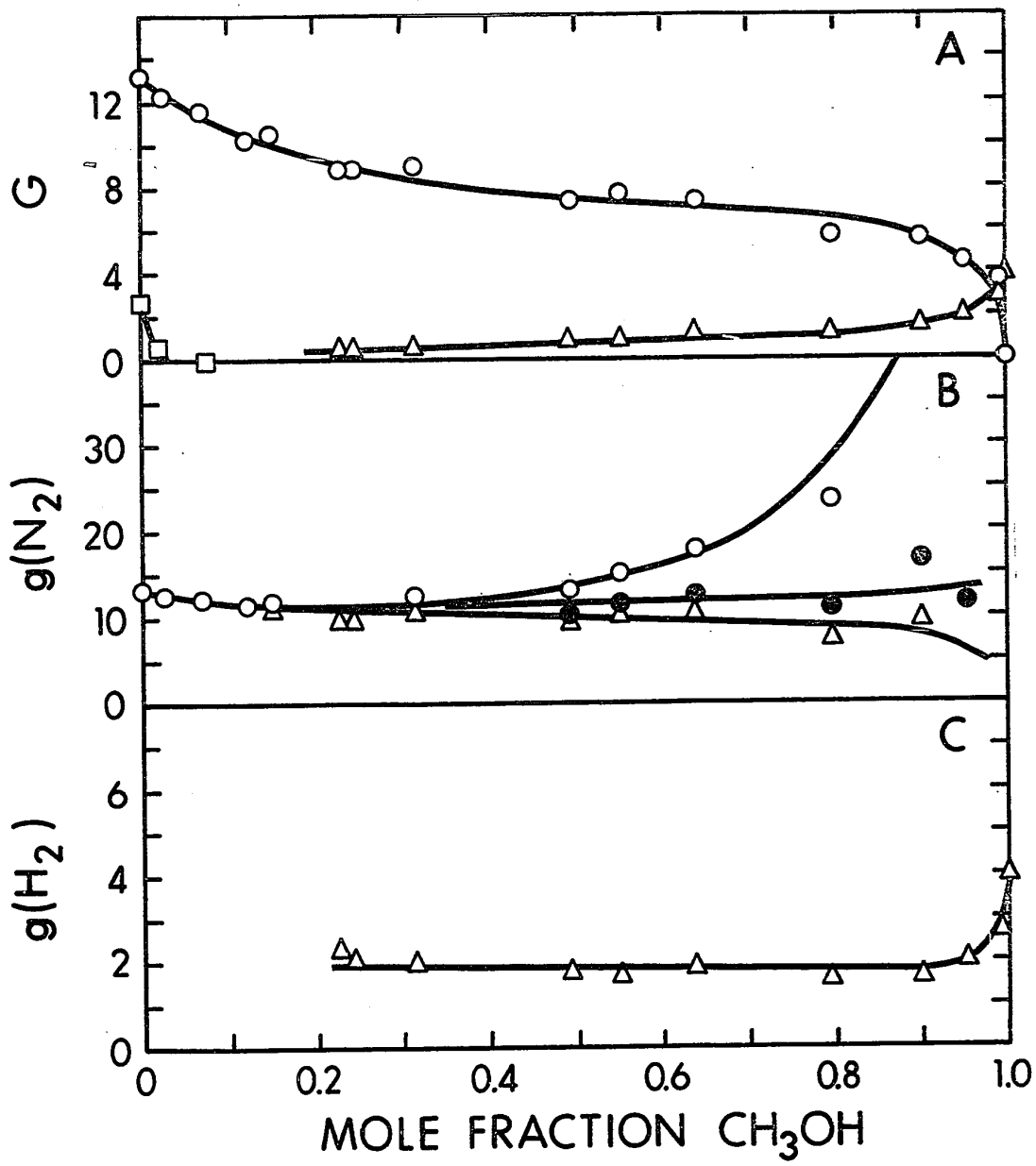

FIGURE III-26 Product Yields with Methanol as the Additive at -90°C.

A ○ Nitrogen, □ Oxygen, △ Hydrogen.

B ○ $g(N_2)_N^0$, ● $g(N_2)_N^4$, △ $g(N_2)_N^5$.

C △ Hydrogen.

On the extreme right in Figure III-26A, the decrease in $G(H_2)$ and increase in $G(N_2)$ is due to the electron released in the methanol during radiolysis being scavenged preferentially by the nitrous oxide. $G(O_2)$ decreases to zero at 0.07 mole fraction of methanol.

In Figure III-26B, the $g(N_2)_N^4$ curve remains constant along most of the concentration range.

The $g(H_2)$ curve in Figure III-26C decreases rapidly with addition of nitrous oxide, then levels off, around a value of 2. This 'levelling off' behaviour is due to the 'unscavengeable' hydrogen (92).

The $G(NO_2)$ curve in Figure III-24A decreases sharply upon small additions of methanol.

(iv) Ethanol

The results are presented in Table III-28 and Figure III-27.

In Figure III-27A, the $G(N_2)$ curve is similar to that of methanol, and $G(O_2)$ decreases to zero at a 0.07 mole fraction addition.

The $g(N_2)_N^5$ curve stays fairly constant up to around 0.8 mole fraction then decreases slowly (Figure III-27B).

The $g(H_2)$ value for pure ethanol is 4.8, and the curve decreases sharply with small additions of nitrous oxide reaching a non-scavengeable plateau of 1.5 (Figure III-27C).

TABLE III-28

G Values Using Ethanol as the Additive at -90°C

Mole Fraction of Additive	$G(N_2)$	$G(O_2)$	$G(H_2)$	$g(N_2)_N^0$	$g(N_2)_N^4$	$g(N_2)_N^5$	$g(H_2)$
0.016	13.1	0.85	0.0	13.3	13.2	13.2	0.0
0.041	11.6	0.17	0.0	12.2	12.0	12.0	0.0
0.073	12.0	0.0	0.0	13.1	12.7	12.6	0.0
0.131	11.3	0.0	0.0	13.3	12.6	12.5	0.0
0.323	9.0	0.0	0.42	14.0	11.8	11.2	1.2
0.401	8.4	0.0	0.67	15.0	11.8	11.0	1.5
0.562	6.7	0.0	0.89	16.9	10.8	9.3	1.5
0.600	6.6	0.0	1.1	18.3	11.2	9.4	1.7
0.764	6.1	0.0	1.2	30.	14.3	10.5	1.5
0.797	6.3	0.0	1.2	36.	17.1	12.5	1.5
0.913	5.4	0.0	1.7	72.	22.1	9.7	1.8
0.949	4.8	0.0	2.0	111.	23.1	1.1	2.1
0.968	4.9	0.0	2.2	178.	35.	(-0.51)	2.3
0.987	3.8	0.0	3.0	343.	(-16.)	(-106.)	3.0
1.000	0.0	0.0	4.8	0.0	0.0	0.0	4.8

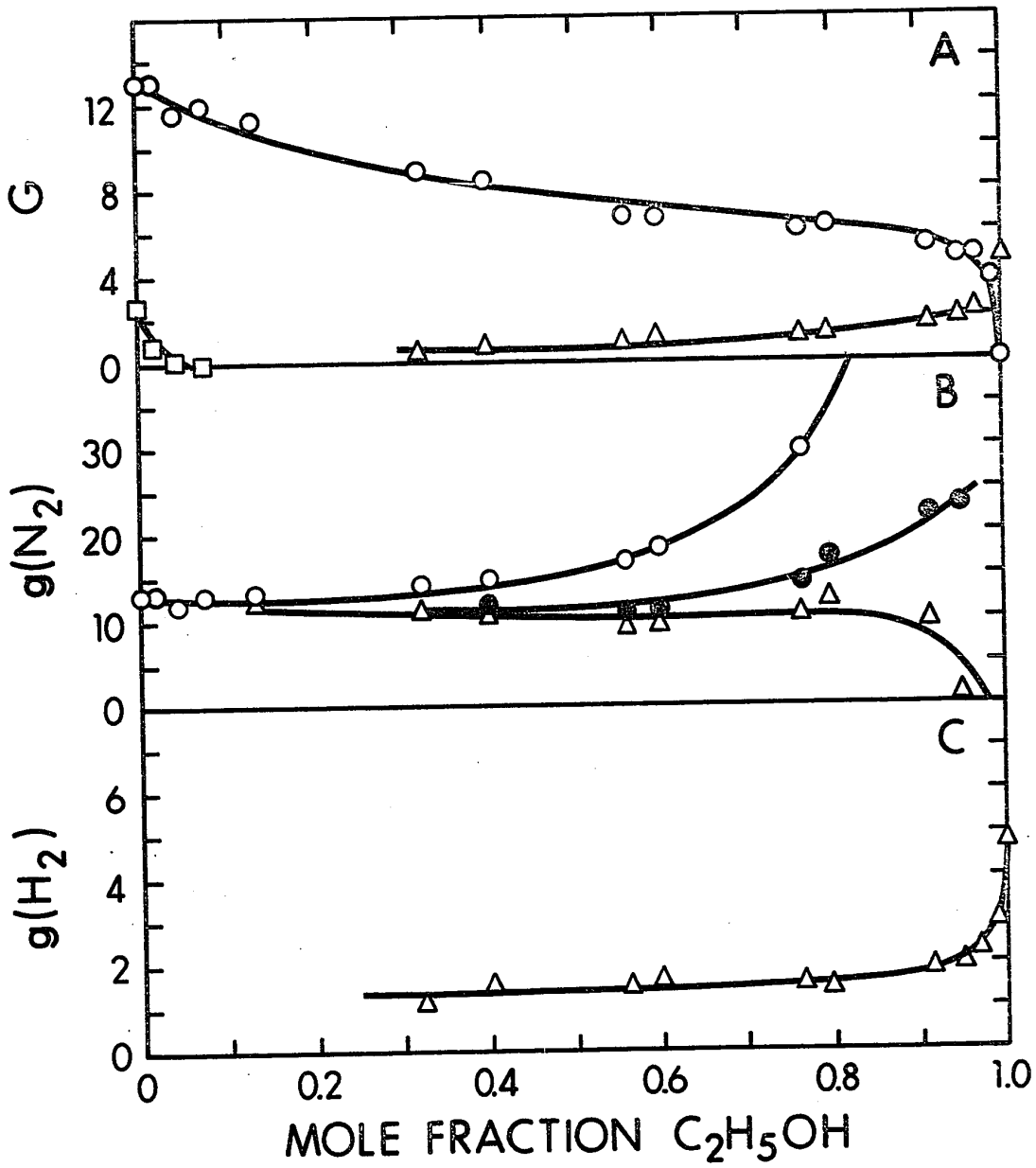

FIGURE III-27 Product Yields with Ethanol as the Additive at -90°C.

A ○ Nitrogen, □ Oxygen, △ Hydrogen.

B ○ $G(N_2)_N^0$, ● $g(N_2)_N^4$, △ $g(N_2)_N^5$.

C △ Hydrogen.

(f) Alkynes

(i) Acetylene

The results are given in Table III-29 and Figure III-28.

The $G(N_2)$ curve in Figure III-28A decreases uniformly with increasing additive concentration. No oxygen was detected at 0.06 mole fraction of acetylene.

In Figure III-28B, the $g(N_2)_N^3$ curve increases only at high concentration of additive.

(ii) Methyl Acetylene

The results are expressed in Table III-30 and Figure III-29.

Referring to Figure III-29A, the $G(N_2)$ curve is higher than that for acetylene. In Figure III-29B, the corrected curve incorporating $g(N_2)_N^5$ displays a plateau over most of the concentration range.

$G(NO_2)$ in Figure III-30C and Table III-31 decreases to zero at a methyl acetylene concentration of 0.05 mole fraction.

(g) Cyclo-compounds

(i) Cyclopentane

The results are presented in Table III-32 and Figure III-31.

In Figure III-31A, with the addition of a few mole % of cyclopentane, the $G(N_2)$ and $G(O_2)$ curves decrease rapidly. On the extreme right of the graph, the decrease in $G(H_2)$

TABLE III-29

G Values Using Acetylene as the Additive at-90°C

Mole Fraction of Additive	$G(N_2)$	$G(O_2)$	$g(N_2)_N^0$	$g(N_2)_N^3$	$g(N_2)_N^4$
0.017	12.8	1.7	12.9	12.9	12.9
0.058	12.4	0.0	12.9	12.8	12.7
0.117	11.6	0.0	12.5	12.2	12.2
0.204	10.8	0.0	12.6	12.1	11.9
0.260	10.2	0.0	12.5	11.8	11.6
0.358	8.9	0.0	12.0	10.9	10.6
0.489	8.5	0.0	13.7	11.9	11.2
0.592	7.3	0.0	14.0	11.2	10.4
0.688	7.0	0.0	16.7	12.5	11.1
0.768	5.8	0.0	17.9	11.6	9.5
0.910	4.7	0.0	35.	15.7	8.8
0.949	3.5	0.0	45.	9.5	(-2.3)
0.986	2.2	0.0	103.	(-31.)	(-77.)
1.000	0.0	0.0	0.0	0.0	0.0

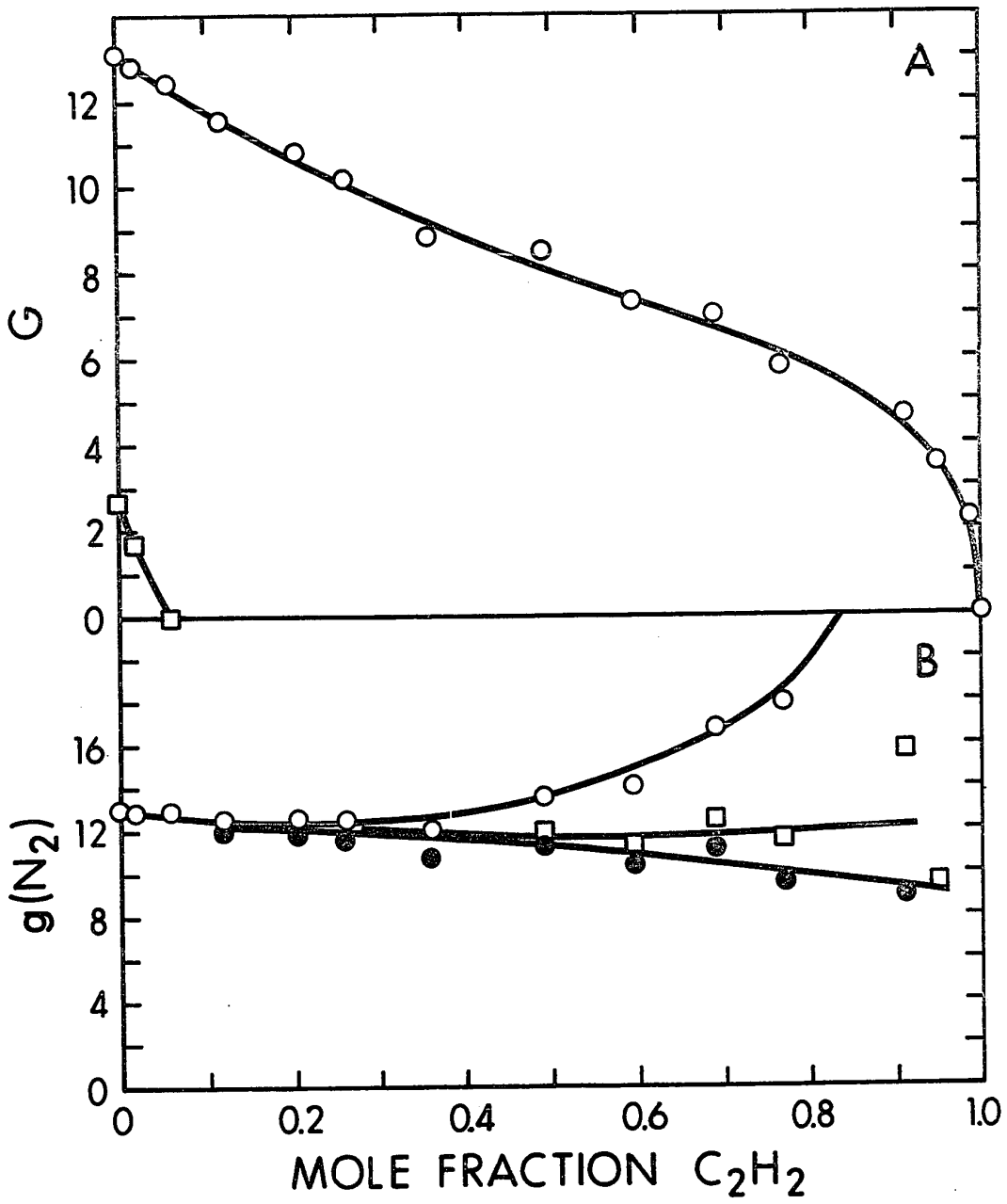

FIGURE III-28 Product Yields Using Acetylene as the Additive at -90°C.

A ○ Nitrogen, □ Oxygen.

B ○ $g(N_2)^0_N$, □ $g(N_2)^3_N$, ● $g(N_2)^4_N$.

TABLE III-30

G Values Using Methylacetylene as the Additive at -90°C

Mole Fraction of Additive	$G(N_2)$	$G(O_2)$	$g(N_2)_N^0$	$g(N_2)_N^4$	$g(N_2)_N^5$
0.035	12.6	1.1	13.1	12.9	12.9
0.114	11.6	0.0	13.1	12.6	12.5
0.201	10.4	0.0	13.0	12.0	11.7
0.331	9.8	0.0	14.6	12.7	12.2
0.613	8.1	0.0	20.8	14.5	12.9
0.719	7.7	0.0	27.	17.0	14.4
0.826	5.8	0.0	33.	14.3	9.6
0.902	5.3	0.0	54.	17.1	7.9
0.948	4.0	0.0	78.	4.6	(-13.7)
0.991	1.5	0.0	168.	(-273.)	(-383.)
1.000	0.0	0.0	0.0	0.0	0.0

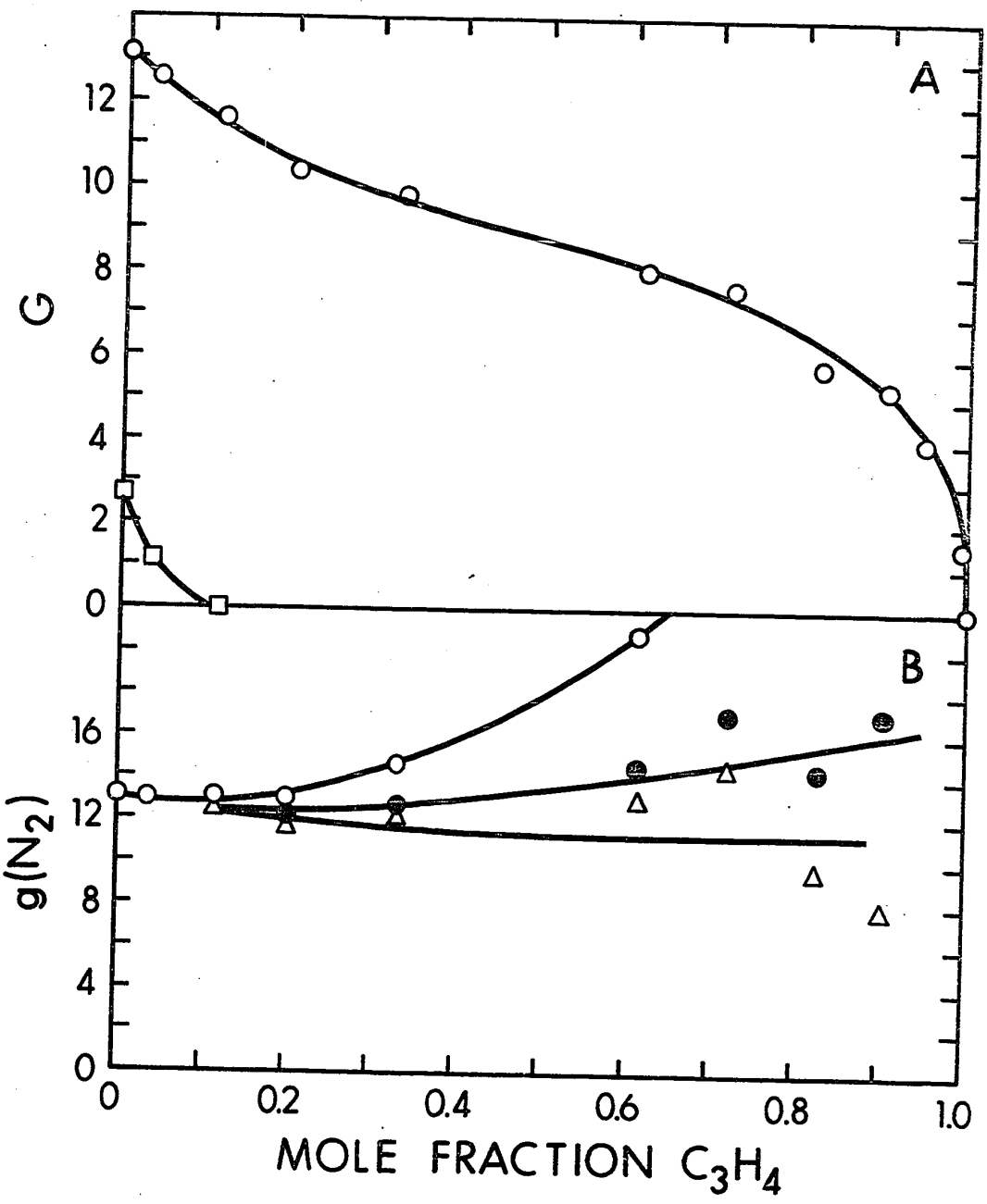

FIGURE III-29 Product Yields with Methyl Acetylene as the Additive at -90°C.

A ○ Nitrogen, □ Oxygen.

B ○ $g(N_2)_N^0$, ● $g(N_2)_N^4$, △ $g(N_2)_N^5$.

TABLE III-31

G Values of Nitrogen Dioxide Using Neohexane, Toluene and Methyl Acetylene as the Additives at -90°C

Mole Fraction of Neohexane	$G(NO_2)$	Mole Fraction of Toluene	$G(NO_2)$	Mole Fraction of Methyl Acetylene	$G(NO_2)$
0.000	5.6	0.000	5.6	0.000	5.6
0.004	4.1	0.011	1.5	0.021	0.6
0.010	1.2	0.017	0.9	0.031	0.1
0.025	0.6	0.041	0.0	0.053	0.0
0.043	0.2				
0.057	0.0				

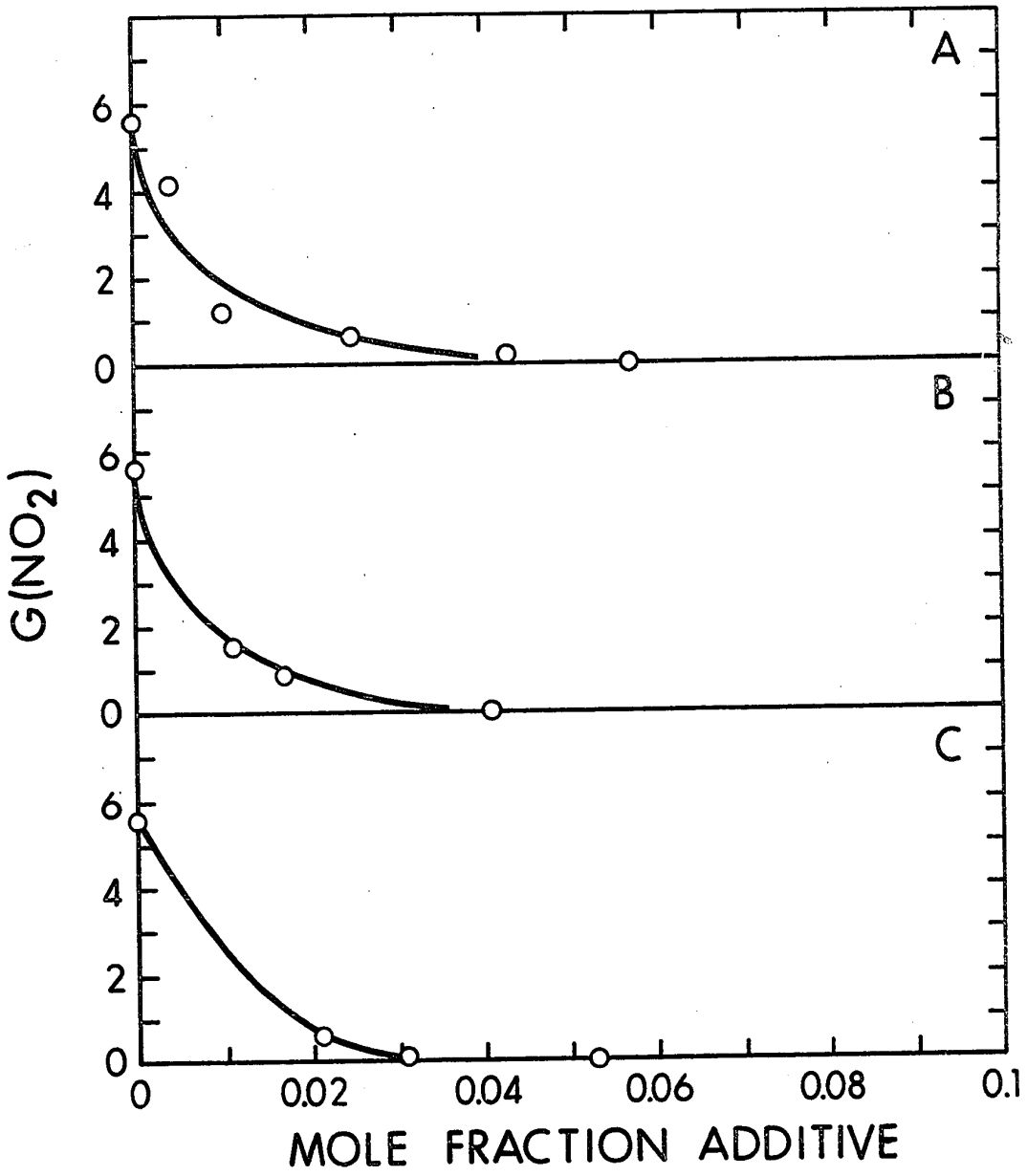

FIGURE III-30 Effect of Various Additives on the $G(NO_2)$ Yield at -90°C.

A Using neohexane , O Nitrogen Dioxide .

B Using toluene , O Nitrogen Dioxide .

C Using methyl acetylene , O Nitrogen Dioxide .

TABLE III-32

G Values Using Cyclopentane as the Additive at -90°C

Mole Fraction of Additive	$G(N_2)$	$G(O_2)$	$G(H_2)$	$g(N_2)_N^0$	$g(N_2)_N^4$	$g(N_2)_N^5$	$g(H_2)$
0.012	11.3	0.95	0.0	11.5	11.5	11.4	0.0
0.038	10.8	0.13	0.0	11.6	11.3	11.2	0.0
0.141	9.7	0.0	0.0	12.6	11.5	11.2	0.0
0.265	8.5	0.0	0.0	14.0	11.4	10.7	0.0
0.375	7.8	0.0	0.11	16.3	11.9	10.8	0.21
0.568	7.4	0.0	0.45	25.	15.5	13.1	0.64
0.703	7.0	0.0	0.71	37.	19.8	15.4	0.87
0.789	6.2	0.0	0.98	49.	21.5	14.7	1.1
0.896	5.6	0.0	1.4	93.	31.	14.8	1.5
0.948	4.5	0.0	1.9	154.	21.8	(-11.4)	2.0
0.993	3.0	0.0	3.1	787.	(-245.)	(-502.)	3.1
1.000	0.0	0.0	5.2	0.0	0.0	0.0	5.2

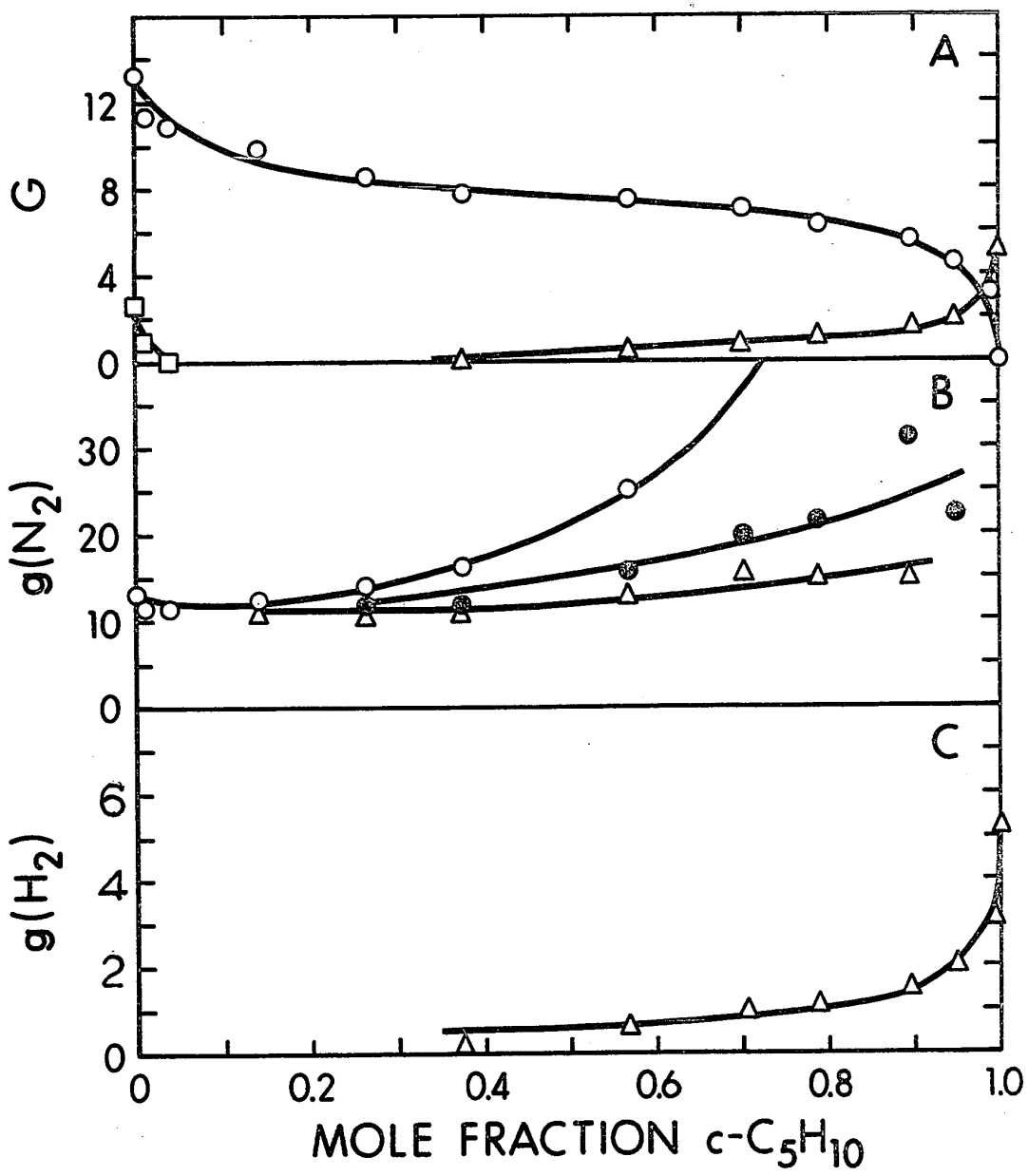

FIGURE III-31 Product Yields Using Cyclopentane as the Additive at -90°C.

A ○ Nitrogen, □ Oxygen, Δ Hydrogen.

B ○ $g(N_2)_N^0$, ● $g(N_2)_N^4$, Δ $g(N_2)_N^5$.

C Δ Hydrogen.

and corresponding increase in $G(N_2)$ is again due to preferential electron scavenging by the nitrous oxide. The $G(N_2)_N^5$ curve in Figure III-31B shows an initial decrease, then increases slowly along the concentration range.

Referring to Figure III-31C, the $g(H_2)$ value for the pure additive is 5.2, and with small quantities of nitrous oxide, the curve dips sharply, levelling off around 0.6.

(ii) Cyclopentene

The results are given in Table III-33 and Figure III-32.

The $G(N_2)$ curve in Figure III-32A drops sharply initially. The rise in $G(N_2)$ proceding right to left on the right side of the graph, is lower when compared to the $G(N_2)$ curve for cyclopentane. This is due to the electron scavenging efficiency of nitrous oxide being lower in alkenes (65).

In Figure III-32B, the $g(N_2)_N^5$ curve remains constant up to around 0.85 mole fraction.

The $g(H_2)$ value for pure cyclopentene is 1.2 (Figure III-32C).

(iii) Cyclopropane

The results are expressed in Table III-34 and Figure III-33.

The $G(N_2)$ curve in Figure III-33A is similar to those for the other cyclo-compounds, but is higher than the

TABLE III-33

G Values Using Cyclopentene as the Additive at -90°C

Mole Fraction of Additive	$G(N_2)$	$G(O_2)$	$G(H_2)$	$g(N_2)_N^0$	$g(N_2)_N^4$	$g(N_2)_N^5$	$g(H_2)$
0.022	11.5	0.60	0.0	11.9	11.8	11.7	0.0
0.080	9.9	0.0	0.0	11.4	10.8	10.7	0.0
0.241	8.6	0.0	0.0	13.2	11.0	10.5	0.0
0.307	7.7	0.0	0.10	13.7	10.6	9.8	0.23
0.572	6.6	0.0	0.33	21.7	12.4	10.1	0.47
0.652	6.4	0.0	0.49	27.	14.1	10.9	0.64
0.731	6.3	0.0	0.62	36.	16.9	12.2	0.75
0.815	5.7	0.0	0.81	49.	18.7	11.1	0.92
0.901	5.0	0.0	0.97	83.	20.2	4.5	1.0
0.952	3.9	0.0	1.0	138.	(-0.83)	(-33.)	1.1
0.992	2.2	0.0	1.1	478.	(-379.)	(-593.)	1.1
1.000	0.0	0.0	1.2	0.0	0.0	0.0	1.2

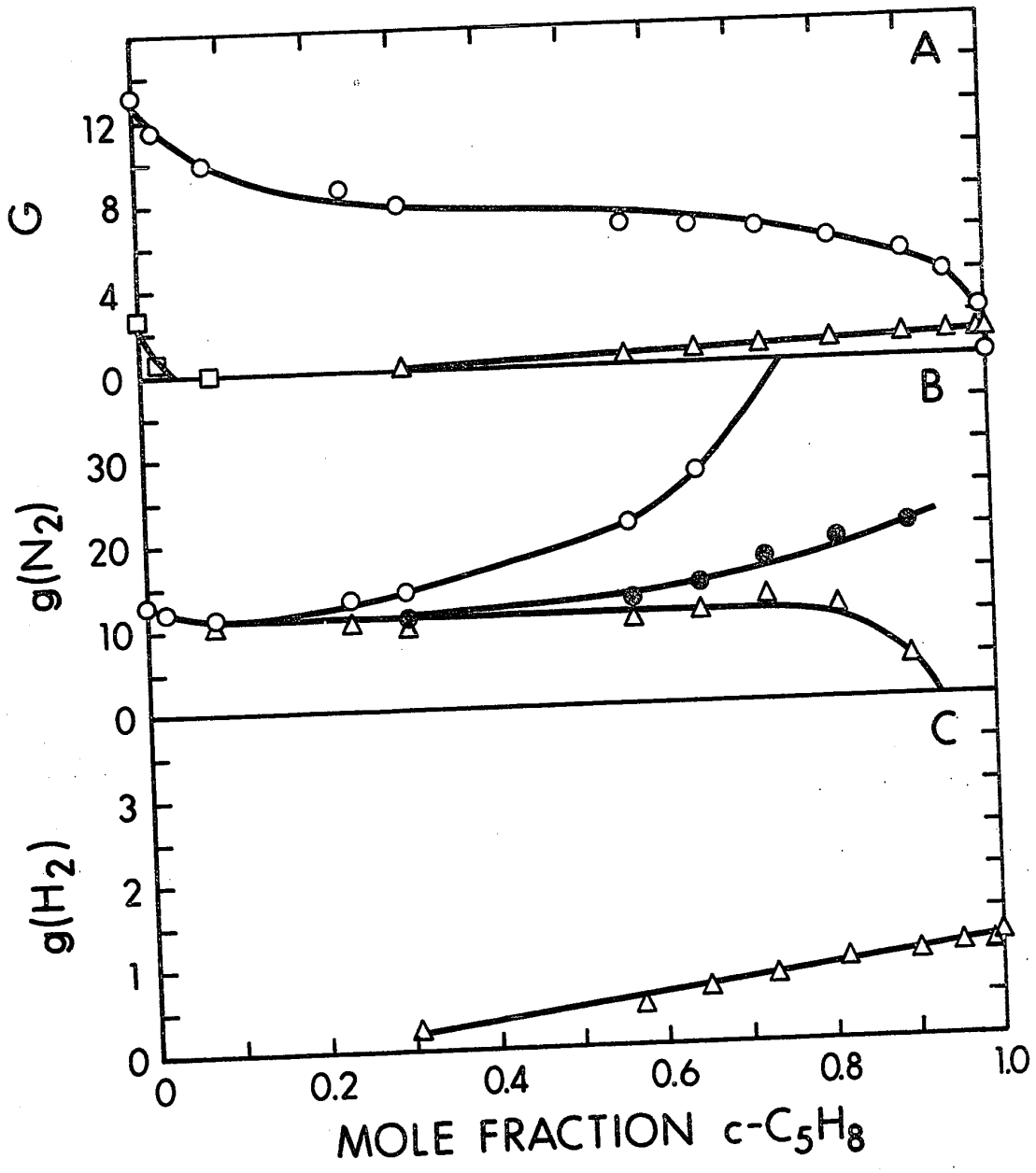

FIGURE III-32 Product Yields with Cyclopentene as the Additive at -90°C.

A ○ Nitrogen, □ Oxygen, △ Hydrogen.

B ○ $G(N_2)^0_N$, ● $g(N_2)^4_N$, △ $g(N_2)^5_N$.

C △ Hydrogen.

TABLE III-34

G Values Using Cyclopropane as the Additive at -90°C

Mole Fraction of Additive	$G(N_2)$	$G(O_2)$	$G(H_2)$	$g(N_2)_N^0$	$g(N_2)_N^4$	$g(N_2)_N^5$	$g(H_2)$
0.015	12.4	1.5	0.0	12.6	12.5	12.5	0.0
0.038	11.3	0.70	0.0	11.8	11.6	11.6	0.0
0.068	10.4	0.30	0.0	11.2	10.9	10.8	0.0
0.242	8.3	0.0	0.10	11.2	9.8	9.5	0.39
0.640	7.1	0.0	0.40	20.7	13.0	11.0	0.61
0.709	7.0	0.0	0.40	25.	14.8	12.2	0.55
0.801	6.3	0.0	0.50	34.	16.2	11.8	0.62
0.850	5.7	0.0	0.55	41.	16.5	10.3	0.64
0.900	5.3	0.0	0.64	57.	17.6	7.8	0.71
0.949	3.6	0.0	0.70	77.	(-4.5)	(-24.8)	0.74
0.989	2.7	0.0	0.85	264.	(-128.)	(-226.)	0.86
1.000	0.0	0.0	1.1	0.0	0.0	0.0	1.1

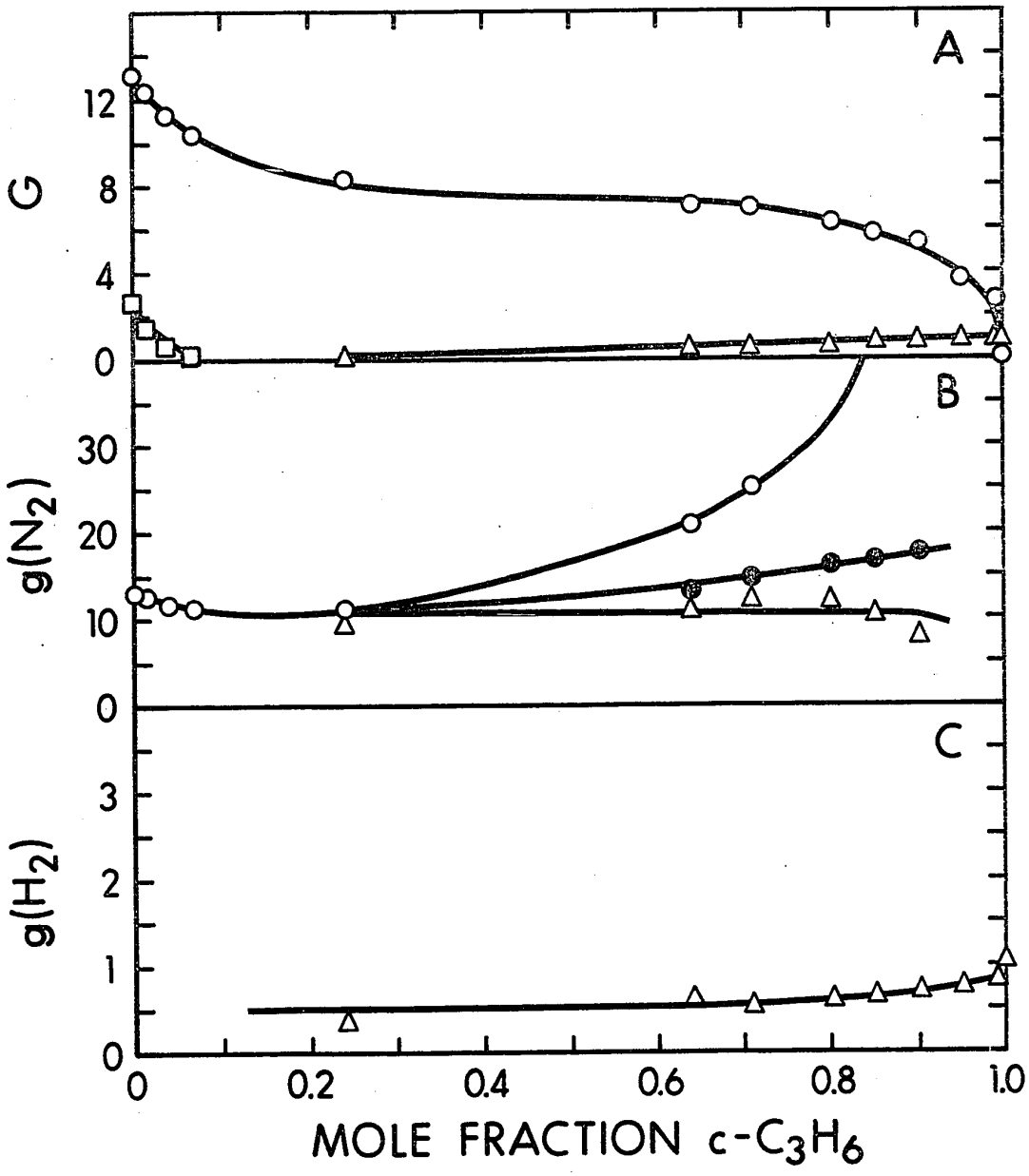

FIGURE III-33 Product Yields Using Cyclopropane as the Additive at -90°C.

A	O	Nitrogen,	□	Oxygen,	Δ	Hydrogen.
B	O	$g(N_2)_N^0$,	●	$g(N_2)_N^4$,	Δ	$g(N_2)_N^5$.
C	Δ	Hydrogen.				

$G(N_2)$ curve for cyclpentene. At 0.07 mole fraction $G(O_2)$ decreases to zero.

In Figure III-33B, the $g(N_2)_N^5$ curve is fairly constant and yields negative values at high cyclopropane concentrations.

The $g(H_2)$ value for the pure additive is 1.1, and after an initial decrease the curve levels out to a limiting value of 0.5 g units.

(h) Miscellaneous

(i) Toluene

The results are reported in Table III-35 and Figure III-34.

In Figure III-34A, the $G(N_2)$ curve decreases steadily with increasing concentrations. No oxygen was detected at 0.06 mole fraction of toluene.

The $g(N_2)_N^4$ curve decreases initially then increases smoothly along the concentration range.

The results for the nitrogen dioxide determinations are given in Table III-31 and Figure III-30B. At 0.04 mole fraction addition of toluene no nitrogen dioxide was detected.

(ii) 1,3-Butadiene

The results are presented in Table III-36 and Figure III-35.

A sharp initial decrease in the $G(N_2)$ curve occurs (Figure III-35A), and the curve is lower than the $G(N_2)$

TABLE III-35

G Values Using Toluene as the Additive at -90°C

Mole Fraction of Additive	$G(N_2)$	$G(O_2)$	$g(N_2)_N^0$	$g(N_2)_N^4$	$g(N_2)_N^5$
0.016	13.0	1.1	13.5	13.4	13.3
0.061	10.8	0.0	12.4	11.8	11.7
0.120	10.3	0.0	13.6	12.3	12.0
0.273	8.4	0.0	15.6	12.2	11.3
0.334	8.6	0.0	18.3	13.7	12.6
0.408	7.3	0.0	18.7	12.5	10.9
0.590	6.7	0.0	29.	15.5	12.3
0.813	5.5	0.0	60.	20.3	10.4
0.830	5.0	0.0	60.	15.6	4.5
0.899	4.5	0.0	95.	14.2	(-6.0)
0.942	3.9	0.0	148.	0.21	(-37.)
1.000	0.0	0.0	0.0	0.0	0.0

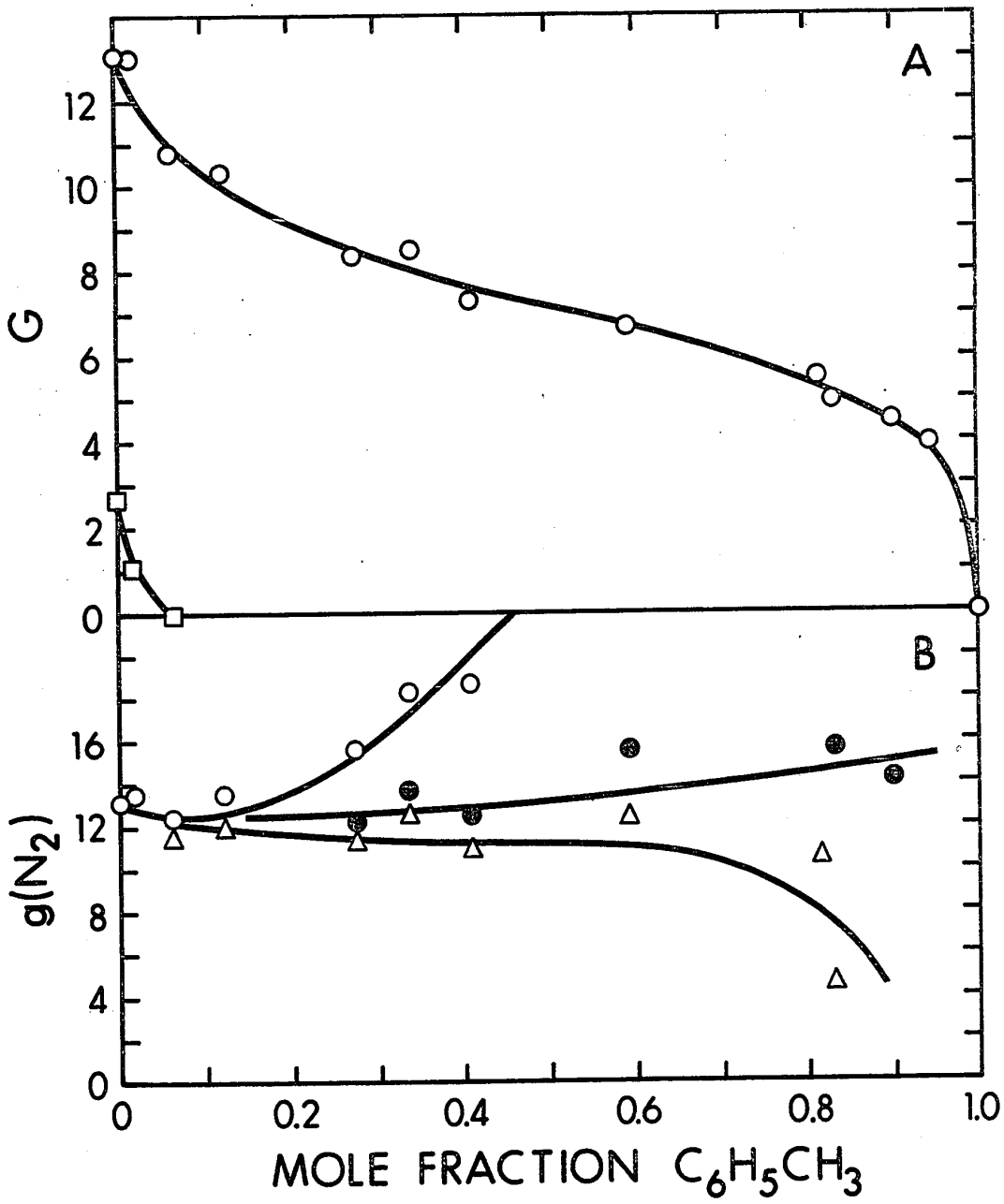

FIGURE III-34 Product Yields Using Toluene as the Additive at -90°C.

A ○ Nitrogen, □ Oxygen.

B ○ $g(N_2)_N^0$, ● $g(N_2)_N^4$, △ $g(N_2)_N^5$.

TABLE III-36

G Values Using 1,3-Butadiene as the Additive at -90°C

Mole Fraction of Additive	$G(N_2)$	$G(O_2)$	$g(N_2)_N^0$	$g(N_2)_N^2$	$g(N_2)_N^3$
0.017	11.6	0.48	11.9	11.8	11.8
0.075	10.4	0.0	11.5	11.3	11.2
0.155	8.9	0.0	11.1	10.6	10.3
0.247	8.0	0.0	11.6	10.7	10.3
0.255	7.6	0.0	11.1	10.2	9.7
0.619	4.6	0.0	14.7	10.3	8.0
0.718	3.8	0.0	16.8	9.8	6.4
0.806	3.2	0.0	21.2	9.9	4.2
0.870	2.6	0.0	26.	7.7	(-1.0)
0.935	1.7	0.0	36.	(-3.0)	(-23.)
0.988	0.72	0.0	81.	(-144.)	(-256.)
1.000	0.0	0.0	0.0	0.0	0.0

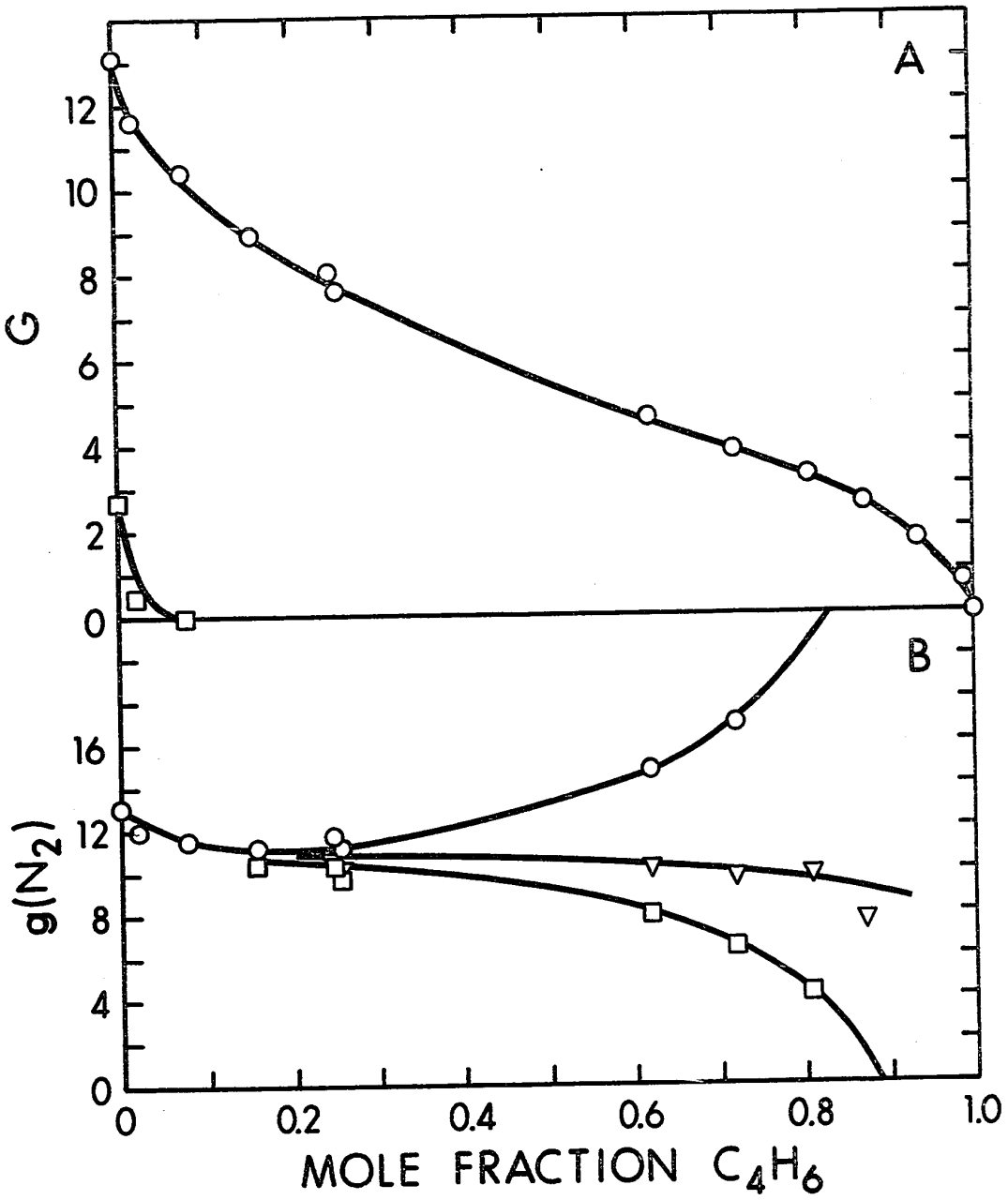

FIGURE III-35 Product Yields with 1,3-Butadiene as the Additive at -90°C.

A ○ Nitrogen, □ Oxygen.

B ○ $g(N_2)^0_N$, ▽ $g(N_2)^2_N$, □ $g(N_2)^3_N$.

curve for 1-butene (Figure III-12A and Table III-13). The electron scavenging efficiency of nitrous oxide is therefore less in a conjugated diene than a mono-olefin. In Figure III-35B, the $g(N_2)_N^2$ curve yields negative values at high concentrations of the diene.

(iii) Neohexane

The results are expressed in Table III-37 and Figure III-36.

$G(O_2)$ decreases to zero at 0.09 mole fraction addition of neohexane. The $G(N_2)$ curve initially decreases quickly then levels off until around 0.95 mole fraction where it drops sharply (Figure III-36A).

In Figure III-36B, $g(N_2)_N^5$ remains constant along most of the concentration range.

The values of hydrogen and methane for the pure additive are 1.8 and 0.8 respectively (Figure III-36C. No nitrogen dioxide (Figure III-30A) was detected at a neohexane concentration of 0.06 mole fraction.

(i) Water Analysis

(i) Using n-Butane as the Additive

The results are given in Table III-38 and Figure III-37.

On small additions of the alkane, the $G(H_2O)$ curve increases rapidly, reaching a plateau level of around 11.4

TABLE III-37

G Values Using Neohexane as the Additive at -90°C

Mole Fraction of Additive	$G(N_2)$	$G(O_2)$	$G(H_2)$	$G(CH_4)$	$g(N_2)_N^0$	$g(N_2)_N^4$	$g(N_2)_N^5$	$g(H_2)$	$g(CH_4)$
0.012	12.9	0.82	0.0	0.0	13.2	13.1	13.1	0.0	0.0
0.048	12.1	0.20	0.0	0.0	13.5	13.0	12.9	0.0	0.0
0.085	11.3	0.0	0.0	0.0	13.7	12.9	12.7	0.0	0.0
0.151	9.4	0.0	0.0	0.0	13.3	11.6	11.2	0.0	0.0
0.344	8.3	0.0	0.67	0.16	18.2	13.4	12.2	1.2	0.30
0.591	6.9	0.0	0.80	0.16	30.	16.4	13.1	1.0	0.21
0.698	6.6	0.0	0.88	0.36	41.	20.0	14.8	1.0	0.43
0.803	5.9	0.0	1.2	0.36	60.	23.1	13.8	1.3	0.40
0.850	5.7	0.0	1.1	0.35	79.	27.	14.2	1.2	0.38
0.897	5.6	0.0	1.4	0.38	116.	37.	16.9	1.5	0.40
0.944	4.8	0.0	1.5	0.45	190.	37.	(-1.3)	1.6	0.46
1.000	0.0	0.0	1.8	0.80	0.0	0.0	0.0	1.8	0.80

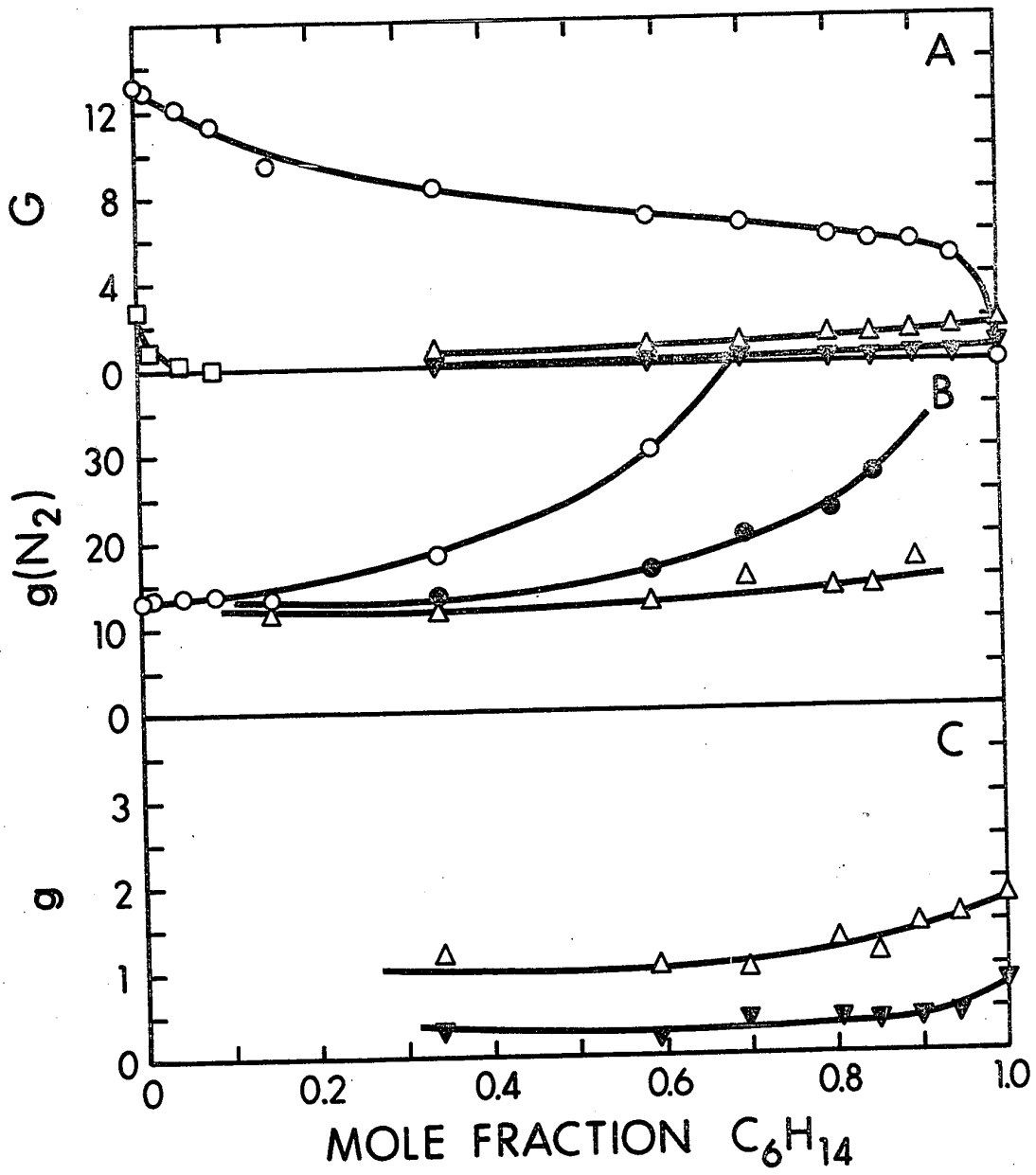

FIGURE III-36 Product Yields with Neohexane as the Additive at -90°C.

A ○ Nitrogen, □ Oxygen, △ Hydrogen, ▼ Methane.

B ○ $g(N_2)^0_N$, ● $g(N_2)^4_N$, △ $g(N_2)^5_N$.

C △ Hydrogen, ▼ Methane.

TABLE III-38

Determination of $G(H_2O)$ in Nitrous Oxide using n-Butane as the Additive at -90°C

Mole Fraction of Additive	$G(H_2O)$
0.000	0.0
0.026	2.7
0.032	5.3
0.039	5.8
0.046	5.7
0.053	7.3
0.095	9.6
0.144	11.6
0.200	11.0
0.237	11.6

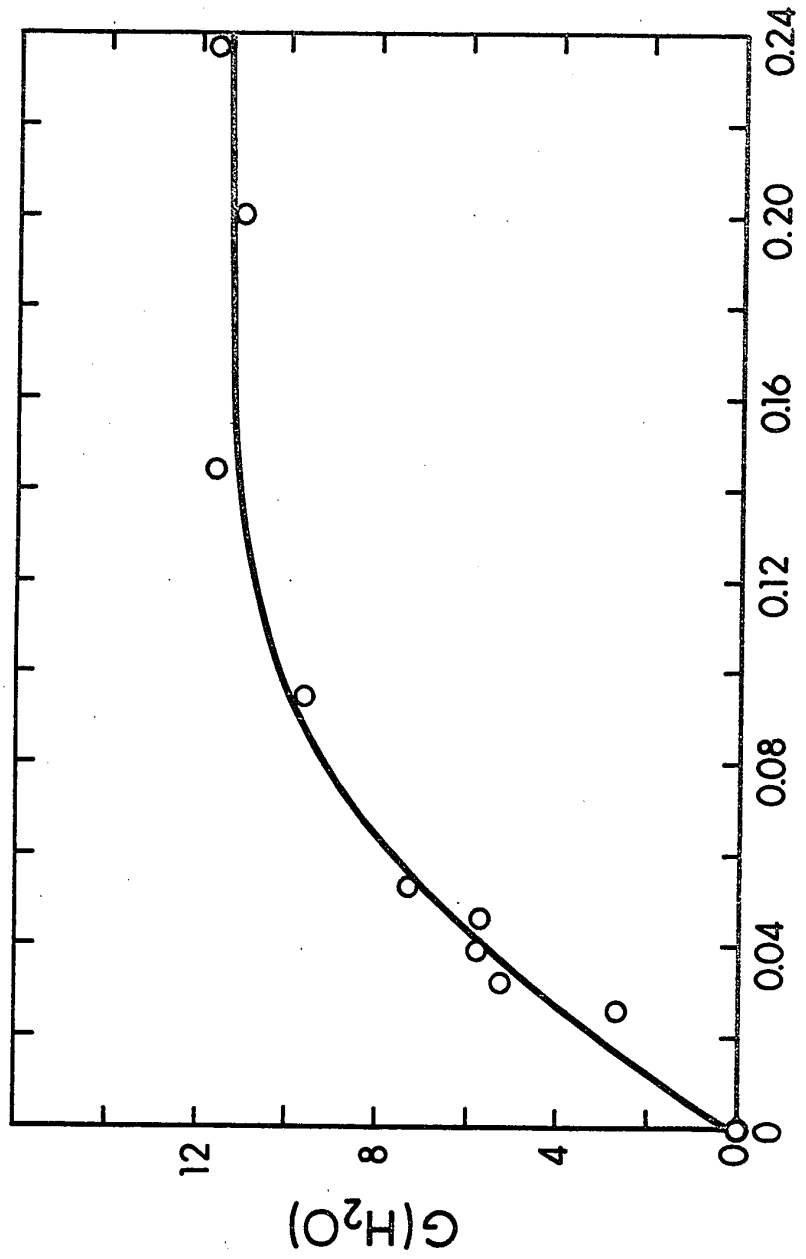

FIGURE II-37 Yield of G(H_2O) Upon Addition of n-Butane at -90°C

O Water.

units at about 0.15 mole fraction addition (Figure III-34).

(ii) Using 1-Butene as the Additive

The results are presented in Table III-39 and Figure III-38.

In Figure III-38, the $G(H_2O)$ curve levels out at around 11.2 at about 0.11 mole fraction of 1-butene. The initial increase of $G(H_2O)$ is steeper for the alkene than for the alkane.

(iii) Alcohol Detection

In both, the above systems, products such as alcohols were expected (81), but none were observed. Therefore, a special column was constructed giving optimum conditions for the detection of alcohols. It is concluded that G(ethanol) < 0.01, G(propanols) < 0.08 and G(butanols) < 0.3.

TABLE III-39

Determination of $G(H_2O)$ in Nitrous Oxide using 1-Butene as the Additive at -90°C

Mole Fraction of Additive	$G(H_2O)$
0.000	0.0
0.022	5.9
0.034	5.4
0.046	7.8
0.077	10.7
0.089	9.0
0.107	10.9
0.117	11.3
0.136	11.1
0.170	10.9
0.232	11.3

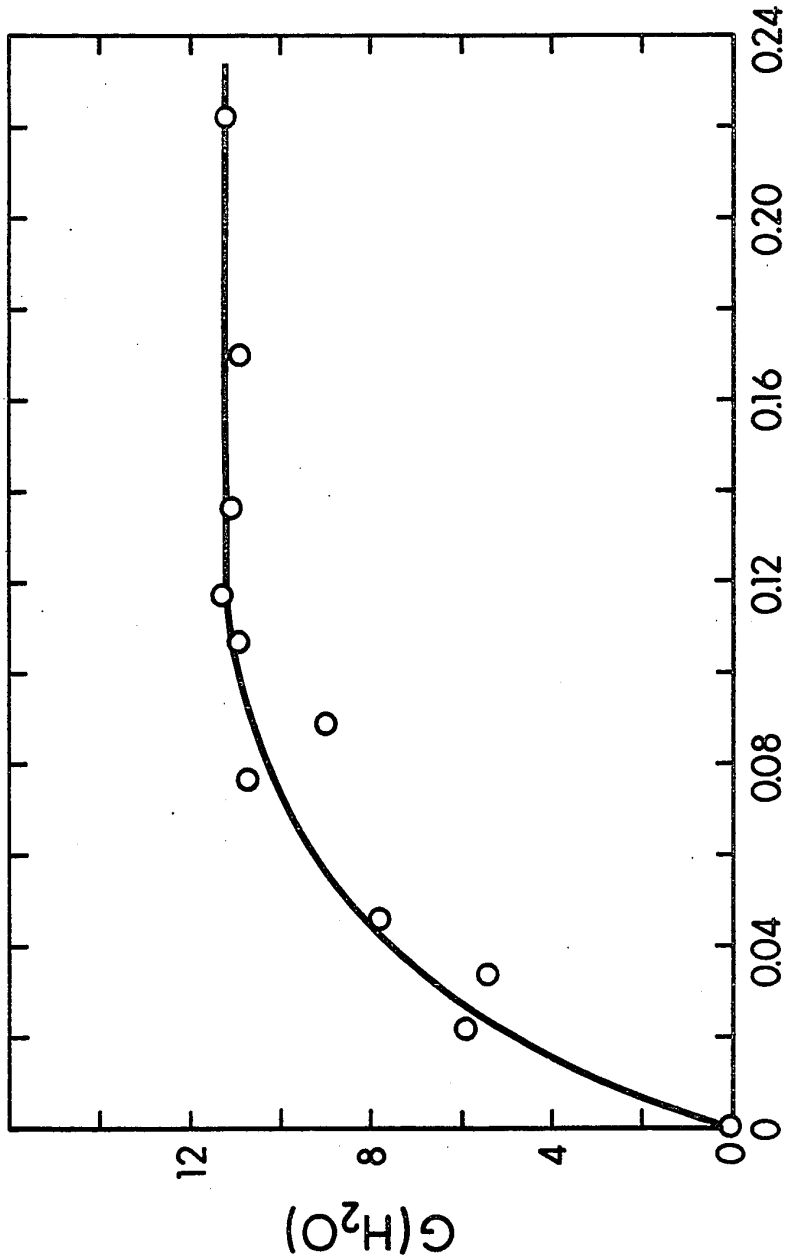

FIGURE III-38 Yield of $G(H_2O)$ Upon Addition of 1-Butene at -90°C
O Water.

D I S C U S S I O N

A. LIQUID NITROUS OXIDE

The G values obtained for the radiolysis of liquid nitrous oxide at -90°C are $G(N_2) = 13.1 \pm 0.2$, $G(O_2) = 2.6 \pm 0.1$, and $G(NO_2) = 5.6 \pm 0.2$.

A mechanism given below is consistent with the results obtained. Some of the included reactions were proposed earlier for the pyrolysis (93,94), photolysis (10,43) and radiolysis (38, 48) of gaseous nitrous oxide. The yield of nitrogen from ionic reactions comes from a novel combination of N_2O^- and N_2O^+ ions in the neutralisation reaction. Another mechanism involving reactions of the O^- ions is also compatible with the results and is included.

$$N_2O \xrightarrow{\sim\sim} N_2O^+ + e^- \quad (39)$$

$$\xrightarrow{\sim\sim} N_2O^* \quad (40)$$

$$N_2O + e^- \longrightarrow N_2O^- \quad (3)$$

$$N_2O^+ + N_2O^- \longrightarrow NO + NO + N_2 \quad (41)$$

$$N_2O^+ + N_2O^- \longrightarrow N_2 + O_2 + N_2 \quad (42)$$

$$N_2O^* \longrightarrow N_2 + O \quad (19)$$

$$O + O + M \longrightarrow O_2 + M \quad (21)$$

$$2NO + O_2 \longrightarrow 2NO_2 \quad (43)$$

The W value of gaseous nitrous oxide is 32.9 eV (23), thus a G(ionisation) value of 3 is incorporated into gas phase mechanisms. As previously discussed, there are

marked differences between processes in the gas and liquid phases. For example, most of the reactive intermediates in the liquid phase undergo geminate recombination and electron affinity values of various species probably differ due to the solvation energies of the species involved (4). Ionisation potentials are also reported to be lower in the liquid phase (24). It is therefore possible that G(ionisation) will be higher in the liquid phase. Three values of G(ionisation) are chosen for trial; these being 3, 4 and 5, and are included in the mechanism in Table IV-1. The G(ionisation) values of 4 and 5 give the better agreement with the data obtained from the radiolysis of nitrous oxide and additive solutions, and will be discussed later.

Experimental evidence gathered so far is slightly weighted towards the formation of the N_2O^- ion, and Mechanism I in Table IV-1 is preferred. This mechanism is quite consistent with the results obtained from additive studies. Another mechanism (Mechanism II) invoking the dissociative attachment of electrons to nitrous oxide is also compatible with the results from the radiolysis of pure liquid nitrous oxide, and is given in Table IV-2.

TABLE IV-1

Material Balance for Mechanism I Using G(ionisation) Values 3, 4 and 5 Respectively

		$G(e^-)=3$ G(step)	$G(e^-)=4$ G(step)	$G(e^-=5)$ G(step)
(39)	$N_2O \rightsquigarrow N_2O^+ + e^-$	3.0	4.0	5.0
(40)	$\rightsquigarrow N_2O^*$	9.9	7.9	5.9
(3)	$N_2O + e^- \longrightarrow N_2O^-$	3.0	4.0	5.0
(41)	$N_2O^+ + N_2O^- \longrightarrow NO + NO + N_2$	2.8	2.8	2.8
(42)	$N_2O^+ + N_2O^- \longrightarrow N_2 + O_2 + N_2$	0.2	1.2	2.2
(19)	$N_2O^* \longrightarrow N_2 + O$	9.9	7.9	5.9
(21)	$O + O + M \longrightarrow O_2 + M$	5.0	4.0	3.0
(43)	$2NO + O_2 \longrightarrow 2NO_2$	2.8	2.8	2.8
	Resulting $G(N_2)$	13.1	13.1	13.1
	$G(O_2)$	2.4	2.4	2.4
	$G(NO_2)$	5.6	5.6	5.6

TABLE IV-2

Material Balance for Mechanism II (Invoking O^- Ions) Using G(ionisation) Values of 3, 4 and 5 Respectively

		$G(e^-)=3$ G(step)	$G(e^-)=4$ G(step)	$G(e^-)=5$ G(step)
(39)	$N_2O \rightsquigarrow N_2O^+ + e^-$	3.0	4.0	5.0
(40)	$\rightsquigarrow N_2O^*$	6.9	3.9	0.9
(27)	$N_2O + e^- \longrightarrow N_2 + O^-$	3.0	4.0	5.0
(28)	$O^- + N_2O \longrightarrow N_2 + O_2^-$	0.2	1.2	2.2
(29)	$O^- + N_2O \longrightarrow NO + NO^-$	2.8	2.8	2.8
(44)	$N_2O^+ + O_2^- \longrightarrow N_2O^* + O_2$	0.2	1.2	2.2
(45)	$N_2O^+ + NO^- \longrightarrow N_2O^* + NO$	2.8	2.8	2.8
(19)	$N_2O^* \longrightarrow N_2 + O$	9.9	7.9	5.9
(21)	$O + O + M \longrightarrow O_2 + M$	5.0	4.0	3.0
(43)	$2NO + O_2 \longrightarrow 2NO_2$	2.8	2.8	2.8
	Resulting $G(N_2)$	13.1	13.1	13.1
	$G(O_2)$	2.4	2.4	2.4
	$G(NO_2)$	5.6	5.6	5.6

Nitrogen atom reactions say from the decomposition of N_2O^+, are not included in these mechanisms. Gorden and Ausloos, in the gas phase radiolysis of $^{15}N^{14}NO$ and NO, estimated the yield of nitrogen atoms to be roughly 1 G unit (37). Oka et al (95,96) detected only "small quantities" of nitrogen containing products such as hydrogen cyanide in the nitrous oxide/ethane system. Therefore, a reasonable conclusion is that processes involving nitrogen atoms play only a minor role in the radiolysis of nitrous oxide.

Takao and Shida (50) suggested the following reaction to explain their results.

$$N_2O^+ + N_2O^- \rightarrow N_2 \text{ and other products} \qquad (46)$$

The positive ion N_2O^+, formed during the radiolysis of nitrous oxide has been confirmed as a primary product by the electron spin resonance studies of Smith and Seddon (15,16) and the existence of a long-lived N_2O^- ion is supported by mounting experimental evidence.

For example, Paulson (54) determined an ion of mass 44 and identified it as N_2O^-. Then Fehsenfeld (97) observed the formation of N_2O^- when O^- interacted with N_2 in a flow system at -193°C. Ferguson et al (98) rebuked the formation of N_2O^- at thermal energies, since the production of a stable bent N_2O^- ion from the linear neutral molecule should require a rather large activation energy. Further

indications to the existence of N_2O^- came from Warman and Fessenden (6) and Phelps and Voshall (5) who demonstrated that a three-body mechanism occurred for the electron capture process by nitrous oxide.

$$e^- + 2N_2O \rightarrow N_2O^- + N_2O \qquad (31)$$

Chantry (99) concluded from his results that at the lower energies the bending mode of vibration is excited, thus lowering the energy necessary for the formation of N_2O^-. Bardsley (100) also discussed the existence of a stable bent N_2O^- ion and its possible energy states. Chaney and Christophorou (101), using electron swarm techniques, determined the formation of N_2O^- as a primary product. Later work by Paulson (102) confirmed the existence of the N_2O^- ion proposing that the ion is formed *via* a charge transfer reaction.

$$NO^- + N_2O \rightarrow NO + N_2O^- \qquad (47)$$

The geometric restrictions towards the formation of N_2O^- may not be quite as severe as those imposed by Ferguson *et al* (98), since Pearson (103), using the rules originated by Walsh (104), pointed out that the first excited state of neutral nitrous oxide assumes the shape of a ground state nitrogen dioxide molecule. The latter is a bent molecule, having an apex angle of 143° (105). Recently Wentworth *et al* (106) obtained a value of 10.4 $\pm$ 0.4 kcal for the

activation energy of dissociative attachment of thermal electrons to nitrous oxide. The energy is thought to be that necessary for the attachment of a thermal electron to the bent form of the neutral nitrous oxide molecule.

Dainton, O'Neill and Salmon (8) established the existence of a stable N_2O^- ion, and gave its lifetime in liquid cyclohexane at 2×10^{-5} sec. Another determination (37) considered that the gas phase lifetime of N_2O^- with respect to dissociation is greater than 10^{-4} sec.

Mechanism II involves the dissociative attachment of electrons to nitrous oxide.

$$e^- + N_2O \longrightarrow N_2 + O^- \qquad (27)$$

Various workers (51, 107,108) have determined that, in the gas phase, O^- is indeed one of the primary negative ions formed. The cross-section for dissociative attachment as a function of electron energy has two peaks, one at low energy (~0.0 eV to ~1.2 eV) and the other at 2.2 eV (108), but the allowed threshold for the appearance of the O^- ion is 0.21 eV.

$$D_{(N_2-O)} - EA_{(O)} = 1.67 - 1.46 = 0.21 \text{ eV}$$

where $D_{(N_2-O)}$ is the bond energy of the N-O bond (109)

$EA_{(O)}$ is the electron affinity of the oxygen atom (110)

Kaufman (109) suggested that the dissociative electron attachment from the higher vibrational levels of nitrous oxide could account for the appearance of O^- at the lower energies, and Schulz (51) postulated that the second intense peak came from dissociative attachment *via* a complex negative ion.

Perhaps Mechanism I and II occur simultaneously in the radiolysis of liquid oxide, with both processes contributing towards the overall mechanism.

(a) Structures of Nitrous Oxide and Its Ions Using Mechanism I.

(i) Nitrous Oxide

Nitrous oxide is a linear molecule in its ground state, containing sixteen valence electrons (105). It possesses a small dipole moment of 0.17 D, and has the following bond lengths.

$$N \xrightarrow{1.13\text{Å}} N \xrightarrow{1.19\text{Å}} O$$

The N-N bond distance of 1.13Å is between a triple N≡N bond distance of 1.1Å and a double -N=N- bond length of 1.25Å. The N-O bond length is 1.19Å between the distances expected for a double -N=O bond 1.15Å and a single =N-O- bond ~1.4Å (111). The molecule is not satisfactorily represented by any one single valence bond structure. Therefore it

is expedient to use the valence bond structures to account for the properties of nitrous oxide. The molecule is best represented by the two main resonance hybrids given below.

I II

(ii) N_2O^+

From the two basic structures I and II, a minimum of two forms of the positive ion can be constructed.

III IV

The linear structure of N_2O^+ is well established, having fifteen valence electrons (105) and being isoelectronic with CO_2^+ and NCS (112). In these latter compounds the unpaired electron is proposed to be concentrated at either end of the molecule with negligible spin density on the central atom (113).

(iii) N_2O^-

Two structures can also be derived for the negative ion.

V VI

The structure of N_2O^- is bent with an apex angle of 134°; it has seventeen electrons and is isoelectronic with nitrogen dioxide (105).

(iii) Combination of the Two Ions

It is interesting to note that in both the negative and positive ions, the free radical ends do not exist in the same positions as the charges, and it is the former that react.

Permutations of these ions, by combining the free radical ends of each species, result in the formation of the products, nitrogen, oxygen and nitric oxide.

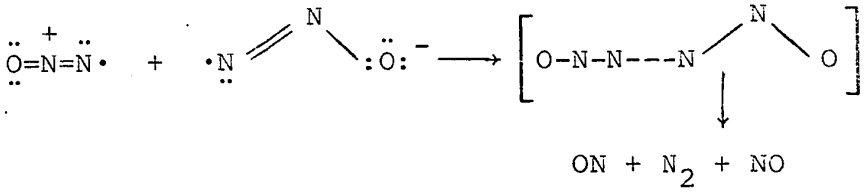

ON + N_2 + NO (48)

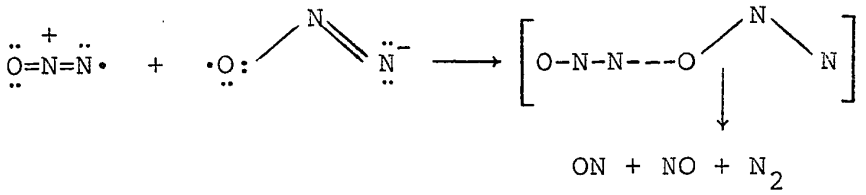

ON + NO + N_2 (49)

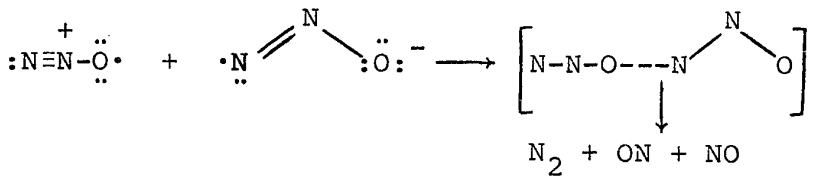

$N_2 + ON + NO$ (50)

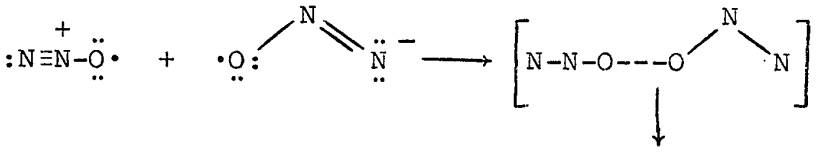

$N_2 + O_2 + N_2$ (51)

If each permutation had an equal probability of reacting, then the following material balance would occur.

$$4N_2O^+ + 4N_2O^- \longrightarrow 6NO + 5N_2 + O_2 \qquad (52)$$

Referring to Table IV-1, the mechanism incorporating a G(ionisation) of 4 has a material balance close to the above.

B. ANALYSIS OF THE ADDITIVE STUDIES

(a) Alkanes

The effects of liquid alkanes on the radiolysis of liquid nitrous oxide are displayed in Figures III-5A to III-9A and also Figure III-36A. Subtraction of the contribution of the electrons from the alkanes to the nitrogen yields gave the curves in Figures III-5B through III-9B and Figure III-36B. From the latter curves, it is observed that the corrected curve $g(N_2)_N^5$ affords the best "plateau"

along most of the concentration range, and this is the case for all the alkanes studied.

The decreases in the nitrogen, oxygen and nitrogen dioxide yields upon addition of the alkanes are presented in Table IV-3a. Four of the alkanes, neohexane, n-hexane, n-butane and propane show nitrogen decreases, $\Delta g(N_2)$, of 1-2 g units, whereas ethane shows a decrease of 2-3 units. A correlation between these calculated results, derived from experimental data, and the theoretical prediction using Mechanism I may be made.

A charge transfer reaction between N_2O^+ and the alkane molecule RH is quite possible, due to the lower ionisation potential of the latter (Table IV-4).

$$N_2O^+ + RH \longrightarrow N_2O + RH^+ \qquad (7)$$

Nitrous oxide will scavenge electrons generated in the radiolytic solution, forming the negative ion N_2O^-, so a neutralisation reaction between the two ions proceeds.

$$N_2O^- + RH^+ \longrightarrow N_2O^* + RH \qquad (53)$$

The excited nitrous oxide molecule then decomposes.

$$N_2O^* \longrightarrow N_2 + O \qquad (19)$$

Referring to Mechanism I in Table IV-1 and using G(ionisation) = 4, elimination of reactions (41) and (42) affords

TABLE IV-3a

Decrease in Product Yields with Addition of the Alkanes

Compound	$\Delta g(N_2)$ using the $g(N_2)_N^5$ curve	$\Delta g(O_2)$ at 0.1 mole fraction alkane	$\Delta g(NO_2)$ at 0.1 mole fraction alkane
neo-C_6H_{14}	1-2	2.7	(5.6)
n-C_6H_{14}	1-2	2.7	5.6
n-C_4H_{10}	1-2	2.7	5.6
C_3H_8	1-2	2.7	(5.6)
C_2H_6	2-3	2.7	5.6

TABLE IV-3b

G Values Obtained for the Pure Alkanes

Compound	$G(H_2)$	$G(H_4)$
neo-C_6H_{14}	1.8	0.8
n-C_6H_{14}	5.0	n.d.
n-C_4H_{10}	5.4	n.d.
C_3H_8	4.3	0.47
C_2H_6	4.8	0.35

TABLE IV-4

Ionisation Potentials of the Alkanes (119)

Compound	Ionisation Potential eV
neo-C_6H_{14}	10.05
n-C_6H_{14}	10.17
n-C_4H_{10}	10.63
C_3H_8	11.07
C_2H_6	11.65
(N_2O	12.89)

a decrease of 5.2 units of nitrogen. The substitution of reaction (7) followed by reaction (53) gives 4 g units of nitrogen. Hence a net decrease of 1.2 units of nitrogen ensues. Similarly, the use of G(ionisation) = 5 would result in a net nitrogen decrease of 2.2 g units. When compared to the calculated decreases, one finds that the theoretical decrease of 1.2 g units of nitrogen, using G(ionisation) = 4, is in reasonable accord with the experimental results for four of the alkanes and only ethane displays a greater calculated decrease. However, the decreases are not precise enough to warrant a separate explanation for ethane and until G(ionisation) is accurately known, an exact conclusion cannot be reached. Further support for Mechanism I can be made by analysing the decreases in the yields of oxygen and nitrogen dioxide with increasing alkane concentration. Thus the addition of a few mole % of an alkane to nitrous oxide eliminates the yields of oxygen and nitrogen dioxide. These observations may be rationalised in terms of Mechanism I as substitution of reaction (53) in place of reactions (41) and (42) essentially cancels all the nitric oxide previously formed and also decreases the oxygen yield. Reactions of oxygen atoms with hydrocarbons are favoured (114,115), so the combination of oxygen atoms, generated in reaction (21), to form oxygen will not occur. Subsequent reactions of oxygen atoms with hydrocarbons are

discussed later. The above results therefore, are quite compatible with Mechanism I.

Referring to Figures III-5A to III-9A for the unbranched alkanes the increase in the nitrogen yield coupled with a decrease in the hydrogen yield upon the addition of nitrous oxide to the alkanes is due to the fact that nitrous oxide is an electron scavenger. Some of the electrons initially generated in the alkane are scavenged by nitrous oxide, thereby altering the neutralisation reaction and thus inhibiting hydrogen formation *via* reaction (2).

$$RH \longrightarrow RH^+ + e^- \qquad (1)$$

$$RH^+ + e^- \longrightarrow H_2 + \text{products} \qquad (2)$$

$$e^- + N_2O \longrightarrow N_2O^- \qquad (3)$$

$$N_2O^- + RH^+ \longrightarrow N_2 \text{ but no } H_2 \qquad (4)$$

The rate constant for the reaction of hydrogen atoms with nitrous oxide at 27°C is estimated at 1 litre/mole sec (116). In solution, the larger value of $k(H + N_2O) \approx 10^4$ litre/mole sec (117) could be enhanced by such factors as the large vibration energy of OH and by the polarity of the solvent. Certainly, reactions of hydrogen atoms with nitrous oxide are negligible as $k(H + \text{alkane}) \approx 10^6$ litre/mole sec (118). Hydrocarbon free radicals also do not

react with nitrous oxide to form nitrogen (64,69).

The addition of nitrous oxide to liquid alkanes therefore results in the formation of nitrogen due to the scavenging of electrons and plateaus are indicated around a value of $G(N_2) = 5$. The plateau in the ethane/nitrous oxide system is clearly shown (Figure III-9A), achieving a value of $G(N_2) = 5.2$ at only 0.001 mole fraction of nitrous oxide. This is interesting as it determines that electron scavenging in ethane is more efficient than in the other alkanes.

The G values of hydrogen and methane obtained from the radiolysis of the pure alkanes are presented in Table IV-3b. The $g(H_2)$ curves (Figures III-5C to III-9C) drop sharply initially, then level off reaching a plateau of unscavengable hydrogen (91). In the case of neohexane, increasing concentrations of nitrous oxide have only a slight effect on the $g(H_2)$ and $g(H_4)$ curves (Figure III-36C).

(b) Alkenes

The decreases in the product yields of pure liquid nitrous oxide with increasing alkene concentration are given in Table IV-5a. In the case of 1-hexene, the $g(N_2)^5_N$ curve affords the best plateau (Figure III-10B), thus providing a greater $\Delta g(N_2)$ when compared to the other alkenes studied. The calculated decreases in nitrogen

TABLE IV-5a

Decrease in Product Yields with Addition of the Alkenes

Compound	$\Delta g(N_2)$ using curves (a) $g(N_2)_N^5$	(b) $g(N_2)_N^4$	$\Delta g(O_2)$ at 0.08 mole fraction alkene	$\Delta g(NO_2)$ at 0.08 mole fraction alkene
$1\text{-}C_6H_{12}$	4-5	-	2.7	5.6
$1\text{-}C_4H_8$	-	2-3	2.7	5.6
C_3H_6	-	2-3	2.7	(5.6)
C_2H_4	-	2-3	2.7	5.6

TABLE IV-5b

$G(H_2)$ Values Obtained for the Pure Alkenes

Compound	$G(H_2)$
$1\text{-}C_6H_{12}$	0.80
$1\text{-}C_4H_8$	0.90
C_3H_6	1.0
C_2H_4	1.2

yields using the $g(N_2)_N^4$ curve for 1-butene, propene and ethene are in the range 2-3 g units (Figures III-12B to III-15B). $G(NO_2)$ and $G(O_2)$ decrease to zero with small additions of the alkenes (Table IV-5a).

The nitrogen decreases may be explained using Mechanism I. A charge transfer reaction is feasible between N_2O^+ and the olefin molecule, ol, as all the ionisation potentials of the alkenes studied are in the range 9-11 eV (Table IV-6) and hence are lower than the ionisation potential of nitrous oxide.

$$N_2O^+ + ol \longrightarrow N_2O + ol^+ \qquad (54)$$

This reaction is then followed by a neutralisation reaction.

$$N_2O^- + ol^+ \longrightarrow N_2O^* + ol \qquad (55)$$

However, excited states of alkenes commonly have triplet state energy levels around 4.4 eV (120-123), thus being in the same range as the lower electronic levels of nitrous oxide (11,51,100,105,124,125) so an alternative to reaction (55) may occur.

$$N_2O^- + ol^+ \longrightarrow N_2O + ol^* \qquad (56)$$

Thus replacement of reactions (41) and (42) by reactions (54) and (55) gives a decrease of 5.2 g units of nitrogen. The increase in nitrogen from reaction (55) now depends on the extent of reaction (56). If, for example,

TABLE IV-6

Ionisation Potentials (119) and Electron Affinities of the Alkenes

Compound	Ionisation Potential eV	Electron Affinity eV
1-C_6H_{12}	9.46	
1-C_4H_8	9.58	
C_3H_6	9.73	
C_2H_4	10.51	-1.69[a]
(N_2O	12.89)	

[a] J. R. Hoyland and L. Goodman, J. Chem. Phys., 36, 21 (1962).

reaction (55) eventually yields 3 g units of nitrogen, then the net decrease is 2.2 units. In the case of the alkanes, a reaction similar to reaction (56) is not favoured as the lowest triplet state energy levels in these compounds are as high as 9 eV (122,126).

The calculated decreases in the nitrogen yields from the experimental data are in the range 2-3 g units. Therefore, reaction (56) which results in no nitrogen formation is proposed to occur in the radiolysis of alkene/nitrous oxide solutions.

As with the alkanes, the addition of alkenes to nitrous oxide eliminates the yields of nitrogen dioxide and oxygen. Again these results are compatible with Mechanism I as replacement of reactions (41) and (42) by reactions (55) and (56) removes all the nitric oxide.

The addition of nitrous oxide to liquid alkenes results in nitrogen formation from the scavenging of electrons by nitrous oxide. However, comparing the $G(N_2)$ curves on the right-hand side, for the alkanes (Figures III-5A to III-9A) and the alkenes (Figures III-10A to III-15A), it is clearly shown that the latter curves are lower than their saturated counterparts.

Sato et al (65) determined that the electron scavenging efficiency of nitrous oxide is lower in alkenes than in alkanes. Schmidt and Allen (127) found that the ion-electron separation distances in the spurs are less in

alkenes than in alkanes. Hence a smaller ion-electron distance leads to a shorter geminate neutralisation time, thus decreasing the possibility of electron capture by nitrous oxide. However, several workers (65,75) have suggested that mono-olefins provide shallow traps for electrons in liquid alkanes, and these electrons may be scavenged by nitrous oxide, eventually leading to nitrogen formation. This conclusion appears to be rather anomalous in light of the present work, as nitrogen yields in alkenes are markedly lower than those in alkanes. Recent work (128) has confirmed that the addition of olefins to alkane solutions has no effect on the nitrogen yield.

In the last year, Robinson and Freeman (83) have studied the effects of nitrous oxide on alkenes and alkanes, and concluded that the smaller efficiency of electron scavenging in such alkenes is largely due to their shorter ion-electron distances. They suggested that these smaller separation distances might indicate a greater energy transfer efficiency from the secondary electrons of the alkenes and this transfer efficiency in the alkenes must be due to the π bond. The π bond, from their results, decreases the electron scavenging efficiency by a factor of 12 in the C_3 hydrocarbons, and by a factor of roughly 40 in the C_2 hydrocarbons. Such marked differences between the olefin and its saturated counterpart increase with decreasing chain length, and hence a correlation

between electron ranges and the nature of polarisability of the molecules was made.

Results from the $g(H_2)$ values (Figures III-10C to III-15C) indicate that the increasing addition of nitrous oxide to liquid alkenes has little effect on the yield of hydrogen, again deviating from the behaviour of their saturated counterparts.

(c) Water Analysis

As previously mentioned, oxygen atoms react readily with hydrocarbons (114,115), resulting in the formation of oxygen-containing products. In the present work, n-butane and 1-butene were added to liquid nitrous oxide and after radiolysis, a specific study was carried out to find any oxygen-containing products formed. The principal product determined was water, other expected products such as alcohols and carbonyl compounds were absent, at least to the limits of detectability of the system ($G(\text{ethanol}) < 0.01$, $G(\text{propanols}) < 0.08$ and $G(\text{butanols}) < 0.3$).

The results obtained are shown in Figure III-37 for the n-butane/nitrous oxide system, and in Figure III-38 using 1-butene as the additive. The $G(H_2O)$ curves, in both cases, level out around a value of 11. These observations may be rationalised in terms of Mechanism I.

(i) n-Butane

Referring back to reaction (53), the neutralisation of RH^+ with N_2O^- results in the formation of an excited nitrous oxide molecule which subsequently decomposes.

$$N_2O^* \longrightarrow N_2 + O \qquad (19)$$

The oxygen atom thus formed can abstract a hydrogen atom from the alkane molecule forming the hydroxyl radical, which undergoes a further hydrogen abstraction reaction, hence forming water.

$$O + RH \longrightarrow OH + R\cdot \qquad (57)$$

$$OH + RH \longrightarrow H_2O + R\cdot \qquad (20)$$

A total $G(H_2O)$ of 4 can be expected for this process. However, remembering that the yield of oxygen decreases to zero upon alkane addition, then reaction (19) in Mechanism I generates further oxygen atom which can undergo like reactions given above to form water. Thus computing the total $G(H_2O)$ value from these two sources gives a theoretical yield of 12 units, in good accord with the experimental results.

(ii) 1-Butene

A similar approach may be made using 1-butene as the additive. Thus reaction (55) results in the formation of

an excited nitrous oxide molecule.

$$N_2O^- + ol^+ \longrightarrow N_2O^* + ol \qquad (55)$$

However, a minor reaction leading to the formation of ol^*, an excited alkene molecule, is proposed to occur, and will reduce the yield of N_2O^*.

$$N_2O^- + ol^+ \longrightarrow N_2O + ol^* \qquad (56)$$

Consideration of the $G(N_2)$ values of the alkenes indicate that reaction (55) yields a $G(N_2O^*)$ of about 3 thus giving $G(H_2O) \approx 3$ from this source. Coupling this value with the total $G(H_2O)$ obtained *via* reaction (19) affords a net $G(H_2O) \approx 11$, comparing well with the observed result.

From comparing the two graphs (Figure III-37 and Figure III-38), it is noted that the $G(H_2O)$ rising slope in the 1-butene/nitrous oxide system is steeper than that in the *n*-butane/nitrous oxide system.

This is perhaps indicative of the relative rates of reaction of oxygen atoms with alkanes and alkenes (129).

Various workers (17,81,130,131) have attempted to determine the yields of water and other oxygen-containing compounds in the hydrocarbon/nitrous oxide system, usually measuring the increase in the hydrogen yield from the reaction of water on sodium.

Sato *et al* (130) estimated $G(H_2O)$ at 4 or 5 in the

radiolysis of gaseous mixtures of hydrocarbons and nitrous oxide. Gaümann et al (17) studying the addition of nitrous oxide to n-hexane at -70°C and using $LiAlH_4$ to produce hydrogen, determined that at 3.8 mole % addition of nitrous oxide, $G(H_2O)$ was 5.5. They could not detect any hexanols or hexanones, and proposed that the formation of water involved initially the neutralisation of N_2O^- with the hexane positive ion to give the OH radical.

Koch et al (131) obtained a value of $G(H_2O) \approx 2$ for the n-pentane/nitrous oxide system, again using the yield of hydrogen from sodium.

Recently Takao et al (81) studied the addition of several hydrocarbons to the gas-phase radiolysis of nitrous oxide. They used a polyethylene glycol-200 column to detect water and other allied compounds, obtaining a $G(H_2O)$ value of 4.8 using n-butane as the additive, and determined $G(H_2O) = 7.2$ for cis-2-butene. The present work, for solutions of nitrous oxide and hydrocarbons, give a $G(H_2O)$ value of about 11 using a Porapak Q column. However, Takao found n-propanol, G(PrOH) = 0.7, using n-butane as the additive, whereas the present study determined G(propanols) < 0.08.

(d) Halo-compounds

The decreases in product yields of nitrous oxide upon addition of the halo-compounds are displayed in Figures III-15A to III-22A, and the $\Delta g(N_2)$ decreases are summarised in Table IV-7a. The curves used to achieve such $\Delta g(N_2)$ decreases merit further comment since a gradation in the use of correction factors is observed in going from methyl fluoride through carbon tetrachloride. Thus, methyl fluoride shows a plateau using the $g(N_2)_N^4$ curve, but methyl iodide affords a plateau with the $g(N_2)_N^2$ curve, and chloroform yields a plateau only in the uncorrected $g(N_2)_N^0$ curve. There is therefore a trend in the decreasing correction factors, which parallels the trend in the electron scavenging efficiencies of the halo-compounds. Virtually all the electrons released during radiolysis in the chloroform/nitrous oxide system are scavenged by chloroform, leading to no nitrogen formation by electron capture; which is exemplified by the use of the $g(N_2)_N^0$ curve. On the other hand, the methyl fluoride/nitrous oxide system yields a plateau with the $g(N_2)_N^4$ curve. This behaviour indicates that most of the electrons generated in the solution are captured by nitrous oxide and that methyl fluoride is a relatively poor electron scavenger.

All the halo-compounds have ionisation potentials

TABLE IV-7a

Decrease in Product Yields with Addition of the Halo-compounds

Compound	$\Delta g(N_2)$ using curves (a) $g(N_2)_N^4$,	(b) $g(N_2)_N^4 - g(N_2)_N^3$,	(c) $g(N_2)_N^3$,	(d) $g(N_2)_N^2$,	(e) $g(N_2)_N^0$	$\Delta g(O_2)$ at 0.1 mole fraction additive	$\Delta g(NO_2)$ at 0.1 mole fraction additive
CH_3F	0-1					2.7	
CH_3Cl		0-1				2.7	5.6
CH_3Br			0-1			2.7	5.6
CH_3I				1-2		2.7	
$n\text{-}C_3H_7Br$			0-1			2.7	
$CHCl_3$					~5	2.7	
CCl_4					5-6	-	

TABLE IV-7b

G Values Obtained for the Pure Halo-compounds

Compound	$G(H_2)$	$G(CH_4)$
CH_3F	1.3	-
CH_3Cl	0.70	2.5
CH_3Br	0.18	0.13
CH_3I	0.28	0.29

(continued.....)

TABLE IV-7b (continued)

Compound	$G(H_2)$	$G(CH_4)$
$n\text{-}C_3H_7Br$	0.50	-
$CHCl_3$	-	-
CCl_4	-	-

below that of nitrous oxide (Table IV-8a), so a charge transfer reaction between the positive ion N_2O^+ and RX the neutral halo-compound molecule may occur. This reaction is followed by a neutralisation between N_2O^- and RX^+ eventually giving nitrogen.

$$N_2O^+ + RX \longrightarrow N_2O + RX^+ \quad (58)$$

$$N_2O^- + RX^+ \longrightarrow N_2O^* + RX \quad (59)$$

Thus, again using G(ionisation) of 4 for nitrous oxide, reaction (58) through reaction (59) gives an increase of 4 units of nitrogen as seen from Table IV-7a, the yields of nitrogen dioxide and oxygen decrease to zero with increasing concentration of the halo-compound. Hence reactions (41) and (42) are cancelled out affording a decrease of 5.2 units of nitrogen and giving a net decrease of 1.2 g units of nitrogen. The $\Delta g(N_2)$ values for the halo-compounds (except methyl iodide, chloroform and carbon tetrachloride) are in the range 0-1 g units, being in fair agreement with the theoretical result.

The experimental values obtained for chloroform and carbon tetrachloride are particularly interesting as both compounds afford calculated nitrogen decreases of about 5 g units.

From Table IV-8a, the electron affinities of these additives are much higher, and the ionisation potentials

TABLE IV-8a

Ionisation Potentials (119) and Electron Affinities of the Halo-compounds

Compound	Ionisation Potential eV	Electron Affinity eV
CH_3F	12.80	
CH_3Cl	11.28	
CH_3Br	10.53	
CH_3I	9.54	
$n\text{-}C_3H_7Br$	10.18	
$CHCl_3$	11.42	1.92[b]
CCl_4	11.47	2.17[a] 2.28[b]

[a] H.O. Pritchard, Chem. Review, 52, 529 (1953).

[b] A.F. Gaines, J. Kay and F. M. Page, Trans. Farad. Soc. 62, 874 (1966).

TABLE IV-8b

$G(N_2)$ Values at 0.01 Mole Fraction Nitrous Oxide

Compound	$G(N_2)$ value at 0.01 mole fraction N_2O
CH_3F	3.0
CH_3Cl	0.99
CH_3Br	0.24
CH_3I	0.15

are lower than those of nitrous oxide. Thus, these halo-compounds can scavenge both positive ions and electrons in the nitrous oxide system.

$$e^- + CHCl_3 \longrightarrow (CHCl_3^-) \qquad (60)$$

$$N_2O^+ + CHCl_3 \longrightarrow N_2O + CHCl_3^+ \qquad (61)$$

$$(CHCl_3^-) + CHCl_3^+ \longrightarrow \text{no } N_2 \text{ formation} \qquad (62)$$

$$e^- + CCl_4 \longrightarrow (CCl_4^-) \qquad (63)$$

$$N_2O^+ + CCl_4 \longrightarrow N_2O + CCl_4^+ \qquad (64)$$

$$(CCl_4^-) + CCl_4^+ \longrightarrow \text{no } N_2 \text{ formation} \qquad (65)$$

The $CHCl_3^-$ and CCl_4^- ions may decompose to form Cl^-, in which case Cl^- would be the negative ion in reactions (62) and (65).

Therefore, using chloroform as the additive, reaction (62) will replace reactions (41) and (42) in Mechanism I, and the neutralisation reaction between ions of chloroform does not lead to nitrogen formation.

Removal of reactions (41) and (42) gives a decrease of 5.2 units of nitrogen. Referring to Figure III-21A, the uncorrected $g(N_2)_N^0$ curve shows a plateau around a value of 8, thus affording a decrease of about 5 g units of nitrogen. The $g(N_2)_N^0$ curve for carbon tetrachloride (Figure III-22B) indicates a levelling-off around a value of 7 to 8, giving a decrease in nitrogen of 5 to 6 units.

These calculated decreases derived from experimental data compare well with the theoretical decrease derived from Mechanism I.

The $G(N_2)$ curves on the extreme right in Figures III-15A through III-20A show the effect of nitrous oxide, and hence the resultant nitrogen yields, on the radiolysis of the halo-compounds. From the respective slopes it is seen that the electron scavenging efficiency of nitrous oxide in methyl fluoride is much greater than in methyl iodide. Taking the $G(N_2)$ value at 0.01 mole fraction nitrous oxide for the methyl halides, the relative efficiencies of electron scavenging in the methyl halides are as follows (Table IV-8b):-

$$CH_3F(3.0) > CH_3Cl(0.99) > CH_3Br(0.24) > CH_3I(0.15)$$

The yields of minor products from the radiolysis of the pure halo-compounds are given in Table IV-7b. Increasing amounts of nitrous oxide have little effect on the hydrogen yields (Figures III-15C to III-20C).

(e) Oxygen-containing Compounds

The effect of these additives on the product yields from the radiolysis of liquid nitrous oxide are given in Figures III-23A through III-27A. The observations are similar to those previously reported in that the yields of nitrogen are reduced, whereas the yields of nitrogen

dioxide and oxygen are eliminated. With the carbonyl compounds, the lower values of $G(N_2)_x$ of 2 and 3 yielding $g(N_2)^2_N$ and $g(N_2)^3_N$ respectively, were calculated, giving the best plateau over most of the concentration range, (Figure III-23B and Figure III-25B). The decreases in product yields are summarised in Table IV-9a.

As the ionisation potentials of these compounds fall below 12.89 eV (the ionisation potential of nitrous oxide) then the charge transfer reaction between N_2O^+ and ROH, the oxygen-containing compound, is favoured. The subsequent neutralisation reaction eventually yields nitrogen, and as reactions (41) and (42) are wiped out, the net theoretical decrease in nitrogen is again 1.2 g units.

$$N_2O^+ + ROH \longrightarrow N_2O + ROH^+ \qquad (66)$$

$$N_2O^- + ROH^+ \longrightarrow N_2O^* + ROH \qquad (67)$$

Comparing the calculated decreases in nitrogen yields in Table IV-9a, fair agreement is obtained with the theoretical value. The $g(N_2)^3_N$ and $g(N_2)^2_N$ curves for acetone and acetaldehyde respectively indicate that these two additives are electron scavengers, and that the trend in the decreasing correction factors equals the trend in the electron scavenging efficiencies, (Figures III-23B and III-25B). The two alcohols used both give nitrogen decreases

TABLE IV-9a

Decrease in Product Yields with Addition of the Oxygen-containing Compounds

Compound	$\Delta g(N_2)$ using curves (a) $g(N_2)_N^5 - g(N_2)_N^4$	(b) $g(N_2)_N^3$	(c) $g(N_2)_N^2$	$\Delta g(O_2)$ at 0.08 mole fraction additive	$\Delta g(NO_2)$ at 0.08 mole fraction additive
CH_3COCH_3	-	0-1	-	2.7	5.6
CH_3CHO	-	-	1-3	2.7	(5.6)
CH_3OH	1-2	-	-	2.7	5.6
C_2H_5OH	1-2	-	-	2.7	(5.6)

TABLE IV-9b

G Values Obtained for the Pure Oxygen-containing Compounds

Compound	$G(H_2)$	$G(CH_4)$	$G(CO)$
CH_3COCH_3	0.95	0.70	-
CH_3CHO	1.3	1.0	1.4
CH_3OH	4.0	-	-
C_2H_5OH	4.8	-	-

TABLE IV-10

Ionisation Potentials of the Oxygen-containing Compounds

Compound	Ionisation Potential eV
CH_3COCH_3	9.75[a]
CH_3CHO	10.25[a]
CH_3OH	10.85 (119)
C_2H_5OH	10.48 (119)

[a] H. Hurzeler, M. G. Ingram and J. D. Morrison, J. Chem. Phys., 28, 76 (1958).

in the range 1-2 g units.

On the extreme right of Figures III-23A through III-27A, the electron generated in the solution is scavenged by nitrous oxide, and the electron scavenging efficiency of nitrous oxide is greater in the alcohols than in the carbonyl compounds. The nitrous oxide is thus interfering with the normal ion-electron neutralisation reactions.

For the alcohols, the addition of nitrous oxide rapidly decreases the hydrogen yields (Figures III-26C and III-27C) until plateaus of 'unscavengable' hydrogen are reached (92).

Acetone yielded hydrogen and methane upon radiolysis and nitrous oxide has little effect upon these yields (Figure III-23C). The situation with acetaldehyde is more complex as carbon monoxide was also detected, but all three products decrease slightly with addition of nitrous oxide (Figure III-25C).

(f) Alkynes

The $G(N_2)$ curves in Figures III-28A and III-29A show the effect of the alkynes on the nitrous oxide system. The trends are similar to those with other additives mentioned insofar as $G(NO_2)$ and $G(O_2)$ decrease to zero and $G(N_2)$ shows a steady decrease along the concentration range. Decreases in terms of g units of nitrogen are given in Table IV-11A.

TABLE IV-11a

Decrease in Product Yields with Addition of the Alkynes

Compound	$\Delta g(N_2)$ using curves (a) $g(N_2)_N^5$	(b) $g(N_2)_N^3$	$\Delta g(O_2)$ at 0.1 mole fraction alkynes	$\Delta g(NO_2)$ at 0.1 mole fraction alkynes
C_2H_2	-	1-2	2.7	(5.6)
C_3H_4	1-2	-	2.7	5.6

TABLE IV-11b

Ionisation Potentials (119) of the Alkynes

Compound	Ionisation Potential eV
C_2H_2	11.41
C_3H_4	10.36

As before, a charge transfer reaction can take place, followed by the neutralisation reaction.

$$N_2O^+ + C_2H_2 \longrightarrow N_2O + C_2H_2^+ \qquad (68)$$

$$N_2O^- + C_2H_2^+ \longrightarrow N_2O^* + C_2H_2 \qquad (69)$$

A similar reaction to reaction (56) producing an excited acetylene molecule is unlikely as the first excited energy levels of the alkynes are in the region 5-7 eV (132-134) well above the first excited (triplet) level of nitrous oxide. Thus the theoretical decrease is 1.2 g units of nitrogen, giving reasonable agreement to the calculated nitrogen decreases derived from the experimental results (Table IV-11a). Also the $g(N_2)^3_N$ curve affords a plateau, indicating that acetylene is an electron scavenger.

The addition of methyl acetylene to nitrous oxide decreases $G(NO_2)$ to zero at 0.05 mole fraction (Figure III-30C) and also the yield of oxygen is eliminated. Hence these results are compatible with Mechanism I as reactions (41) and (42) are replaced by reaction (69), and thus no nitrogen dioxide is formed.

(g) Cyclo-compounds

Three cyclo-compounds were studied in conjunction with nitrous oxide and the decrease in product yields with increasing additive concentration are given in Table IV-12a. In all three cases, the $g(N_2)^5_N$ curve gives the flattest

TABLE IV-12a

Decrease in Product Yields with Addition of the Cyclo-compounds

Compound	$\Delta g(N_2)$ using the $g(N_2)_N^5$ curve	$\Delta g(O_2)$ at 0.1 mole fraction additive
$c\text{-}C_5H_{10}$	1-2	2.7
$c\text{-}C_5H_8$	1-2	2.7
$c\text{-}C_3H_6$	1-2	2.7

TABLE IV-12b

$G(H_2)$ Values Obtained for the Pure Cyclo-compounds

Compound	$G(H_2)$
$c\text{-}C_5H_{10}$	5.2
$c\text{-}C_5H_8$	1.2
$c\text{-}C_3H_6$	1.1

curve over most of the concentration range (Figures III-31B to III-33B), and thus afford $\Delta g(N_2)$ values in the range 1-2 g units. Since the ionisation potentials of these cyclo-compounds are in the range 9-11 eV, whereas that of nitrous oxide is 12.89 eV, then the following charge transfer reaction is favoured, followed by the neutralisation reaction.

$$N_2O^+ + c\text{-}RH \longrightarrow N_2O + c\text{-}RH^+ \qquad (70)$$

$$N_2O^- + c\text{-}RH^+ \longrightarrow N_2O^* + c\text{-}RH \qquad (71)$$

As previously mentioned, reaction (71) replaces reactions (41) and (42) in Mechanism I, and results in a net decrease of 1.2 g units of nitrogen, being in fair accord with the experimentally determined decreases of 1-2 g units.

The yield of oxygen from nitrous oxide decreases to zero with addition of small quantities of the cyclo-compounds, in agreement with the results obtained from the alkanes and alkene additive studies.

In analysing the effect of the addition of nitrous oxide to the cyclo-compounds (Figures III-31A to III-33A), it is seen that the electron scavenging efficiency of nitrous oxide is greater in cyclopentane than in cyclopentene. The $g(H_2)$ curve in Figure III-31C for cyclopentane decreases sharply with addition of nitrous oxide as the electron scavenger inhibits hydrogen formation by interfer-

TABLE IV-13

Ionisation Potentials (119) of the Cyclo-compounds

Compound	Ionisation Potential eV
$c\text{-}C_5H_{10}$	10.52
$c\text{-}C_5H_8$	9.01
$c\text{-}C_3H_6$	11.06

ing with reaction (72), until a non-scavengable plateau

$$c\text{-}RH^+ + e^- \longrightarrow H_2 + \text{Products} \qquad (72)$$

of hydrogen is reached. For the $g(H_2)$ curve in cyclopentene, increasing nitrous oxide concentration only slightly depresses the curve. The lower $G(N_2)$ curve in cyclopentene is attributed to shorter geminate neutralisation times as a result of the shorter ion-electron separation distances in the alkenes (127), thus decreasing the probability of electron scavenger by nitrous oxide.

In cyclopropane, the addition of nitrous oxide has little effect on the yield of hydrogen (Figure III-33C).

(h) Miscellaneous

Continuing with the classification given in the Results Section, this group comprises of an aromatic compound and a conjugated diene. The decrease in product yields of nitrous oxide with addition of these additives is given in Table IV-14a. Similar trends to the other additives are retained with these compounds in that the oxygen yield decreases to zero within 0.1 mole fraction of additive, and for toluene and 1,3-butadiene, no nitrogen dioxide was detected at 0.06 mole fraction of additive.

(i) Toluene

The $g(N_2)$ decrease derived from Figure III-34B is

TABLE IV-14a

Decrease in Product Yields with Addition of the Miscellaneous Compounds

Compound	$\Delta g(N_2)$ using curves (a) $g(N_2)_N^5$	(b) $g(N_2)_N^5 - g(N_2)_N^4$	(c) $g(N_2)_N^2$	$\Delta g(O_2)$ at 0.1 mole fraction additive	$\Delta g(NO_2)$ at 0.1 mole fraction additive
$C_6H_5CH_3$	-	1-2	-	2.7	5.6
C_4H_6	-	-	2-3	2.7	(5.6)

TABLE IV-14b

Ionisation Potentials of the Miscellaneous Compounds

Compound	Ionisation Potential eV	Electron Affinity eV
$C_6H_5CH_3$	8.82	
C_4H_6	9.07	~ 0.04 (4)

in the range of 1-2 g units. The theoretical decrease in nitrogen using Mechanism I and invoking a charge transfer reaction between N_2O^+ and the toluene molecule; followed by a neutralisation reaction, which replaces reactions (41) and (42), gives a yield of 1.2 g units.

(ii) 1,3-Butadiene

The $G(N_2)$ curve in Figure III-35A is lower than similar curves for the alkenes, showing that the electron scavenging efficiency of nitrous oxide is less in a conjugated diene than in a mono-olefin. Referring to Figure III-35B, the $g(N_2)^2_N$ curve affords the flattest curve over most of the concentration range; the necessity of using such curves shows that 1,3-butadiene is an efficient electron scavenger. The decrease in nitrogen is in the range 2-3 g units. Thus this decrease may be interpreted as follows.

$$N_2O^+ + \text{diol} \longrightarrow N_2O + \text{diol}^+ \qquad (73)$$

$$N_2O^- + \text{diol}^+ \longrightarrow N_2O^* + \text{diol} \qquad (74)$$

where diol is the 1,3-butadiene molecule. The lowest excited states of dienes however fall in the same regions as those for nitrous oxide, so an excited diene molecule can also result from the neutralisation reaction (121,135).

$$N_2O^- + \text{diol}^+ \longrightarrow N_2O + \text{diol}^* \qquad (75)$$

The calculated decrease in nitrogen (2-3 g units) indicate that $G(N_2O^*)$ from reaction (74) is about 3. Hence replacement of reactions (41) and (42) in the mechanism by the neutralisation reactions (74) and (75) affords a theoretical decrease of about 2.2 g units of nitrogen.

(i) High Electron Affinity Compounds

This group comprises of three electron scavengers namely sulphur hexafluoride, carbon dioxide and nitrogen dioxide, and the decreases in nitrogen, oxygen and nitrogen dioxide upon addition of such compounds are shown in Figures III-1A to III-4A, and are summarised in Table IV-15a.

(i) Sulphur Hexafluoride

The addition of a high electron affinity compound, such as sulphur hexafluoride, to the nitrous oxide system is therefore expected to reduce the yields of nitrogen, oxygen and nitrogen dioxide by eliminating reactions (41) and (42). Thus the electron generated in the nitrous oxide is preferentially scavenged by the additive.

$$e^- + SF_6 \longrightarrow SF_6^- \qquad (76)$$

A charge transfer reaction between N_2O^+ and SF_6 is not likely, as the ionisation potential of sulphur hexafluoride is higher than that of nitrous oxide (Table IV-15b). The

TABLE IV-15a

Decrease in Product Yields with Addition of the High Electron Affinity Compounds

Compound	$\Delta g(N_2)$ using curves (a) $g(N_2)_N^4$	(b) $g(N_2)_N^0$	$\Delta g(NO_2)$ at 0.1 mole fraction additive
SF_6	~2	-	~2
CO_2	~1.5	-	-
NO_2	-	5.6	-

TABLE IV-15b

Ionisation Potentials (119) and Electron Affinities of the High Electron Affinity Compounds

Compound	Ionisation Potential eV	Electron Affinity eV
SF_6	19.3	1.52[a], 1.47[b]
CO_2	13.79	>2.0[c]
NO_2	9.78	3.99[a], 3.90[e]
N_2O	12.89	<1.47[d]

[a] H. O. Pritchard, Chem. Rev., 52, 529 (1953).

[b] J. Kay and F. M. Page, Trans. Farad. Soc., 60, 1042 (1964).

[c] G.J. Schulz, Phys. Rev., 128, 178 (1962).

[d] W.J. Holtslander and G.R. Freeman, J. Phys. Chem., 71, 2562 (1967).

[e] S. Tsuda and W.J. Hamill, Advan. Mass. Spect., 3, 249 (1966).

negative ion SF_6^- has an estimated lifetime of 10^{-4} sec (9,136), so the following neutralisation reaction can occur.

$$SF_6^- + N_2O^+ \longrightarrow SF_6 + N_2O^* \qquad (77)$$

The excited nitrous oxide molecule may then decompose.

Referring again to Mechanism I and using G(ionisation) of 4, elimination of reactions (41) and (42) affords a decrease of 5.2 units of nitrogen, and substitution of reaction (76) through (77) gives 4 g units of nitrogen. This results in a net decrease of 1.2 units of nitrogen.

The $g(N_2)_N^4$ curve in Figure III-1B indicates a plateau around a value of 11. Thus the calculated decrease is about 2 units of nitrogen, giving only fair agreement with the theoretical value. Several solutions of sulphur hexafluoride and nitrous oxide were irradiated at -45°C, and it is seen from Figure III-1A that elevation of temperature has little effect on the product yields.

At a concentration of 0.12 mole fraction of sulphur hexafluoride, the decrease in $g(NO_2)$ is only about 2 units, whereas Mechanism I would predict $g(NO_2)$ equals zero at this concentration. The reason for this discrepancy is not clear. Perhaps the excited nitrous oxide molecule formed in reaction (51) decomposes forming not only ground state but also excited oxygen atoms. The latter would then react with nitrous oxide yielding an additional source of nitric oxide.

$$N_2O^* \longrightarrow N_2 + O \qquad (19)$$

$$\longrightarrow N_2 + O^* \qquad (78)$$

$$O^* + N_2O \longrightarrow N_2 + O_2 \qquad (33)$$

$$\longrightarrow 2NO \qquad (34)$$

In fact, reactions involving excited oxygen atoms and nitrous oxide have been introduced into several proposed mechanisms (55,81), and such reactions would decrease the postulated yields of reactions (40), (41), (42) and (19) in Mechanism I. Takao et al (81) suggested that the excited oxygen atom produced in reaction (52) is in the ^1D or ^1S state.

Another explanation is that the electron affinity of nitrous oxide could be comparable to that of sulphur hexafluoride, and that both would compete favourable for the electron. Obviously more research in this direction is needed, especially in determing the electron affinity of nitrous oxide.

In the final stages of writing this thesis Willis et al (137) proposed a mechanism for the radiolysis of gaseous nitrous oxide using high dose rate Febretron pulses (10^{26} - 10^{28} eV g^{-1} s^{-1}). The yields for pure nitrous oxide of $G(N_2) = 12.4 \pm 0.3$, $G(O_2) = 4.8$ and $G(NO) = 5.6$ are not inconsistent with the yields obtained in the liquid at lower dose rates. The main features of

their mechanism include dissociative neutralisation of N_2O^+ by electrons and excitation of nitrous oxide yielding mainly nitrogen and the excited oxygen atom in the ^1D state. The $O(^1D)$ atom is suggested to react with nitrous oxide forming nitrogen, oxygen and nitric oxide.

(ii) Carbon Dioxide

Using the $g(N_2)_N^4$ curve in Figure III-3B, the calculated decrease is 1.5 units of nitrogen. As previously mentioned, the theoretical decrease using G(ionisation) of 4 for nitrous oxide is 1.2 g units. Therefore, it is expected that the following electron scavenging reaction occurs.

$$e^- + CO_2 \longrightarrow CO_2^- \qquad (79)$$

The CO_2^- ion has been observed in the gas phase as a direct product of electron collisions with organic molecules, with a measured lifetime of 3×10^{-5} sec (138). Positive ion scavenging by carbon dioxide is improbable due to the higher ionisation potential of the former over that of nitrous oxide (Table IV-15b). The dominant neutralisation reaction is probably

$$CO_2^- + N_2O^+ \longrightarrow CO_2 + N_2O^* \qquad (80)$$

The excited nitrous oxide molecule decomposes yielding nitrogen. Thus the theoretical decrease of 1.2 g units

of nitrogen agrees well with the calculated decrease, obtained from experimental data, of 1.5 g units of nitrogen. However, an excited carbon dioxide molecule can also result from reaction (80), and depending on the extent of reaction

$$CO_2^- + N_2O^+ \longrightarrow CO_2^* + N_2O \qquad (81)$$

(81), would result in a theoretical decrease of >1.2 units of nitrogen.

(iii) Nitrogen Dioxide

From Table IV-15b, it is noted that the electron affinity of this additive is much higher than that of nitrous oxide, and the ionisation potential value of 9.78 eV is lower than the ionisation potential of nitrous oxide (12.89 eV). So nitrogen dioxide can scavenge positive ions and electrons in the nitrous oxide system.

$$e^- + NO_2 \longrightarrow NO_2^- \qquad (82)$$

$$N_2O^+ + NO_2 \longrightarrow N_2O + NO_2^+ \qquad (83)$$

These resultant ions can undergo neutralisation.

$$NO_2^- + NO_2^+ \longrightarrow \text{negligible } N_2 \text{ formation} \qquad (84)$$

Reaction (84) replaces reactions (41) and (42) in Mechanism I. The neutralisation reaction between ions of nitrogen dioxide does not lead to nitrogen formation, as the radiolysis of pure nitrogen dioxide gives $G(N_2) < 0.1$. Thus using

G(ionisation) of 4 for nitrous oxide, removal of reactions (41) and (42) gives a decrease of 5.2 units of nitrogen. Referring to Figure III-4B, the $g(N_2)_N^0$ curve levels out around 7.5 giving a decrease of 5.6, which is in reasonable agreement with the theoretical value.

REFERENCES

1. J. W.T. Spinks and R. J. Woods, 'An Introduction to Radiation Chemistry', Wiley, New York (1964).
2. L. I. Bone, L. W. Sieck and J. H. Futrell, J. Chem. Phys., 44, 3367 (1966).
3. G. R. A. Johnson and J. M. Warman, Trans. Far. Soc., 61, 1709 (1965).
4. G. R. Freeman, Rad. Res. Rev., 1, 1 (1968).
5. A. V. Phelps and R. E. Voshall, J. Chem. Phys., 49, 3246 (1968).
6. J. M. Warman and R. W. Fessenden, J. Chem. Phys., 49, 4718 (1968).
7. W. J. Holtslander and G. R. Freeman, Can. J. Chem., 45, 1661 (1967).
8. F. S. Dainton, P. O'Neill and G. A. Salmon, Chem. Comm., 1001 (1972).
9. C. E. Klotts, J. Chem. Phys., 46, 1197 (1967).
10. M. Zelikoff and L. M. Aschenbrand, J. Chem. Phys., 22, 1680,1685 (1954).
11. R. A. Young, G. Black and T. G. Slanger, J. Chem. Phys., 49, 4769 (1968).
12. R.A. Holroyd, J. Y. Yang and F. M. Servedio, J. Chem. Phys., 46, 4540 (1967).
13. J. Y. Yang, F. M. Servedio and R. A. Holroyd, J. Chem. Phys., 48, 1331 (1968).

14. R. A. Holroyd, J. Phys. Chem., 72, 759 (1968).

15. D. R. Smith and W. A. Seddon, Chem. Phys. Lett., 3, 640 (1969).

16. D. R.Smith and W. A. Seddon, Can. J. Chem., 48, 1803 (1970).

17. A. Menger and T. Gaümann, Helv. Chim. Acta 52, 2477 (1969).

18. W. A. Noyes Jr., J. Chem. Phys., 5, 807 (1937).

19. G. R. Freeman, J. Chem. Phys., 38, 1022 (1963).

20. G. R.Freeman and J. M. Fayadh, J. Chem. Phys., 43, 86 (1965).

21. F.W. Schmidt and A. O. Allen, J. Phys. Chem., 72, 3730 (1968).

22. P. H. Tewari and G. R. Freeman, J. Phys. Chem., 51, 1276 (1969).

23. G. G. Meisels, J. Chem. Phys., 41, 51 (1964).

24. C. Vermeil, M. Matheson, S. Leach and F. Muller, J. Chim. Phys., 61, 598 (1964).

25. T.W. Woodward and R. A. Back, Can. J. Chem., 41, 1463 (1963).

26. W. J. Holtslander and G. R. Freeman, Can. J. Chem., 45, 1661 (1967).

27. G.R. Freeman and E. D. Stover, Can. J. Chem., 46, 3235 (1968).

28. G. R. Gedye, Trans. Farad. Soc., 27, 474 (1931).

29. G. R. Gedye, J. Chem. Soc., 3016 (1931).

30. P. Harteck and S. Dondes, Nucleonics 14 No. 3 66 (1956).

31. B. J. Burtt and J. F. Kircher, Rad. Res., 9, 1 (1958).

32. F. Moseley and A. E. Truswell, A.E.R.E. Harwell Report No. AERE-R3078 (1960).

33. J. A. Hearne and R. W. Hummel, Rad. Res., 15, 254 (1961).

34. G. R. A. Johnson, J. Inorg. Nucl. Chem., 24, 461 (1962).

35. D. A. Fluory, Nucleonics 21 No. 12 50 (1963).

36. D. Kubose, Trans. Am. Nucl. Soc., 7, 318 (1964).

37. R. Gorden Jr. and P. Ausloos, J. of Research of NBS 69A, 79 (1965).

38. F.T. Jones and T. S. Sworski, J. Phys. Chem., 70, 1546 (1966).

39. A. R. Anderson, B. Knight and J. A. Winter, Trans. Farad. Soc., 62, 359 (1966).

40. C. Willis, O. A. Miller, A. E. Rothwell and A. W. Boyd, Advan. Chem. Ser., 81, 539 (1968).

41. A. W. Boyd, C. Willis and O. A. Miller, Can. J. Chem., 47, 351 (1969).

42. J. P. Doering and B. H. Mahan, "Chemical Reactions in the Lower and Upper Atmosphere" Stanford Research Institute Symposium, Interscience Publishers, New York p.327 (1961).

43. J. P. Doering and B. H. Mahan, J. Chem. Phys., 36, 1682 (1962).

44. H. Essex and A. D. Kolumban, J. Chem. Phys., 8, 450 (1940).

45. H. Essex and N. T. Williams, J. Chem. Phys., 16, 1153 (1948).

46. R. W. Hummel, Chem. Comm., 1518 (1968).

47. S. Takao, S. Shida, Y. Hatano and H. Yamazaki, Bull. Chem. Soc. Japan, 41, 2221 (1968).

48. J. T. Sears, J. Phys. Chem., 73, 1143 (1969).

49. R. W. Hummel, Chem. Comm., 995 (1969).

50. S. Takao and S. Shida, Bull. Chem. Soc. Japan, 43, 2766 (1970).

51. G. J. Schulz, J. Chem. Phys., 34, 1778 (1961).

52. B. P. Burtt and J. Henis, J. Chem. Phys., 41, 1510 (1964).

53. P. J. Chantry, J. Chem. Phys., 51, 3380 (1969).

54. J. F. Paulson, Advan. Chem. Ser., 58, 28 (1966).

55. M. G. Robinson and G. R. Freeman, J. Phys. Chem., 72, 1394 (1968).

56. F. S. Dainton and D. B. Peterson, Nature, 186, 878 (1960).

57. F. S. Dainton and D. B. Peterson, Proc. Roy. Soc. (London) A267, 443 (1962).

58. J. T. Allan and C.M. Beck, J. Am. Chem. Soc., 86, 1483 (1964).

59. G. Scholes and M. Simic, Nature 202, 895 (1964).

60. G. Scholes, M. Simic, G. E. Adams, J. W. Boag, and B. D. Michael, Nature 204, 1187 (1964).

61. Y. Okada, J. Phys. Chem., 68, 2120 (1964).

62. P. J. Dyne, Can. J. Chem., 43, 1080 (1965).

63. G. Meissner and A. Henglein, Ber. Bunginges physik. Chem., 69, 264 (1965).

64. R. Blackburn and A. Charlesby, Nature 210, 1036 (1966).

65. S. Sato, R. Yugeta, K. Shinsaka and T. Terao, Bull. Chem. Soc. Japan 39, 156 (1966).

66. W. V. Sherman, J. Chem. Soc., A599 (1966).

67. J. W. Warman, Nature 213, 381 (1967).

68. L. A. Rajbenbach, J. Am. Chem. Soc., 47, 242 (1967)

69. N. H. Sagert and A. S. Blair, Can. J. Chem., 45, 1351 (1967).

70. D. A. Head and D. C. Walker, Can. J. Chem., 45, 2051 (1967).

71. G. R. A. Johnson and M. Simic, J. Phys. Chem., 71, 1118 (1967).

72. J. M. Warman, J. Phys. Chem., 71, 4066 (1967).

73. R. A. Holroyd, Advan. Chem. Series 82, 488 (1968).

74. J. C. Russell and G. R. Freeman, J. Chem. Phys., 48, 90 (1968).

75. M. G. Robinson and G. R. Freeman, J. Chem. Phys., 48, 983 (1968).

76. R. R. Hentz and S. J. Rzad, J. Phys. Chem., 72, 1027 (1968).

77. R. R. Hentz and R. J. Knight, J. Phys. Chem., 72, 4684 (1968).

78. N. H. Sagert, R. W. Robinson and A. S. Blair, Can. J. Chem., 46, 3512 (1968).

79. J. M. Warman, K.-D. Asmus and R. H. Schuler, Advan. Chem. Ser., No. 82 25 (1968).

80. K. Takeuchi, K. Shinsaka, S. Takao, Y. Hatano and S. Shida, Bull. Chem. Soc. Japan, 44, 2004 (1971).

81. S. Takao, Y. Hatano and S. Shida, J. Phys. Chem., 75, 3178 (1971).

82. C. E. Burchill and G. P. Wollner, Can. J. Chem., 50, 1751 (1972).

83. M. G. Robinson and G. R. Freeman, J. Chem. Phys., 55, 5644 (1971).

84. R. Cooper and R. M. Mooring, Australian J. Chem., 21, 2417 (1968).

85. P. Alder and H. K Bothe, Z. Naturforsch, 20a, 1700 (1965).

86. M. G. Robinson and G. R. Freeman, Can. J. Chem., (in press).

87. "Methods for the Determination of Toxic Substances in Air", 16.1 (1961), International Union of Pure and Applied Chemistry, Butterworths, London (1962).

88. A. O. Allen, "The Radiation Chemistry of Water and Aqueous Solutions", D. Van Nostrand, Princeton, N.J., (1961).

89. J. N. Pitts, J. H. Sharp and S. I. Chan, J. Chem. Phys., 39, 238 (1963).

90. J. W. Gerstmayr, P. Harteck and R. R. Reeves, J. Phys. Chem., 76, 474 (1972).

91. H. A. Dewhurst, J. Phys. Chem., 62, 15 (1968).

92. J. H. Baxendale and F. W. Mellows, J. Am. Chem. Soc., 83, 4720 (1961).

93. H. S. Johnson, J. Chem. Phys., 19, 663 (1951).

94. L. Friedman and J. Bigeleisen, J. Am. Chem. Soc., 75, 2215 (1953).

95. T. Oka, R. Kato, S. Sato and S. Shida, Bull. Chem. Soc. Japan, 41, 2192 (1968).

96. T. Oka and S. Sato, Unpublished results (1968).

97. F. C. Fehsenfeld, Private communication (1968).

98. E.E. Ferguson, F. C. Fehsenfeld and A. L. Schmeltekopk, J. Chem. Phys., 47, 3085 (1967).

99. P. J. Chantry, J. Chem. Phys., 51, 3380 (1968).

100. J. N. Bardsley, J. Chem. Phys., 51, 3384 (1969).

101. E. J. Chaney and L. G. Christophorou, J. Chem. Phys., 51, 883 (1969).

102. J. F. Paulson, J. Chem. Phys., 52, 959 (1970).

103. R.G. Pearson, Chem. Phys. Lett. 10(1), 31 (1971).

104. A. D. Walsh, J. Chem. Soc., 2266 (1952).

105. G. Hertzberg, "Electronic Spectra of Polyatomic Molecules", D. Van Nostrand, Princeton, N.J., (1966).

106. W. E. Wentworth, E. Chen and R. Freeman, J. Chem. Phys., 55, 2075 (1971).

107. R. K. Curran and R. E. Fox, J. Chem. Phys., 34, 1590 (1961).

108. D. Rapp and D. D. Briglia, J. Chem. Phys., 43, 1480 (1965).

109. F. Kaufman, J. Chem. Phys., 46, 2449 (1967).

110. L. M. Branscomb, D. S. Burch, S. J. Smith and S. Geltman, Phys. Rev., 111, 504 (1958).

111. W. L. Jolly, "The Inorganic Chemistry of Nitrogen", W. A. Benjamin, N.Y., (1964).

112. D. A. Ramsay, "Determination of Organic Structures by Physical Methods Vol. 2", Academic Press, N.Y., (1962).

113. M. C. R. Symons, Advan. Chem. Ser., 36, 76 (1962).

114. H. W. Ford and N. Endow, J. Chem. Phys., 27, 1277 (1957).

115. R. Atkinson and R. J. Cvetanović, J. Chem. Phys., 55, 659 (1971).

116. C.P. Fenimore and G. W. Jones, J. Phys. Chem., 63, 1154 (1959).

117. F. S. Dainton and S. A. Sills, Proc. Chem. Soc., 223 (1962).

118. D. Perner and R. H. Schuler, J. Phys. Chem., 70, 317 (1966).

119. R.W. Kiser, "Introduction to mass spectrometry and its applications", Prentice-Hall Inc., Englewood Cliffs, N.J., (1965).

120. J. P. Manion and M. Burton, J. Phys. Chem., 56, 560 (1952).

121. D. F. Evans , J. Chem. Soc., 1735 (1960).

122. C. R. Bowman and W. D. Millar, J. Chem. Phys., 42, 681 (1965).

123. J. P. Doering, J. Chem. Phys., 46, 1194 (1967).

124. H. Sponer and L. G. Bonner, J. Chem. Phys., 8, 33 (1940).

125. M. Zelikoff, K. Watanabe and E. C. Y. Inn, J. Chem. Phys., 21, 1643 (1953).

126. B. A. Lombos, P. Sauvageau and C. Sandorfy, Chem. Phys. Lett., 1, 382 (1967).

127. W.F. Schmidt and A. O. Allen, J. Chem. Phys., 52, 2345 (1970).

128. F. Busi and G. R. Freeman, J. Phys. Chem., 75, 2560 (1971).

129. R. J. Cvetanović, J. Chem. Phys., 25, 376 (1968).

130. S. Sato, K. Shinsaka and T. Terao, Bull. Chem. Soc. Japan, 39, 156 (1966).

131. R. O. Koch, J. P. W. Houtman and W. A. Cramer, J. Am. Chem. Soc., 90, 3326 (1968).

132. L. G. Ross, Trans. Farad. Soc., 48, 973 (1952).

133. T. Nakayama and K. Watanabe, J. Chem. Phys., 40, 538 (1964).

134. S. Trajmar, J. K. Rice, P. S. P. Weir and A. Kupperman Chem. Phys. Lett., 1, 703 (1968).

135. G. S. Hammond, N. J. Turro, and P. A. Leersmaker, J. Phys. Chem., 66, 1144 (1962).

136. D. Edelsen, J. E. Griffiths, and K. B. McAfee Jr., J. Chem. Phys., 37, 917 (1962).

137. C. Willis, A. W. Boyd and P. E. Bindner, Can. J. Chem., 50, 1557 (1972).

138. C. D. Cooper and R. N. Compton, Chem. Phys. Lett., 14, 29 (1972).

END OF REEL

-30